UNIVERSITY OF OKLAHOMA

GRADUATE COLLEGE

EFFECTS OF WATER AND ALUMINUM DISTRIBUTION ON CATALYTIC PERFORMANCE OF ZEOLITES

A DISSERTATION

SUBMITTED TO THE GRADUATE FACULTY

in partial fulfillment of the requirements for the

Degree of

DOCTOR OF PHILOSOPHY

By

TRAM NGOC PHAM

Norman, Oklahoma

2022

EFFECTS OF WATER AND ALUMINUM DISTRIBUTION ON
CATALYTIC PERFORMANCE OF ZEOLITES

A DISSERTATION APPROVED FOR THE

SCHOOL OF CHEMICAL, BIOLOGICAL, AND MATERIALS ENGINEERING

BY THE COMMITTEE CONSISTING OF

Dr. Steven Crossley, Chair

Dr. Bin Wang

Dr. Daniel Resasco

Dr. Lance Lobban

Dr. Daniel Glatzhofer

Xin dành tặng gia đình thân yêu!

To my beloved family

ACKNOWLEDGMENTS

First, I would like to thank Dr. Steven Crossley for his tremendous support, guidance, and kindness. He is an excellent person with a combination of knowledge, creativity, and enthusiasm. I have learned many things from him, both in research and in life. He gives me a lot of ideas and positive energies every time we have discussions about research. He realizes my potential, always believes in me, and encourages me to pursue excellence. I am so grateful to have such an amazing advisor.

I would like to thank our collaborators, including Vy Nguyen, Dr. Bin Wang and Dr. Jeffery White. I especially thank Vy Nguyen for her hard work in supporting this dissertation. I am so lucky to be involved in this project and to work with such a great team. This dissertation is hardly completed without their thoughtful scientific contributions.

I would like to express my great gratitude to Dr. Resasco, for being such a great mentor. He is an amazing researcher and professor who is a great model for young people like me. He always encourages me to improve myself to become whom I want to be. All my accomplishments during my time in OU would not have been possible without his support. In addition, I would like to thank Dr. Lance Lobban and Dr. Daniel Glatzhofer for being my committee members. They are very supportive and give me many advice to improve my Ph.D. work.

I would like to thank all members of OU catalysis group for their support and discussions. I especially thank Vy, Phat, Han, Tien, Nhung, a Tuong, Gengnan, Ana, Alejandre, Nilson, Reda, and Ismaeel. I would like to thank my other Vietnamese friends, including Quy, Thao, c Nhung, a Tien, c Vi, and a Vinh, Y. They make my time at OU delightful.

Finally, I would like to acknowledge a great deal of supports from my family. I would like to thank my husband, Tuan Vu, for constantly supporting me to pursue my dreams and our little son, Albert, for always loving me. They motivate me to go through this long journey and make it more enjoyable. I would also like to thank my parents and my sister for always helping and encouraging me to get through difficult times. I am so lucky to have them by my side all the time.

There are many people that I could not mention here, but I appreciate and will remember all supports I have received during this journey.

This material is based upon work supported by the National Science Foundation. The DFT calculations were performed by Vy Nguyen, Dr. Bin Wang's group, using computational resources at the OU Supercomputing Center for Education & Research (OSCER) at the University of Oklahoma. NMR spectra were conducted by Dr. Jeffery White's group, School of Chemical Engineering, Oklahoma State University.

Contents

LIST OF FIGURES

LIST OF TABLES

LIST OF SCHEMES

ABSTRACT

Zeolites are used in numerous industrially relevant reactions such as cracking, isomerization, and alkylation. The activity of Brønsted acid sites contained within the microporous zeolite channels might be influenced by the location and resulting local confining environment that stabilizes reaction intermediates and transition states. The presence of active sites nearby and extra-lattice species may modify the environment surrounding active sites, which have been proposed to alter reaction rates significantly. Thus, understanding the effect of these factors on the reactivity of zeolites is essential for the design and synthesis of solid acid catalysts to improve their catalytic performance.

It is well-known that extra-framework Al species generated due to the exposure of zeolites to water at high temperatures can significantly modify the catalytic reactivity of neighboring Brønsted acid sites. Hydrothermal treatment and steaming might lead to the generation of synergistic sites between Brønsted acid sites and extra-framework Al species with high activity for alkane cracking reaction. The generation of these synergistic sites is strongly influenced by the formation, diffusion, and stabilization of extra-framework Al species inside the zeolite pores. Thus, this dissertation aims to reveal the influence of water and other structural properties of zeolites, including the density and the distribution of framework and non-framework Al species in the generation of highly active sites that regulate the catalytic performance of catalysts. In particular, newly developed treatment methods by pulsing water are employed to decouple the rate enhancement due to the generation of highly active sites without the hydrolysis of framework Al sites. The experiment results combined with Density Functional Theory calculations show that cations such as sodium and calcium prefer to exchange with protons associated with highly

active sites in zeolites. These cations inhibit the generation of these sites under water treatment. This approach allows quantifying the number of highly active sites and accesses the activation energies for cracking reactions on different types of active sites. Various pre-treatments of catalysts are conducted to modify the cracking rate via enhancement of mobility of extra-framework Al species inside zeolite pores or transformation of these species leading to the generation of new actives sites. Conclusions regarding the generation of highly active sites in MFI zeolite are expanded to other zeolite topologies (FAU, BEA, MOR, MEL, FER, and TON) to understand the impact of confinement and topologies on the reactivity of the catalyst.

CHAPTER 1: Introduction

1.1 Zeolite and their use in catalytic cracking

Due to the strong growth in energy demand, it is crucial to enhance the efficiency of refining processes to produce fuels and chemicals from crude oil. For several decades, zeolites have been utilized widely as acid catalysts in many industrial reactions. These crystalline oxides consist of SiO_4 and AlO_4^- tetrahedra structures forming pores and cavities of diameter ~0.2-2 nm. Besides strong acidity, zeolites possess thermal robustness and flexibility in tailoring the shapes, size, and connectivity of framework channels, making them useful in many industrial catalysis and separation processes. Figure 1 presents different zeolite frameworks, some of which are the focus of this work.

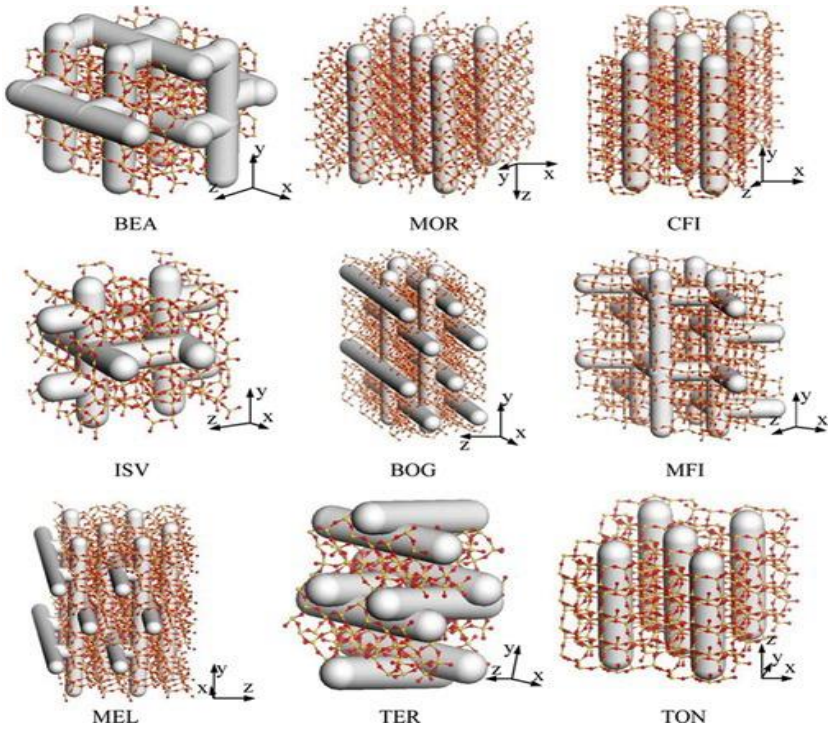

Figure 1. Representations of various zeolite frameworks, adapted from elsewhere.[1]

Y zeolite, a large pore zeolite with a faujasite (FAU) framework structure, is mainly utilized as a catalyst for fluid catalytic cracking (FCC), which convert heavy components of crude oil to fuels and chemical products.[2, 3] The second most used zeolite after Y is ZSM-5 catalysts with MFI structure. ZSM-5 is an essential additive for FCC catalyst to enhance the octane number of the gasoline fraction and reduce the coke formation. In addition, cracking in the presence of steam, known as steam cracking, is the principal method to produce light olefins, including ethylene and propylene. These olefins are one of the most critical starting products in the petrochemical industry with many applications, such as producing plastics and other polymers.

The catalytic cracking reactions generally happen at a very high temperature (~500^{o}C) for a short contact time between the reactants and acid catalysts. The presence of water in this condition might have both positive and negative effects on the reactivity of the zeolite catalysts. It has been observed that steaming treatment under mild conditions can significantly enhance the catalyst's reactivity. In addition, with the same zeolite framework, some zeolites exhibit higher cracking activity than others. For many years, researchers have proposed various hypotheses to explain the differences in the reactivities of zeolite in the presence and absence of water exposure leading to many contradicting claims in the literature. These issues motivate us to conduct this work to provide more insights into the relationship between the structural properties of zeolites and their catalytic performance, especially for alkane cracking reactions. In the scope of this dissertation, we revealed the role of water, the Al site distribution, including concentration and location of framework and extra-framework Al atoms, and the topologies of zeolites on the reactivity of alkane

cracking reaction. This knowledge provides critical information for the synthesis and design of zeolites for catalytic purposes.

1.2 Framework and non-framework Al species in zeolites.

These catalysts' typical active centers are Brønsted acid sites (BAS) created by the charge balance of tetrahedrally-coordinated aluminum atoms in the zeolite frameworks. The nature, the number, and the strength of acid sites in zeolite have been studied intensively for decades.[4, 5] The reactivity of these acid sites is generally influenced by many factors such as diffusion, acid strength, confinement around the active sites, and the density of active sites, etc.[6-9] These factors can affect the adsorption of molecules and stabilization of the transition states leading to the differences in the reaction rate on different active sites.

It is well-known that exposure of zeolite to different temperature conditions and in the presence of water can lead to hydrolysis of framework Al atoms. As a result, framework-associated Al atoms and extra-framework Al (EFAL) might be generated, as shown in Scheme 1. While framework-associated Al atoms can be formed at low temperatures, they can be converted to EFAL species at higher temperature treatment in the presence of water. Therefore, it is challenging to decouple the effect of these two species on the reactivity of the catalysts. In general, EFAL species are usually generated during steaming at a high temperature which is believed to be responsible for the higher alkane cracking rate of steamed zeolites.[10-16] The nature of these EFAL species has been investigated, but the catalytic consequences of each are not entirely known.

Scheme 1. A summary of generation of different non-framework Al atoms in zeolites. [17]

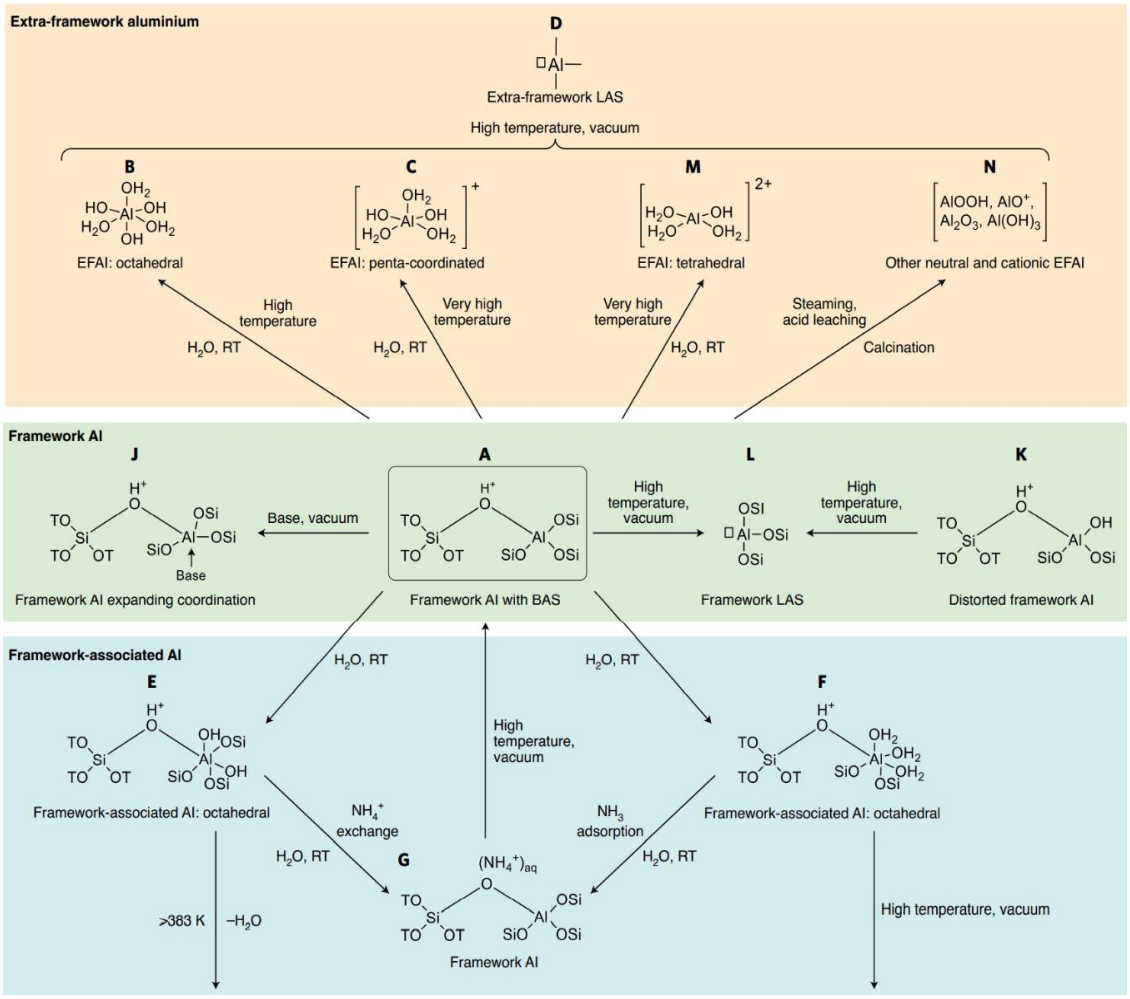

In general, two forms of EFAL have been proposed: the cationic species including Al^{3+}, AlO^{+}, $Al(OH)^{2+}$, $Al(OH)_2^{+}$ and neutral compounds such as AlO(OH), $Al(OH)_3$, Al_2O_3. The generation and stabilization of these species under steaming treatment are strongly influenced by the BAS density and topologies of parent zeolites. Figure 2 illustrates the stabilization of different EFAL species at intersections of MFI zeolite. The Al atom in the framework is utilized to balance the charge of cation EFAL species. The interaction between the water molecules or acidic protons can convert one form of EFAL species into others.[18] In steaming conditions, these EFAL species can be mobilized and aggregated to

form aluminum clusters. The mobility and stabilization of these species are influenced by zeolite's structural properties, which will be investigated in this work.

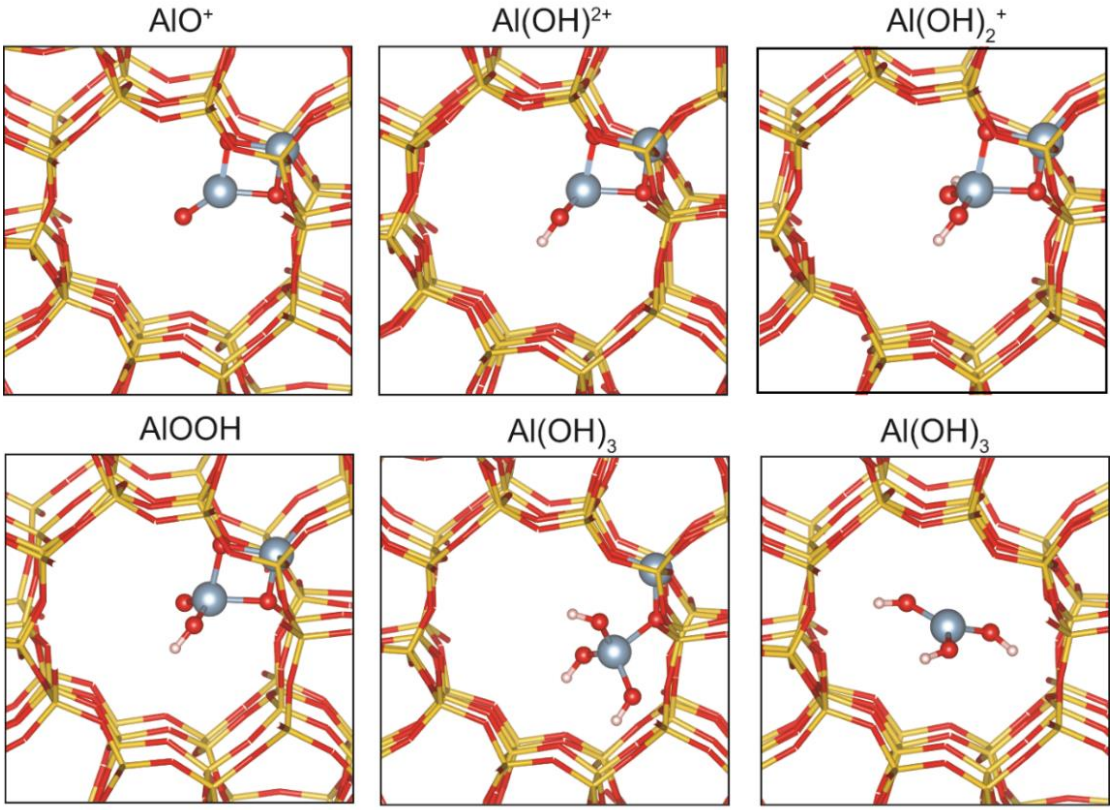

Figure 2. Optimized structures of EFAL species inside MFI zeolite

1.3 Alkane cracking reaction

Alkane cracking is one of the most important reactions for producing fuels and chemicals from hydrocarbons and emerging processes such as biomass and waste polymer conversion. It is generally accepted that selective monomolecular alkane cracking occurs at high reaction temperatures (≥ 450 ^{o}C), low reactant pressures, and low conversions resulting in simple product distribution. Many researchers utilize this reaction to investigate the catalytic activity or the acidity of zeolites.[10, 12, 19-22] The cracking of hexane,

known as (α) alpha test, has been used for decades as a convenient measure of catalytic activity [23, 24] and will be utilized as a probe reaction to investigate different types of active sites and the effect of the Al distribution on the reactivity of catalysts in this study. The rate of this reaction is not affected by the pore diffusion.[25] The pathway of hexane conversion is illustrated in Scheme 2. Besides the main reaction as protolytic cracking and dehydrogenation, other bimolecular reactions such as H-transfer can happen that strongly affect the product distribution of the reaction. Thus, it is crucial to operate the reaction at the first-order regime and low conversion level to avoid secondary reactions.

Scheme 2. Reaction pathways of paraffin over zeolite, adapted from elsewhere. [26]

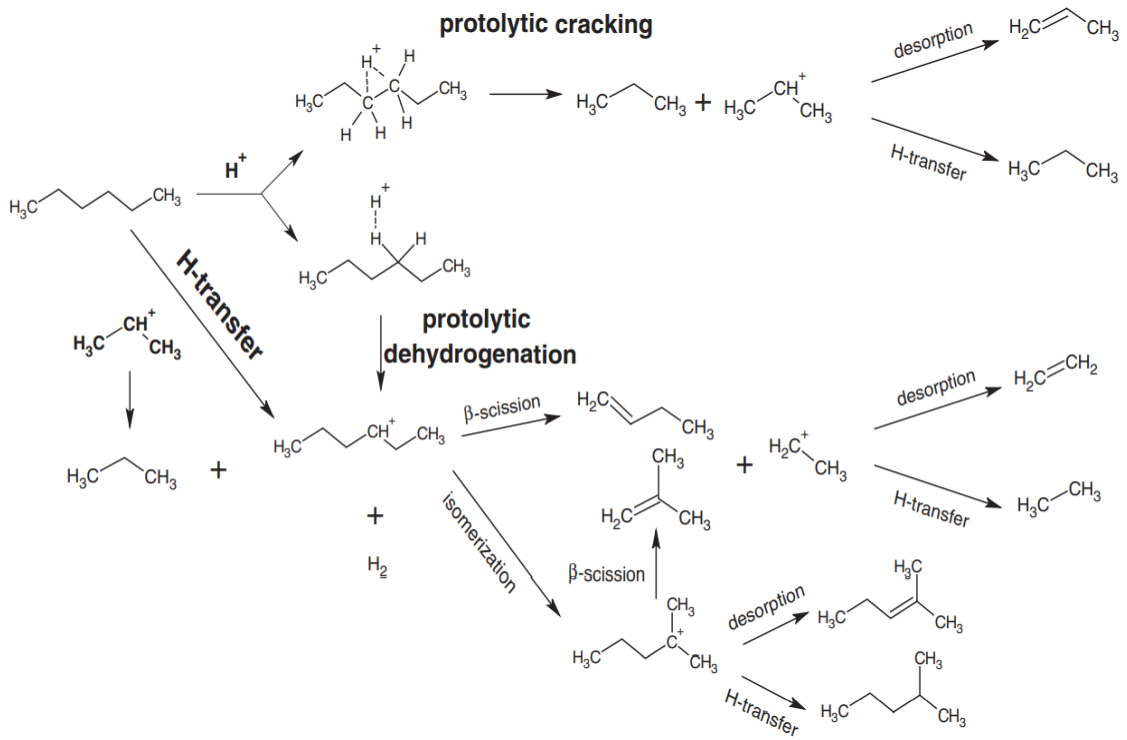

Haag et al. have reported that the activity per framework Al for hexane cracking is similar on synthesized HZSM-5 samples varying Al concentration in 3 orders of magnitude.[27, 28] The authors observed a consistent reactivity with a variant of proton distribution and

location. Another explanation for these results is that these investigated samples have similar distributions of specific protons.[29] The previous works reported that the product distribution of hexane cracking is identical for all zeolites.[21, 30, 31] In general, the high olefin to paraffin ratio, the low selectivity to is-C5 and iso-C4, as well as the absence of C7+ products, suggest that the bimolecular cracking reactions do not likely to happen. The ratio of propylene to propane is greater than one. In addition, there is a significant amount of methane but no pentene is observed. These results suggest that larger olefins quickly undego secondary cracking reactions. This analysis of cracking products is similar to the experiment results observed in this work.

1.4 Outline

This work aims to systematically investigate the effect of EFAL species, zeolite structure parameters, and the Al distribution on the monomolecular cracking reaction. Hexane cracking is used as a probe reaction to measure and compare the reactivity of parent and modified zeolites obtained by water or ammonium nitrate treatment and cation exchange procedures.

In chapter 2, the pulsing water treatment method was introduced to modify the reactivity of alkane cracking on zeolite. In this treatment, we reveal the role of water in enhancing the mobility of existing EFAL species without hydrolyzing existing framework Al species and reducing site density. It is observed that rate enhancements after pulsed water exposure beyond those observed in a typical framework site are a strong function of the framework site density, implying an intriguing element of framework site location and proximity on the ultimate generation of highly active sites. The activation energy of the cracking reaction

associated with synergistic sites and the energy required to generate these new sites are estimated.

In chapter 3, we employed a combination of cation titration, pulsed water treatments, and activity measurements to reveal the influence of Al distribution, including acid sites in proximity and their location in the generation of highly active sites for alkane cracking. The work proposed two types of synergistic sites might present in MFI zeolites. One type is associated with Al in proximity. In addition, the high selectivity of cation titration of synergistic sites using calcium and sodium enables the quantification of these highly active sites in different MFI samples. The preferred locations for highly active site formation were also discussed. The new approach using pulsing water and cation titration allows decoupling from traditional sites such that barriers for alkane cracking may be independently estimated over these sites.

Chapter 4 reported that several pre-treatments with water and ammonium nitrate solutions might significantly enhance the catalyst's reactivity for cracking reactions. These treatments do not modify the density of BAS; thus, the higher cracking rate on these zeolites is attributed to the enhancement of mobility of EFAL species or the transformation of these species into “active” EFAL forms. The influence of BAS density and the H-bond network inside zeolite pore might strongly influence the mobility of EFAL species, evidenced by experiment results and DFT calculations.

Finally, we investigate the effect of Si/Al ratios, confinement, and topologies on the catalytic activities of different zeolites. The activity of the fresh and those after water treatment are compared to reveal the effect of zeolite structure on the generation of new

highly active sites. Activation barriers for hexane cracking are estimated for these catalysts showing the effects of both confinement and the presence of highly active sites on the reactivities of these catalysts. The preference for sodium titration with these highly active sites in MOR and MEL zeolites will be investigated and compared with results observed in MFI zeolites.

REFERENCES

1. Lu, L.; Zhu, Y.; Wu, X.; Wang, S.; Cao, W.; Lu, X., Adsorption of N-Butane/I-Butane in Zeolites: Simulation and Theory Study. *Separation Science and Technology* **2014,** *49* (8), 1215-1226.

2. Degnan, T. F., Applications of zeolites in petroleum refining. *Topics in Catalysis* **2000,** *13* (4), 349-356.

3. Vogt, E. T. C.; Weckhuysen, B. M., Fluid catalytic cracking: recent developments on the grand old lady of zeolite catalysis. *Chemical Society Reviews* **2015,** *44* (20), 7342-7370.

4. Derouane, E. G.; Védrine, J. C.; Pinto, R. R.; Borges, P. M.; Costa, L.; Lemos, M. A. N. D. A.; Lemos, F.; Ribeiro, F. R., The Acidity of Zeolites: Concepts, Measurements and Relation to Catalysis: A Review on Experimental and Theoretical Methods for the Study of Zeolite Acidity. *Catalysis Reviews* **2013,** *55* (4), 454-515.

5. Resasco, D. E.; Wang, B.; Crossley, S., Zeolite-catalysed C–C bond forming reactions for biomass conversion to fuels and chemicals. *Catalysis Science & Technology* **2016,** *6* (8), 2543-2559.

6. Derouane, E. G.; Andre, J.-M.; Lucas, A. A., Surface curvature effects in physisorption and catalysis by microporous solids and molecular sieves. *Journal of Catalysis* **1988,** *110* (1), 58-73.

7. Noh, G.; Shi, Z.; Zones, S. I.; Iglesia, E., Isomerization and β-scission reactions of alkanes on bifunctional metal-acid catalysts: Consequences of confinement and diffusional constraints on reactivity and selectivity. *Journal of Catalysis* **2018,** *368*, 389-410.

8. Gorte, R. J.; Crossley, S. P., A perspective on catalysis in solid acids. *Journal of Catalysis* **2019,** *375*, 524-530.

9. Crossley, S. P.; Resasco, D. E.; Haller, G. L., Clarifying the multiple roles of confinement in zeolites: From stabilization of transition states to modification of internal diffusion rates. *Journal of Catalysis* **2019,** *372*, 382-387.

10. Masuda, T.; Fujikata, Y.; Mukai, S. R.; Hashimoto, K., Changes in catalytic activity of MFI-type zeolites caused by dealumination in a steam atmosphere. *Applied Catalysis A: General* **1998,** *172* (1), 73-83.

11. Schallmoser, S.; Ikuno, T.; Wagenhofer, M. F.; Kolvenbach, R.; Haller, G. L.; Sanchez-Sanchez, M.; Lercher, J. A., Impact of the local environment of Brønsted acid sites in ZSM-5 on the catalytic activity in n-pentane cracking. *Journal of Catalysis* **2014,** *316*, 93-102.

12. van Bokhoven, J. A.; Tromp, M.; Koningsberger, D. C.; Miller, J. T.; Pieterse, J. A. Z.; Lercher, J. A.; Williams, B. A.; Kung, H. H., An Explanation for the Enhanced Activity for Light Alkane Conversion in Mildly Steam Dealuminated Mordenite: The Dominant Role of Adsorption. *Journal of Catalysis* **2001,** *202* (1), 129-140.

13. Li, S.; Zheng, A.; Su, Y.; Zhang, H.; Chen, L.; Yang, J.; Ye, C.; Deng, F., Brønsted/Lewis Acid Synergy in Dealuminated HY Zeolite: A Combined Solid-State NMR and Theoretical Calculation Study. *Journal of the American Chemical Society* **2007,** *129* (36), 11161-11171.

14. Chen, K.; Abdolrahmani, M.; Horstmeier, S.; Pham, T. N.; Nguyen, V. T.; Zeets, M.; Wang, B.; Crossley, S.; White, J. L., Brønsted–Brønsted Synergies between

Framework and Noncrystalline Protons in Zeolite H-ZSM-5. *ACS Catalysis* **2019**, 6124-6136.

15. Zhang, Y.; Zhao, R.; Sanchez-Sanchez, M.; Haller, G. L.; Hu, J.; Bermejo-Deval, R.; Liu, Y.; Lercher, J. A., Promotion of protolytic pentane conversion on H-MFI zeolite by proximity of extra-framework aluminum oxide and Brønsted acid sites. *Journal of Catalysis* **2019,** *370*, 424-433.

16. Maier, S. M.; Jentys, A.; Lercher, J. A., Steaming of Zeolite BEA and Its Effect on Acidity: A Comparative NMR and IR Spectroscopic Study. *The Journal of Physical Chemistry C* **2011,** *115* (16), 8005-8013.

17. Ravi, M.; Sushkevich, V. L.; van Bokhoven, J. A., Towards a better understanding of Lewis acidic aluminium in zeolites. *Nature Materials* **2020,** *19* (10), 1047-1056.

18. Liu, C.; Li, G.; Hensen, E. J. M.; Pidko, E. A., Nature and Catalytic Role of Extraframework Aluminum in Faujasite Zeolite: A Theoretical Perspective. *ACS Catalysis* **2015,** *5* (11), 7024-7033.

19. Kung, H. H.; Williams, B. A.; Babitz, S. M.; Miller, J. T.; Haag, W. O.; Snurr, R. Q., Enhanced hydrocarbon cracking activity of Y zeolites. *Topics in Catalysis* **2000,** *10* (1), 59-64.

20. Zholobenko, V. L.; Kustov, L. M.; Kazansky, V. B.; Loeffler, E.; Lohser, U.; Peuker, C.; Oehlmann, G., On the possible nature of sites responsible for the enhancement of cracking activity of HZSM-5 zeolites dealuminated under mild steaming conditions. *Zeolites* **1990,** *10* (4), 304-306.

21. van Bokhoven, J. A.; Williams, B. A.; Ji, W.; Koningsberger, D. C.; Kung, H. H.; Miller, J. T., Observation of a compensation relation for monomolecular alkane

cracking by zeolites: the dominant role of reactant sorption. *Journal of Catalysis* **2004,** *224* (1), 50-59.

22. Janda, A.; Bell, A. T., Effects of Si/Al Ratio on the Distribution of Framework Al and on the Rates of Alkane Monomolecular Cracking and Dehydrogenation in H-MFI. *Journal of the American Chemical Society* **2013,** *135* (51), 19193-19207.

23. Weisz, P. B.; Miale, J. N., Superactive crystalline aluminosilicate hydrocarbon catalysts. *Journal of Catalysis* **1965,** *4* (4), 527-529.

24. Miale, J. N.; Chen, N. Y.; Weisz, P. B., Catalysis by crystalline aluminosilicates: IV. Attainable catalytic cracking rate constants, and superactivity. *Journal of Catalysis* **1966,** *6* (2), 278-287.

25. Haag, W. O.; Lago, R. M.; Weisz, P. B., Transport and reactivity of hydrocarbon molecules in a shape-selective zeolite. *Faraday Discussions of the Chemical Society* **1981,** *72* (0), 317-330.

26. To, A. T.; Jentoft, R. E.; Alvarez, W. E.; Crossley, S. P.; Resasco, D. E., Generation of synergistic sites by thermal treatment of HY zeolite. Evidence from the reaction of hexane isomers. *Journal of Catalysis* **2014,** *317*, 11-21.

27. Olson, D. H.; Haag, W. O.; Lago, R. M., Chemical and physical properties of the ZSM-5 substitutional series. *Journal of Catalysis* **1980,** *61* (2), 390-396.

28. Haag, W. O.; Lago, R. M.; Weisz, P. B., The active site of acidic aluminosilicate catalysts. *Nature* **1984,** *309* (5969), 589-591.

29. Haag, W. O., Catalysis by Zeolites – Science and Technology. In *Studies in Surface Science and Catalysis*, Weitkamp, J.; Karge, H. G.; Pfeifer, H.; Hölderich, W., Eds. Elsevier: 1994; Vol. 84, pp 1375-1394.

30. Narbeshuber, T. F.; Vinek, H.; Lercher, J. A., Monomolecular Conversion of Light Alkanes over H-ZSM-5. *Journal of Catalysis* **1995,** *157* (2), 388-395.

31. Kotrel, S.; Rosynek, M. P.; Lunsford, J. H., Intrinsic Catalytic Cracking Activity of Hexane over H−ZSM-5, H−β and H−Y Zeolites. *The Journal of Physical Chemistry B* **1999,** *103* (5), 818-824.

CHAPTER 2: Quantifying the Influence of Water on the Mobility of Aluminum Species and their Impacts on Alkane Cracking in Zeolites

ABSTRACT

The role of extra framework Al species on industrially important reactions such as alkane cracking has been extensively discussed and debated. We have long known that water treatments influence the framework aluminum sites and, in some cases, can modify activity. However, what is less understood is the direct relationship between the structural modifications and altered reactivity of essential reactions such as alkane cracking and isomerization. Collective understanding of the multiple roles that water plays in the modification of zeolites and influencing reaction rates is continuously evolving. Extra lattice Al species close to a framework Brønsted acid site have been proposed to modify the energies associated with surface intermediates and kinetically relevant transition states, enhancing alkane cracking reaction rates. However, the role of water on the migration of these extra framework alumina species to generate highly active sites is less understood and is the focus of this study. Water is introduced in controlled pulses to ZSM-5 zeolites with various Si/Al ratios and densities of extra framework Al species with n-hexane cracking activity used to investigate the catalytic activity due to the generation of new active sites. A pulse technique allows decoupling of water dosing, lattice rearrangement, and drying, thereby enabling the quantification of activation energies associated with the generation of new active sites without losses in crystallinity or total density of Brønsted acid site.

Further, by subtracting the contributions to the reaction rate associated with isolated Brønsted acid site, the reaction rate associated with the newly created sites is estimated. The results show that the energy barrier required for cracking on highly active sites is much lower than those observed on traditional Brønsted sites (75 kJ/mol vs. 110 kJ/mol). The temperature dependence for the generation of these new sites reveals a 44 kJ/mol activation energy for the kinetically relevant step associated with the generation of these sites in the presence of water vapor, which to the best of our knowledge has not been previously quantified. It is reported that while water vapor is essential for the generation of these new active sites, it also binds to these sites and strongly inhibits the cracking rate. These findings clarify some of the conflicting reports regarding the role of water in activity enhancement.

2.1 Introduction

The activity and selectivity within the microporous environments of zeolites are easily influenced by diffusion, and local confinement effects can play an important role in many reactions on zeolites.[1-4] While it is well established that modifying active sites by exposing zeolites to high-temperature steaming can lead to activity enhancement, the consensuses regarding the mechanisms are challenging to attain. Steam treatments often lead to modification of active sites in parallel with consequences on zeolite crystal structure such as the generation of mesopores and crystal collapse, all of which can affect catalytic activity. It is well-known that exposure of zeolites to moisture, even at room temperature, can lead to a variety of partially coordinated Al species in equilibrium with framework Al atoms. Some of these species have been suggested as responsible for reactivity rates for facile low temperature reactions such as H/D exchange. Our recent observations that partially coordinated Al species can be removed by ammonium hexafluorosilicate (AHFS) washing and there is some correlation between the concentration of these species and high temperature cracking reactivity suggests that these could be precursors to form extra lattice species under more severe conditions.[5, 6] More severe steam treatments can lead to the removal of framework Brønsted acid sites to create extra lattice species. Excessive exposure to high temperature steam environments eventually leads to pore collapse, however, several studies report enhancements in catalytic activity after exposure to steam at mild conditions or short time for some reactions.[7-9] The extra framework aluminum (EFAL) species created by dealumination during steaming could be responsible for these enhancements in catalytic activity in some instances. The migration of EFAL species upon steam treatment have been observed by quantitative 3D fluorescence imaging,[10] with

resulting consequences on pore accessibility and furfuryl alcohol oligomerization activity. Several hypotheses have been proposed to explain the increase in activity observed for a variety of reactions over catalysts that contain extra framework species, including higher acid strength,[11] enhanced heat adsorption of reaction intermediates,[12] and the polarization of alkane molecules by Lewis acidic sites.[13] Despite the variety of potential explanations, researchers generally agree that two types of Brønsted acid sites coexist including isolated BAS (I-BAS) and synergistic sites, or acid site where the activity is synergistically enhanced by the presence of extra framework (EFAL) species near a traditional framework Brønsted site (EFAL-BAS). Many models focus on the generation and the rate enhancement on these synergistic sites. [5, 9, 12, 14-17] Li et al. provided the evidence for the detailed spatial proximities of Lewis/Brønsted acid sites in dealuminated HY zeolite by ^{1}H DQ-MAS NMR. They utilized NMR and density functional theory (DFT) calculations to reveal that EFAL species, such as $Al(OH)_3$ and $Al(OH)^{2+}$ could coordinate to the oxygen atom of the nearest BAS. The authors observed the downfield shift of the carbonyl carbon in ^{13}C NMR spectra of adsorbed 2-^{13}C-acetone as the hydrogen bond between the acidic proton and an oxygen atom of adsorbent and attributed this to the increase in acidity of active sites.[15] An alternative explanation for enhancement of acidity by EFAL species is proposed by Iglesia et al.[18-20] They claimed the observed enhancement in activity is mainly associated with tighter confinement due to the presence of EFAL species, resulting in more stabilized transition states. Meanwhile, the acid strength determined by deprotonation energies is insensitive to the location and confinement of the corresponding framework Al atoms. NMR experiments combined with chemical washing with ammonium hexafluorosilicate (AHFS) was applied to study synergies between framework aluminum

and EFAL species in these zeolites, revealing the emerge of a specific proton due to the presence of extra lattice Al species that is removed after AHFS treatment.[5, 21, 22] Recently, Zhang et al. utilized pyridine and pentane adsorption on BAS manifested in the IR spectra to observe the interaction between EFAL oxide and acid sites. The authors claimed that the turnover frequencies of pentane cracking on these sites are about 52 ± 2 times higher than on isolated Brønsted acid sites.[16]

Part of the confusion surrounding alterations in zeolite structure and correlation to catalytic activity arise from improper application of characterization techniques to study solid acids. For instance, ammonia is not considered as a good probe molecule to measure acid site strength by Temperature Programmed Desorption (TPD) as the peak temperature is strongly affected by diffusion and resorption of ammonia within catalyst pores or along the catalyst bed. Reaction rates might be a more reliable indicator of the strength of a Brønsted acid site, but rates are also easily influenced by other factors such as diffusion, surface coverage, the confining environment surrounding an acid site, and adsorption geometry.[3] Gounder et al. revealed that the estimation of framework aluminum content in faujasite zeolites by ^{27}Al MAS NMR spectra may not be accurate as some distorted Al structures detected as framework Al sites are not associated with acidic protons, while other Al species may not be accurately quantified via NMR. This leads to disagreement in the number of protons measured by this technique when compared with more reliable titration methods.[18] Conversely, relatively good agreement between ^{1}H solid-state NMR and IPA TPD has been achieved for the proton amount in some MFI catalysts.[5] In addition, depending on the identity of the coordinating species (such as H_2O, NH_3) and the temperature, coordinatively-unsaturated aluminum species in these zeolites can reversibly

convert between different forms, tetrahedral and octahedral coordination.[23, 24] Therefore, the ^{27}Al MAS NMR representation at lower temperatures may not accurately reflect the concentration under reaction conditions.

While much has been studied regarding potential stable species after steam treatments, one must note that the degree of enhancement in reaction rates is highly dependent on steaming conditions and initial zeolite Al distribution. The generation of synergistic sites is generally assumed to require an extra lattice Al species in the proximity of a Brønsted site; however, this involves not only hydrolysis of framework Al to generate an extra lattice site, but also the subsequent migration of this extra framework Al. The critical migration step has received much less attention than the initial hydrolysis. Further, it is well known that provided enough time in a high temperature steaming environment, these extra lattice species may combine to form a more thermodynamically stable Al_2O_3 phase. It is highly challenging to decouple extra lattice Al migration from its formation, limiting our ability to better understand the dynamic role of steam treatment on the generation of these synergistic sites.

In this work, the role of water on the creation of synergistic sites is investigated over HZSM-5 zeolites varying Si/Al ratio using a unique pulsed steaming approach. This method of water treatment is employed to inhibit the modification of zeolite structure during continuous steaming, and independently evaluate the role of water on Al migration independent of pore collapse and hydrolysis of framework Al species. Instead of exposing the catalyst to vapor water continuously, several pulses of water were introduced to change the activity of the catalyst for n-hexane cracking. After subsequent drying, this approach is demonstrated as an effective strategy to maintain the quantity of framework Brønsted sites

while having a significant influence over cracking activity. Water pulses are compared with a continuous steam environment, and the resulting influence on BAS density and activity of the catalysts is quantified. In addition, the results show that the BAS density and EFAL concentration in the parent material play an important role in the potential for activity enhancement by pulsing water treatments when additional dealumination is insignificant. Quantifying activity enhancements allow for measurement of activation energy associated with cracking over synergistic sites independently of isolated framework sites. Further, by carrying out these pulsed treatments as a function of temperature, the activation energy associated with the migration of EFAL species and creation of these sites themselves is measured, which is challenging or impossible to measure via other means.

2.2 Experimental section

2.2.1 Catalyst preparation

NH_4-ZSM5 catalysts with various Si/Al ratios obtained from Zeolyst and HZSM-22 catalyst from ACS Material were utilized in this study. Catalysts were calcined at 873 K for 5 hours in air with an initial slow ramp rate of 2K/min to convert NH_4^+ form to H^+ form. Table 1 lists the catalysts used in this study and their physical properties. After calcination, all ZSM-5 catalysts in proton form are indicated by HZSM5 followed by their Si/Al ratio. HZSM5-15 (Si/Al=15) washed with ammonium hexafluorosilicate (AHFS), denoted as HZSM5-15-AHFS, was obtained using standard methods.[25] The detail of the preparation and characterization of HZSM5-15-AHFS sample utilized in this work was described elsewhere.[5]

Water pulsing/ steaming zeolite. Several pulses of water with water vapor partial pressure of 18.6 kPa were applied to control the water treatment of catalyst at 480°C. The size of

the loop and other conditions of pulsing water are described in section 2.3. Meanwhile, the steamed catalysts were obtained by exposing the catalysts to the same temperature and partial pressure of water vapor in He flow (40 ml/min). It is noted that the water vapor pressures in these two cases are similar; however, the water vapor in the loop has very short contact time (~1-2 seconds) with the catalyst bed carried by the He flow as 75 ml/min while in steaming, catalysts were exposed to water all the time. The diagram of the pulse experiment is illustrated in Figure S3.

Table 1. Properties of investigated zeolite samples

Zeolite	Si/Al ratio	BAS density [mmol. g^{-1}]			Calculated EFAL[c] [mmol. g^{-1}]
		Calculated[a]	IPA-TPD[b]	Literature	
HZSM5-11.5	11.5	1.33	1.08	1.09 [26, 27]	0.25
HZSM5-15	15	1.04	0.73	0.76 [5, 14]	0.31
HZSM5-15-AHFS	__	__	0.70	0.74 [5]	__
HZSM5-25	25	0.64	0.48	0.54 [14]	0.16
HZSM5-40	40	0.41	0.38	0.35 [14, 26]	0.03
HZSM-22	32.5 - 40	0.4 - 0.5	0.31	__	__
HZSM5-140	140	0.12	0.10	0.094 [27]	__

[a] Calculated based on Si/Al ratio and Al framework type. [b] Determined by IPA-TPD. [c] Determined by subtracting the number of BAS sites measured by IPA-TPD from the theoretical BAS density calculated based on the Si/ Al ratio.

2.2.2 Catalyst characterization

Surface area and X-ray diffraction measurements. N_2 physisorption was carried out at -198ºC on a Micromeritics ASAP 2010. The samples were degassed for 10 hours under vacuum at 250°C prior to the absorption. X-ray diffraction (XRD) studies of catalysts were conducted on a Rigaku diffractometer, utilizing Cu Kα radiation generated at 44 mA and 40kV; the diffraction angle range is $2\theta = 2-70°$.

Solid-state NMR Spectroscopy. ^{1}H MAS NMR spectra were collected on a Bruker Avance 400 spectrometer. The detail of the procedure and measurement conditions as described in previous works.[5, 21, 22]

IPA-TPD experiment. BAS density was measured by the temperature-programmed desorption of isopropylamine (IPA-TPD). The catalyst was pre-treated at 480ºC, the temperature of the cracking reaction for 2 h to remove moisture, and cooled down to 100ºC under the helium flow rate of 30 ml/min. Then, it was exposed to specific 2 µL pulses of IPA. After that, weakly adsorbed IPA was removed from the catalyst by flushing He for a few hours at the same temperature. The catalyst was heated up to 600ºC with a 10ºC/min linear heating ramp. A sharp peak of propylene as a product of the reaction between Brønsted sites and IPA was observed at the high-temperature range of 300-390ºC. This peak was used to determine the number of Brønsted sites. The analysis was elaborated by utilizing MKS Cirrus mass spectrometer, tracking m/z = 17, 41, 58 for ammonia, propylene, and IPA, respectively. The intensity of propylene signal (m/z = 41) was calibrated by several 500 µL pulses of propylene.

Kinetic measurements. The activity of each catalyst for the conversion of n hexane cracking was evaluated by a micro-pulse reactor at 120 KPa pressure using helium as carrier gas. The amount of 5-70 mg catalyst pelletized to 0.25-0.35 mm particles then mixed with glass beads was used for the reaction. Before reaction, the catalyst was treated under the reaction temperature of 480^{o}C for 2h with the helium flow of 75 ml/min. Several pulses of the hydrocarbon reactant diluted in helium (0.48 μmol HC/pulse, 3.7 mol% of HC in He) were then sent over the catalyst bed. The size of the loop is 500 μL. During the period between continuous pulses, the catalyst was exposed to a helium flow. A Shimadzu QP-2010 GCMS/FID system using a HP-PLOT/Al_2O_3/''S'' column connected to the reactor outlet was applied to analyze the products of the reaction.

2.2.3 DFT calculations

All DFT calculations were carried out using the Vienna ab initio simulation package (VASP)[28]. The projected augmented waves (PAW)[29, 30] methods and the GGA-PBE exchange-correlation function[31] were used. To include the van der Waals interactions, the DFT-D3 semiempirical method[32] was employed. The HZSM-5 unit cell used in all calculations consists of 96 T sites and 192 O atoms. The lattice constants were set to a = 20.078 Å, b = 19.894 Å and c = 13.372 Å as in our previous studies [5, 6, 33]. The structure was fully relaxed until the atomic force is smaller than 0.02 eV Å^{-1}. The kinetic cut off energy was set to 400 eV. To assess the migration of $[Al(OH)_2]^+$, the migration barriers were investigated at the intersection. A framework Al site was set at T10 in 5-member ring to compensate the charge of the EFAl cation. At the intersection, $[Al(OH)_2]^+$ migrates from a position facing to a T7 site to one facing to a T11 site, and then to one close to a T12 site. The nudged elastic band (NEB)[34] method was used to calculate the transition state.

2.3 Results and discussion

2.3.1 n-hexane cracking

The interpretation of reaction rates when feeds are pulsed across a catalyst is different from that of the continuous flow reactor.[35, 36] The partial pressure of n-hexane exhibits a Gaussian peak, as shown in Figure S1, with the overall conversion used to measure the average activity of the catalysts. To more precisely reflect the rates for kinetic measurement purposes, the rate is reported as an averaged rate over the entire pulse, while the partial pressure is varied by modifying the concentration of n-hexane diluted in He in the loop. More details regarding the analysis of rate and activation energies in this reactor are provided in the Supplemental Information. No significant deactivation is observed over the course of the experiment under the conditions used in this study. The reaction order of the reaction at various temperatures on HZSM-5 catalysts is close to 1, shown in Figure 3, which along with the product distribution shown in Figure S2, suggests a monomolecular cracking mechanism in agreement with literature reports.[37] The ratios of alkanes/alkene deviate from unity due to the secondary reactions such as cracking of hexenes and pentenes, enhancing the selectivity to lighter alkenes.

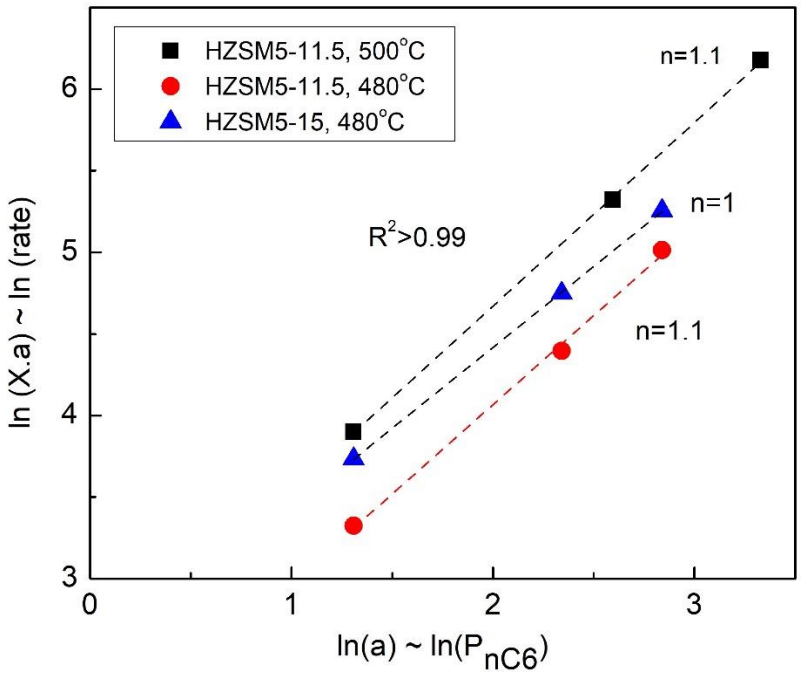

Figure 3. Determination of order of n-hexane cracking reaction, a is mole percent of n-hexane in the loop, X is the reaction conversion, see SI.

2.3.2 The role of acid site proximity and extra-framework aluminum

Figure 4 presents the catalytic activity per site of catalysts of various HZSM-5 catalysts. The discrepancy in turnover frequency values could be explained by the greater concentration of EFAL species, in the various catalysts. While prior reports have indicated that rates of alkane cracking over isolated BAS (I-BAS) are much lower when compared to those over synergistic sites (EFAL-BAS),[16] the activity observed is influenced by both. It is important to note that the conversion per mol_{BAS} is calculated by normalizing the activity per mass unit of the catalyst (% conv./mg) by the mole of Brønsted acid sites (mmol/g). Thus, activity enhancements beyond the value reported for the AHFS washed HZSM-5-15 (where the number represents the Si/Al ratio) catalyst reflects rate enhancements due to the presence of synergistic sites. HZSM5-140, HZSM5-40, and

HZSM5-15-AHFS catalysts have insignificant amounts of EFAL in their structure. As a result, the activity per site is comparable for each of these catalysts.

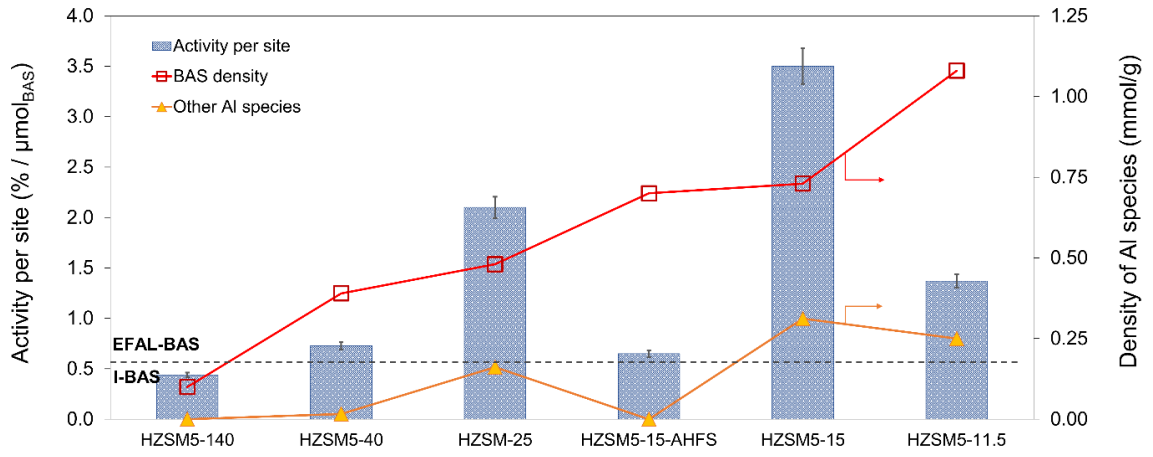

Figure 4. Conversion of n-hexane cracking per site on various HZSM-5 catalysts. Reaction condition: T = 480°C, PnC6 = 4.5 kPa with 0.48 µmol of n-hexane injected in each pulse, amount of catalysts varying to achieve conversions within 5-15%).

The activity per site of these catalysts should reflect the activity of isolated Brønsted sites. HZSM5-40 has slightly higher activity per site since it has a very small population of synergistic sites. The activity of HZSM5-140 is lower than that of HZSM5-15-AHFS, which could be attributed to the difference in either BAS density or distribution of acid sites in these two catalysts.[38, 39] Note that for all of the catalysts tested, those with a higher BAS density, such as HZSM5-25, HZSM5-15, and HZSM5-11.5, also exhibit a greater fraction of Al species that are not framework BAS in their structure. This suggests that BAS proximity and/or the EFAL density might play an important role in the activity enhancement. The parent HZSM5-15 and the AHFS washed HZSM5-15 catalyst to selectively remove EFAL species have the same framework Al density based on IPA TPD;

however, their catalytic activities are significantly different. This illustrates that acid site proximity or density alone cannot be responsible for the loss in activity of the AHFS washed HZSM5-15, which must be related to the absence of EFAL species. If the EFAL species is in the vicinity of a framework BAS, a synergistic site having higher activity could be generated. It is logical to assume that catalysts with higher BAS density will have more framework sites in close proximity and, therefore, a local charge that encourages interaction of EFAL cationic species in the vicinity of an adjacent BAS. As a result, higher initial site density (more sites in close proximity) should exhibit a greater potential for the formation of synergistic sites, given the presence of EFAL cationic species. This hypothesis is evidenced by the higher activity enhancement due to water treatment of higher density BAS catalysts, discussed in section 3.2. As previously stated, the activity is not only affected by the BAS density but also the presence of EFAL. The fact that activities of HZSM5-25 and HZSM5-15 are higher than that of HZSM5-11.5 could be explained by the higher fraction of EFAL over BAS leading to the higher possibility to create more BAS-EFAL synergistic sites in the parent zeolites. We acknowledge that the generation of synergistic sites might be affected by not only EFAL concentration but also the migration of EFAL species and the ability of zeolite structure to stabilize them in an environment necessary to create the synergistic sites. For instance, DFT calculations from Silaghi et al. suggest the thermodynamic stability of hydrated EFAL species depends highly on the local confining environment, with the channel intersections being the most preferred locations for EFAL cations.[40] Follow-up studies focusing on the form of EFAL species and other factors such as the number of paired sites and the location of the framework Al are needed in the future, as all of these may influence the formation of synergistic sites.

2.3.3 Water treatment by steaming and pulsing

The difference between the two methods. A clear distinction exists when subjecting a zeolite to the continuous partial pressure of steam vs. very small water pulses. This is clear by observing the discrepancy in BAS evolution and resulting activity for n-hexane cracking when the two methods are applied. Figure 5 presents the change in the activity during these two treatments.

a)

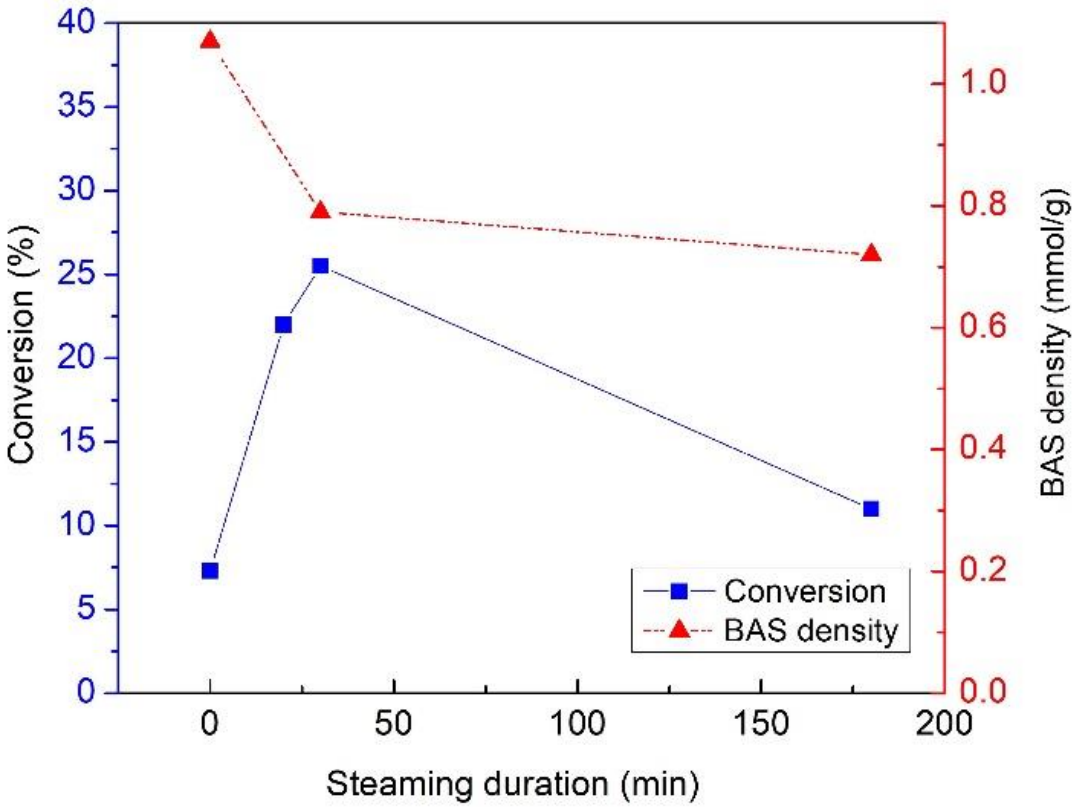

b)

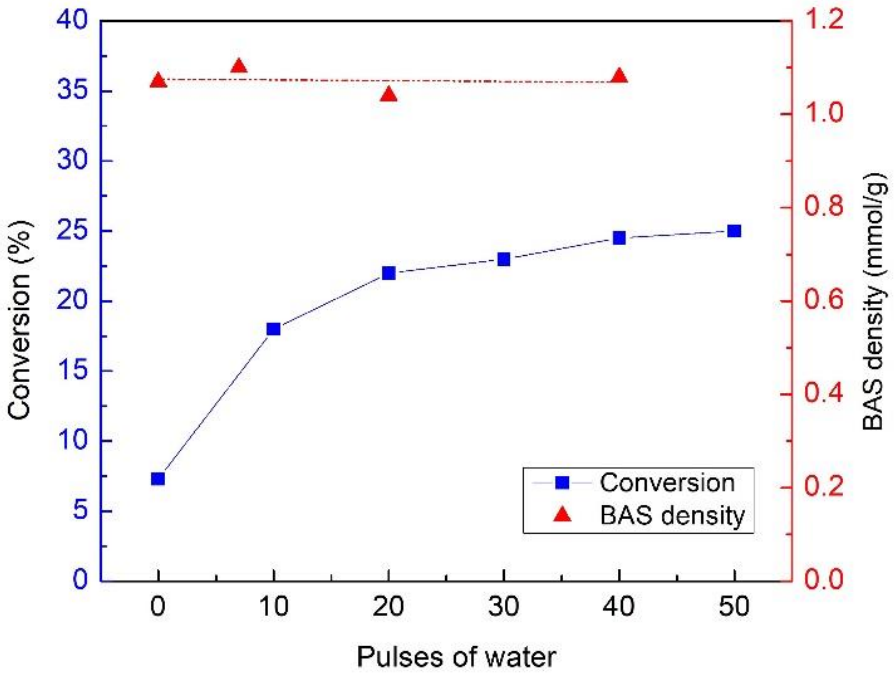

Figure 5. Conversion of n-hexane cracking on HZSM5-11.5 catalyst and BAS density (determined by IPA-TPD) as a function of a) steaming duration (catalyst was treated by steaming) and b) number of pulses of water (catalyst was treated by pulsing water). Steam treatment at 480°C in both cases, with a partial water pressure of 18.6 kPa either continuously or in the pulse. Reaction condition: T = 480°C, P_{nC6} = 4.5 kPa with 0.48 µmol of n-hexane injected in each pulse, 5 mg amount of catalyst. BAS density of HZSM5-11.5-0.5hS and HZSM5-11.5-3hS is 0.79 and 0.73 mmol/g. Diagram of pulse experiment was shown in Figure S4.

First, we discuss the implications of the cracking rate due to pulsing water. The catalysts were exposed to several pulses of 2.85 µmol of water spaced at 10 minutes intervals, followed by 3-10 hours of drying in He flow. The activities were measured by conducting

the reaction with pulses of n-hexane. Drying time depends on the number of pulses of water that catalysts were exposed to during the water treatment. The conversion of hexane cracking increases until the drying time is sufficient. When at least two continuous pulses of hexane gave the same conversion, the activity of catalyst were reported. BAS densities of the catalysts were measured via IPA TPD after exposing different batches of catalysts to 10, 20, and 40 pulses of water. HZSM5-11.5 catalyst treated by pulses of water does not show the loss of BAS sites, which is expected to be less significant in catalysts having lower BAS density. In addition, no significant changes in the product distribution and the order of the reaction are observed as the catalytic activity is modified by water treatment. To compare product selectivity at iso-conversion, higher loading of HZSM-5 in the absence of water treatment was compared with the catalysts after exposure to water pulses, and the product distributions of the two cases are not significantly altered, see Supplementary, Figure S2, S3. These results suggest that water treatment modifies the activity of the catalyst but not the mechanism of the reaction. Further, the lack of shift in selectivity when secondary reactions occur while clearly the activity within each crystallite is enhanced indicates that these results are not influenced by internal diffusion within the zeolite crystals.

Contrasting the pulsing results, catalysts were also exposed to steaming conditions where a consistent stream of water vapor at the same partial pressure as described in the pulse loop above was passed across the catalyst for prolonged times. After steaming, the catalyst was dried overnight prior to performing the n-hexane activity tests. In contrast to the pulsing techniques, the more common continuous steaming exhibited the enhancement of catalytic activity followed by a decrease at prolonged steam exposure, in good agreement

with prior observations in literature.[16, 41] Nitrogen absorption indicates that the surface areas of HZSM5-11.5 catalysts are comparable, ~ 345-353 m^2/g, shown in Table S1, which are comparable with the values in the previous work.[5] In addition, the XRD patterns of these samples shown in Figure 6 indicate that the crystallinity of the zeolites was not significantly altered due to water treatments.

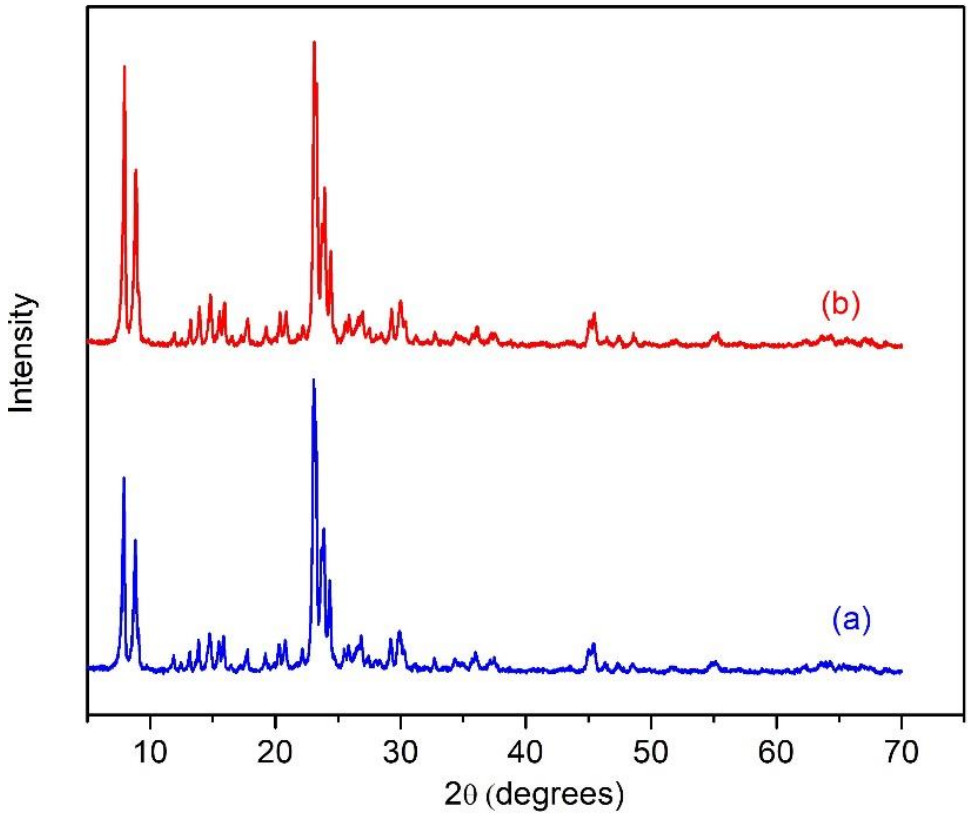

Figure 6. XRD patterns of (a) fresh HZSM5-11.5 and (b) HZSM5-11.5-3hS

The results also show that the activity of the catalyst is increased approximately 3-3.5 fold by both methods of treatment. In cases of pulsing water, the activity of the catalyst does not change after reaching the maximum, while in steaming, the activity passes through the maximum and declines quickly with prolonged steaming times. Since it was hypothesized

that the generation of synergistic sites increases the activity, it is likely that in the pulsing experiment, the catalytic activity will increase until the maximum number of the pair of Brønsted acid sites and active EFAL species in the structure is achieved. These sites are metastable species that remain for the duration of the pulse treatments. In contrast, when a continuous steam treatment is used, the number of Brønsted sites diminishes due to either dealumination or pore collapse. Further, extended steam treatments may eventually migrate these metastable synergistic sites to form Al_2O_3 clusters. The rate of these events depends on steaming time, partial water pressure, and the temperature of the treatment. The IPA-TPD results show that under the condition of steaming treatment in this study, Brønsted site density rapidly reduces after short steaming times, about 25% loss after 30 minutes, with a diminished rate of decline in BAS density with prolonged steaming times. A similar result was also observed in literature.[41]

Figure 7 illustrates ^{1}H MAS NMR spectra of parent HZSM5-11.5 catalyst, HZSM5-11.5 sample after exposure to 50 pulses of water, and two others with different steaming duration. The spectra show no significant modifications of the catalyst treated by pulsing water compared to the parent zeolites; therefore, the activity enhancement must be related to the mobility of EFAL species. Since the loss of BAS represented by the peak at 4.2 ppm is compensated by the generation of AlOH species other than the BAS species, both steaming samples, show increases in the peak corresponding to non-BAS AlOH species located at 2.8 ppm and 12-15 ppm compared to the ones of fresh catalysts. Recently, the appearance of these two signals in the ^{1}H NMR spectra of H-ZSM-5 catalysts at room temperature, along with other broad, poorly-resolved signals in the 5-7 ppm region, has been associated with Al-OH species that are best described as partially-coordinated

framework species based on high-field, multiple quantum, and solvent-treatment experiments.[6, 22, 42] Although these signals were previously attributed to framework/extra-framework interactions,[5] and have recently also been reported in H-FER catalysts,[43] more recent data indicate that in these particular catalysts before water exposure at high-temperature, there are no detectable amounts of EFAl,[44] or Al which can be assigned as trivalent Al.[45] However, these partially-coordinated species can be precursors to the generation of EFAl species after water exposure at high temperature,[40] which may then interact synergistically with existing framework sites through a variety of previously proposed mechanisms.[15, 46]

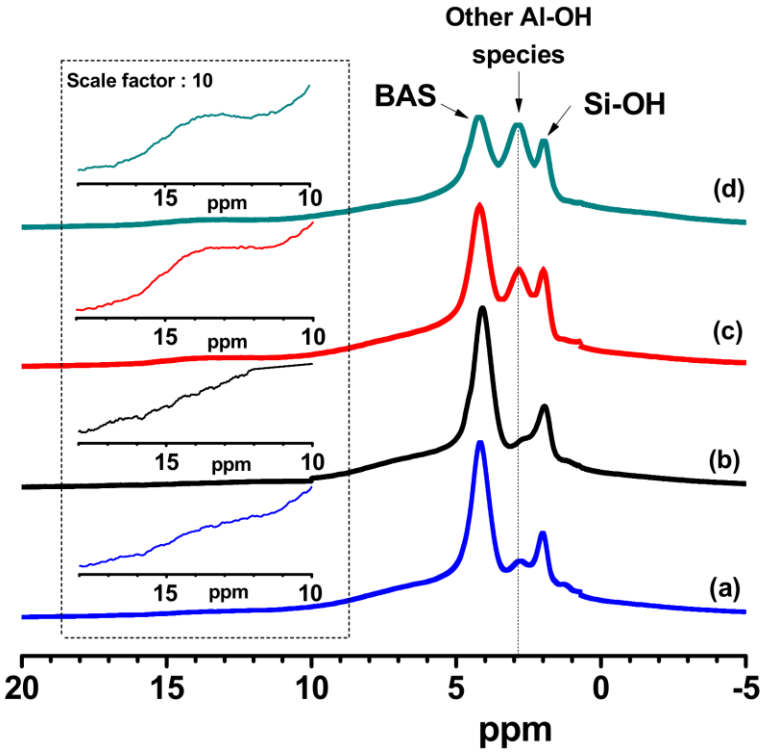

Figure 7. 1H MAS NMR spectra of HZSM5-11.5 after being exposed to 50 pulses of water (a); fresh HZSM5-11.5 (b), HZSM5-11.5 treated by steaming for 0.5 hour (c) and 3 hours (d).

As demonstrated here, the appearance of these signals in room-temperature catalyst spectra appears to correlate with activity differences for high-temperature reactions following exposure to water. It is noted that compared to the activity of 0.5 h steaming sample, a significant loss in activity was observed on 3 h steaming sample with a comparable loss of Brønsted sites. This indicates that the number of synergistic sites was reduced due to the loss of the Brønsted sites or/and active EFAL corresponding to these sites during steaming. Water may interact with and assist the mobility of EFAL species to form more stable Al_2O_3 clusters at longer steaming times.

Implications on catalytic activity by pulsing water. Since pulsing water does not lead to significant dealumination, which decreases the number of Brønsted acid sites and ultimately collapses the zeolite structure, this method is crucial to evaluate the change of catalytic activity by water vapor without convoluted effects of modified zeolite pores or collapse of the crystal. Figure 8 shows the change in reactivity of various HZSM-5 catalysts as a function of sequential pulses of water. It is observed that water pulses have the greatest positive influence on reactivity for HZSM5-11.5 and HZSM5-15, which have higher BAS density and a significant amount of AlOH species that are not from the framework BAS in their parent structure. In addition, HZSM5-15 and HZSM5-15-AHFS have the same BAS density and the distribution of sites, but the only slight activity enhancement by the water treatment is observed on the catalyst HZSM5-15-AHFS where most of EFAL was removed. This evidence suggests that water interacts with existing EFAL species to create new sites with enhanced catalytic activity during the pulsing water treatments.

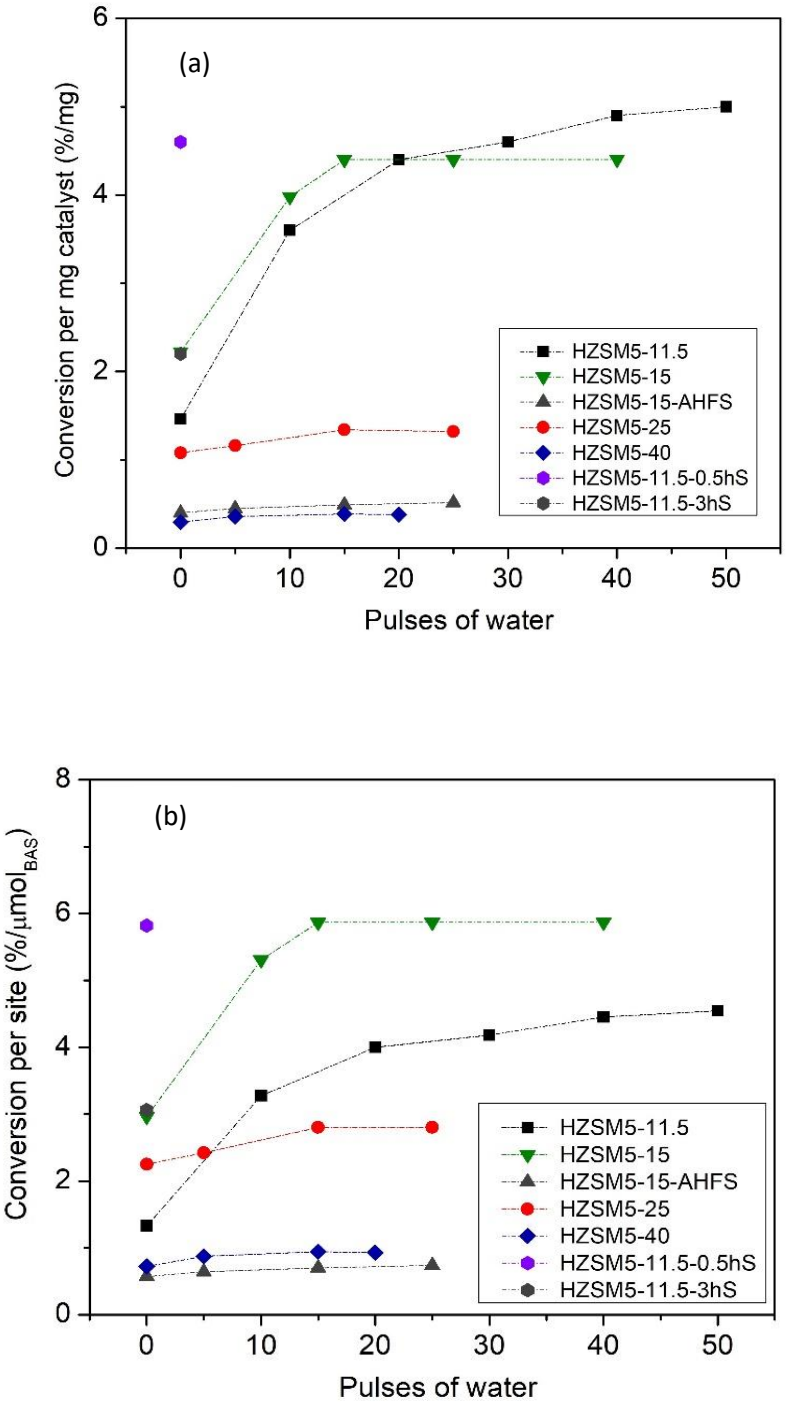

Figure 8. Conversion normalized by a) amount of utilized catalyst and b) number of molBAS of various HZSM-5 zeolites as a function of pulses of water treatment. Reaction

condition: T = 480°C, P_{nC6} = 4.5 kPa, amount of catalyst varying to achieve initial conversions within 5-15%). A Diagram of the pulse experiment is shown in Figure S3.

For the same reason, the low concentration of EFAL species in HZSM5-40 leads to a lower possibility to form the synergistic sites; therefore, we did not observe the significant rate enhancement in this catalyst under pulsing treatment. In the case of HZSM5- 25, we observed high activity in the parent zeolite while pulsing water treatment does not help to enhance the reactivity of this catalyst; although, the concentration of EFAL species and BAS density of this catalyst are relatively high. This leads us to a conclusion that other factors, such as the number of BAS-BAS pairs, the form of EFAL species, etc., likely play an essential role in the formation of synergistic sites.

In summary, under this condition of pulsing treatment, water does not lead to further dealumination of the zeolite framework but likely interacts with existing EFAL species to improve their migration rate. These EFAL species are possibly mobile until they are kinetically trapped at stable positions closed to BAS to form these synergistic sites. We know that severe steaming for longer times can facilitate further migration of EFAL species to form Al_2O_3 clusters but hypothesize that the steam contact time required for this degree of migration is far greater than that observed in these pulses. These sites are stable under the treatment condition, and the activity likely remains once it reaches the maximum. We hypothesize that the Brønsted/Brønsted pair sites might help to stabilize the EFAL species and kinetically trap these species.

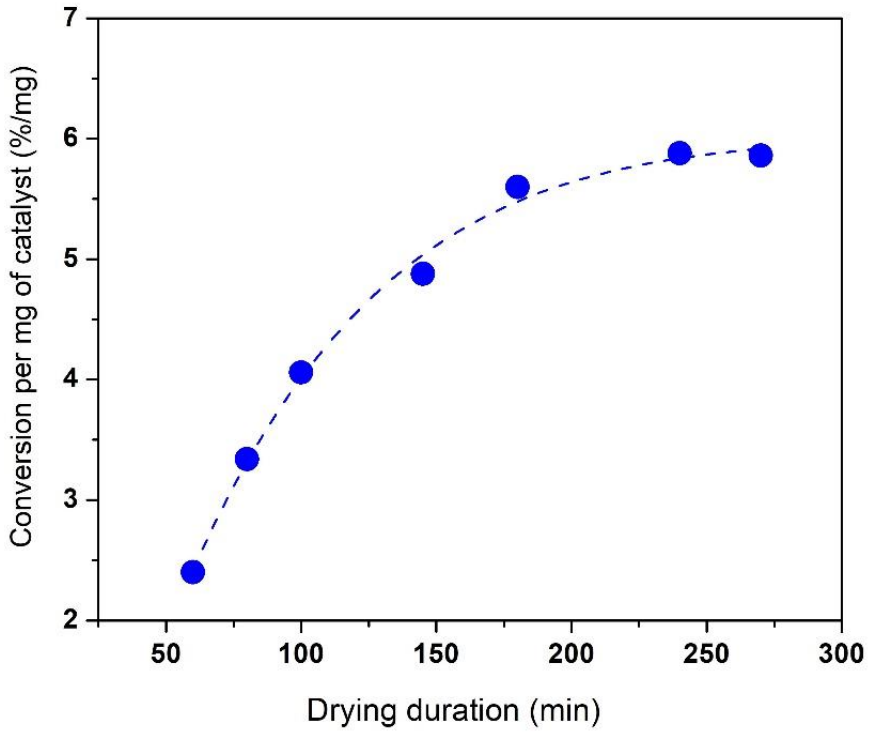

Figure 9. Effect of drying duration after catalyst HZSM5-11.5 was exposed to 50 sequential pulses of water. Water treatment condition: T = 480°C, water partial pressure as 18.6 kPa and 2.85 µmol of water in each pulse; cracking reaction condition: T = 480°C, P_{nC6} = 4.5 kPa with 0.48 µmol of n-hexane injected in each pulse, 5 mg of catalyst.

The strong inhibition of cracking rate is observed when the HZSM5-11.5 catalyst is exposed to 50 pulses of water shown in Figure 9. The catalyst is exposed to only 2.85 µmole of water in each pulse under high temperature, 480°C, and the contact time between the catalyst and water is very short in the pulsing treatment. However, the drying time to reach the maximum activity is up to 6 hours. Since the activity of synergistic sites is much higher compared to that of traditional sites, the change of activity is strongly affected by the number of these sites. This strong inhibition of the rate might be explained by the absorption of water on the synergistic sites or the interaction of water with EFAL species

belonging to these highly active sites. As the interconversion of various EFAL species happens inside zeolite in the presence of water,[47] water likely converts EFAL species into their "inactive" hydrated forms, possibly generating AlOH species. The dehydration of these species and removal of residual moisture requires a high energy barrier as evidenced by the prolonged needed thermo-treatment at high temperatures to recover activity. Note that it is difficult to decouple the dehydration of EFAL species with their migration during the drying process since we believe both happen concurrently. In the more severe condition of treatment like steaming, the measured activity might be significantly influenced by the presence of water. This might help to explain some of the contradicting claims in the literature regarding the catalytic role of created sites.

Table 2. Steaming conditon and the change of catalytic activity measured by converting n-hexane cracking of zeolite samples.

Sample	Conversion per site of fresh catalyst (%/μmol$_{BAS}$)	Steaming conditions			Conversion per mg catalyst (%/mg)	
		Duration [h]	Temperature [C]	Pressure [kPa]	Fresh zeolite	Steamed zeolite
HZSM5-40	0.73	4	480	10	0.29	0.51
HZSM5-15-AHFS	0.6	4	480	10	0.44	1.38
HZSM-22	0.45	10	480	10	0.14	0.14
		4	480	18.6	0.14	0.11 (*)
HZSM5-140	0.44	4	480	18.6	0.044	0.044

(*) BAS density of HZSM-22 after 4h steaming at 18.6 KPa of water vapor is 0.26 mmol/g.

Generating EFAL species by steaming.

Dealumination leading to the generation of additional EFAL can occur under continuous steaming conditions. Table 2 lists the steaming conditions investigated for several catalysts that exhibit no activity enhancement by simply pulsing water. The partial water pressure used in the steaming treatments shown in Table 2 was lower when compared to the conditions used in the pulsing treatment to minimize the rate of modification to the framework.

Considering an alternative framework of TON, HZSM-22, with exhibits 10 membered rings without the intersections present in HZSM-5 catalysts, the influence of site location may be evaluated. It should be noted that while HZSM-22 exhibits the same number of T sites per ring, the shape of the opening is mildly compressed, so while confinement effects induced by MFI straight or zig-zag channels cannot be compared exactly, it does serve as a surrogate to determine the influence that confinement in general plays on these rates. Interestingly, the rate per BAS for the fresh HZSM-22 catalyst is comparable to that observed over HZSM5 with a Si/Al ratio of 140, where we would anticipate the majority of active sites are present in the channel intersections.[39] Further, higher steam partial pressures were required to significantly create EFAL sites in the HZSM-22 catalyst. Interestingly, the rate per proton did not vary, indicating both that the reaction appears to not be influenced by internal diffusion, and that the local environment of the EFAL species alone does not influence the rate in catalysts with low framework Al density. Rather, it reinforces the concept that framework sites in close proximity are required to generate these synergistic active sites.

Another interesting yet expected observation is the correlation between framework site density and the resulting rate of dealumination. This is most pronounced for the Si/Al 140 MFI catalyst, where no significant reduction in BAS density is observed after steam treatment that is far more severe than the MFI catalysts with higher site densities were exposed to. This is in line with the diminished rate of BAS loss with prolonged steaming time as the framework acid site density decreases with time as shown in Figure 5 and in agreement with general practices for other zeolite families, such as USY zeolites commonly employed for catalytic cracking.

2.3.4 Estimation of activity and number of active acid sites

The rate and activation energy associated with synergistic sites can be calculated based on the observed n-hexane cracking activity. This is accomplished by simply estimating the activity per isolated Brønsted acid sites and determining the activity resulting from a synergistic active site. This is accomplished by the following:

$\bar{X}_{total}$, $\bar{X}_{\text{I-BAS}}$, $\bar{X}_{\text{EFAL-BAS}}$: conversion associated with each site per mg catalyst (% per mg)

$X'_{\text{I-BAS}}$, $X'_{\text{EFAL-BAS}}$: conversion per site (% per µmol)

$N_{\text{BAS-total}}$, $N_{\text{I-BAS}}$, $N_{\text{EFAL-BAS}}$: the number of total Brønsted sites, isolated Brønsted sites and synergistic sites per mg, respectively (mmol per g).

$$\bar{X}_{total} = \bar{X}_{I-BAS} + \bar{X}_{EFAL-BAS} = N_{I-BAS}.X'_{I-BAS} + N_{EFAL-BAS}.X'_{EFAL-BAS} \quad \text{Eqs.(1)}$$

$$\bar{X}_{total} = (N_{BAS-total} - N_{EFAL-BAS})\,X'_{I-BAS} + N_{EFAL-BAS}.X'_{EFAL-BAS}$$

Since the activity of a synergistic site is much higher than an isolated BAS ($X'_{\text{EFAL-BAS}}/X'_{\text{I-BAS}} = 52\pm2$, reported by Zhang et al.[16]) and the fraction of EFAL-BAS sites is small,

the term $X'_{I\text{-}BAS} \times N_{EFAL\text{-}BAS}$ is negligible. The conversion attributed to the synergistic sites can be calculated from Eqs. (1) as:

$$\bar{X}_{EFAL-BAS} = N_{EFAL-BAS}.X'_{EFAL-BAS} = \bar{X}_{total} - N_{BAS-total}.X'_{I-BAS} \quad \text{Eqs. (2)}$$

In which, $X'_{I\text{-}BAS}$ was determined by the conversion per micro mol BAS site on HZSM5-15-AHFS at corresponding reaction temperature. Assuming that the activity of synergistic sites in all HZSM-5 catalysts is similar, the value $\bar{X}_{EFAL\text{-}BAS}$ is proportional to the number of these sites in catalysts and represents the rate of reaction corresponding to the synergistic sites.

^{1}H MAS NMR might be utilized to determine the number of different proton species. HZSM5-15 and HZSM5-15-AHFS catalysts in this section are identical to the ones used by Chen et al.[5] Table S2 lists the distribution of H species from ^{1}H MAS NMR of two catalyst samples adapted from that study. Assumed that the 12-15 ppm peak correspond to the synergistic sites,[5] the number of synergistic sites in HZSM5-15, $N_{EFAL\text{-}BAS}$, is estimated as 0.059 mmole/g. At 480°C, $X'_{I\text{-}BAS}$ = 0.6 % per μmol was estimated by the conversion of reaction on HZSM5-15-AHFS and the value of activity on the synergistic sites, $X'_{EFAL\text{-}BAS}$, estimated from Eqs. (1) is 32.2 % per μmol. Once the values of $X'_{I\text{-}BAS}$, $X'_{EFAL\text{-}BAS}$ and $\bar{X}_{total}$ were known at 480°C, the number of synergistic sites of given catalyst can be calculated by Eqs. (1). We note that quantifying of the small number of synergistic sites can be challenging, especially for the samples after exposing to water treatment. Any uncertainty in this number due to additional species overlapping within the 12-15ppm peak, could result in mild overestimations in site counting. Similarly, any additional peaks that are not considered here some have proposed to also correlate with synergistic sites could lead to underestimations in site counting. Regardless, the number of

sites is a small fraction of the total Brønsted sites present in the zeolite, and critically for this exercise the activation energy values attributed to these sites, as well as to their creation will still be accurate.

2.3.5 Activation energy of n-hexane cracking reaction

The turnover rates of the first order reaction at low coverage are given by:

$$rate = k_{int}\, C_{A(z)} = k_{int}\, K_{ads} P_A \;=\; k_{meas} P_A$$

with $C_{A(z)}$ indicating the surface concentration of adsorbed alkanes.

The intrinsic activation energies (E_{int}) can be calculated from these measured activation energies (E_{meas}) and the enthalpies of adsorption as following:

$$E_{meas} = E_{int} + \Delta H_{ads}$$

Since the rate of reaction is proportional to the conversion of the pulse, the Arrhenius plots of the natural logarithm of conversion of reaction as a function of inverse temperature are reported to determine the activation energy of the n-hexane cracking on synergistic sites and isolated sites (Figure 10). The activation energy of ~110 kJ/mol was measured on isolated BAS sites utilizing catalysts with an insignificant number of synergistic sites HZSM5-15-AHFS, HZSM5-40 and HZSM5-140. This barrier is comparable to those reported in reported in previous work.[48, 49] Meanwhile, the rate attributed to synergistic sites was calculated by subtracting the rate observed at different temperatures corresponding to isolated sites (Eqs.(2)).

a)

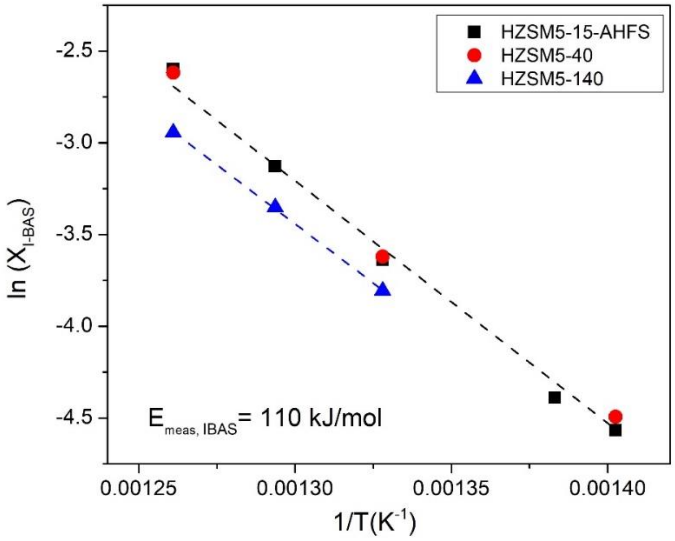

b)

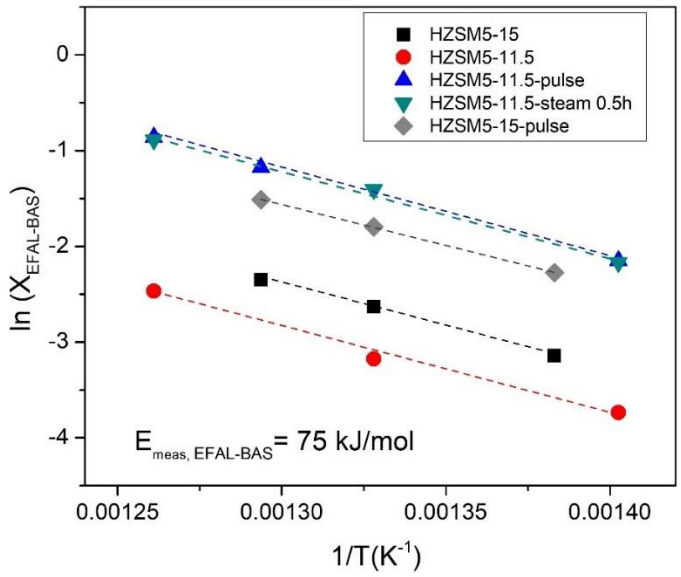

Figure 10. Arrhenius plot of depicting conversion versus inverse temperature on a) isolated Brønsted acid sites and b) synergistic EFAL-BAS sites. Reaction condition: T = 480°C, P_{nC6} = 4.5 kPa, amount of catalysts varying to achieve conversions within 5-15%).

Remarkably, regardless of the Si/Al ratio or subsequent treatments employed, the apparent energy barrier observed over the synergistic sites was quite similar, ~ 75 kJ/mol. The results show that the enhancement in activity is due to the increase in the number of generated active sites while the intrinsic activity of the synergistic site is not altered. This identical observed barrier also suggests that the reaction is not limited by internal or external diffusion mass transfer regime even at the high rate per catalyst particle. Iglesia and others have attributed activity enhancements to modifications to the local confining environment surrounding the active site for a variety of reactions.[19, 50] In this particular case, an EFAL species in proximity to a framework Brønsted site may modify the local confinement of the transition state. Regardless of the nature of activity enhancement, by stabilization of kinetically relevant transition states or by enhancing adsorption of reactive intermediates, the nature of the enhanced sites to lower the apparent enthalpy of reaction appears to be consistent across a wide range of catalysts studied. Alternative proposals, such as the suggestion that enhancements due to synergistic sites are simply due to modifications in transition state entropies [16] appear to not fully explain the behavior observed here for this reaction in question, as a clear shift in apparent activation enthalpy is observed. Further studies are necessary to determine how EFAL species manipulate the adsorbed intermediates and transition states leading to these remarkable rate enhancements.

2.3.6 Activation energy of generation of synergistic sites

Prior to inferring site generation details, we clarify our hypothesis regarding the nature of the synergistic sites in question. Many arguments have been made regarding the nature of active sites within zeolite pores. These arguments are confounded by the fact that certain surface features may be highly active for specific reactions of interest. All arguments proposed here correlate with sites responsible for n-alkane cracking. Differences in activity have been reported for various T site locations within MFI crystals, such as within intersections vs. pore channels, for some families of reactions.[20] In the cases reported here for n-alkane activation, however, activity enhancements are observed without perturbing total site density. Sites responsible for observed rate enhancements cannot be due to modifications in T site location, but migration of more mobile species. We have also reported previously the intriguing role of partially coordinated species for more facile reactions.[6] It is important to note here that, while partially coordinated sites are likely responsible for some chemistry, their presence can shift based on interaction with heteroatoms such as moisture, and some have speculated that at the high temperatures required for more demanding hydrocarbon chemistry these features may no longer exist. [23, 24] Supportive of such an argument is the fact that the synergistic active sites in question here are only apparent after extended drying periods at elevated conditions (Figure 9). Furthermore, if these sites are created in HZSM5-15 parent during pulsing water treatment, they should be formed in AHFS washed HZSM5-15 catalyst, too. However, the fact that we did not observe the rate enhancement when exposing AHFS washed HZSM5-15 catalyst to pulses of water suggests that the partially coordinated sites, if being formed under that condition, are not responsible for the reaction rate enhancement. Further, the

barrier that was quantified for the creation of these sites is more typical of EFAl migration than framework hydrolysis, which generally requires much larger activation energies.[40] We are careful to note, however, that these partial coordinated may be precursors to the extra lattice species required for alkane cracking rate enhancements. Therefore, we hypothesize that the role of water under these conditions is simply to accelerate the formation of these synergistic sites via migration of existing extra framework species, and the pulse reactor employed here allows direct quantification of activation barriers associated with this migration.

To estimate the energy barrier of this process, the activity of various HZSM-5-11.5 samples after treatment at different temperatures is measured while the partial pressure of water in the pulse, residence time, and all other conditions remain constant. A significant number of 40 pulses of water with a break of 10 minutes in intervals between pulses was utilized in all cases to observe significant differences in the activity for the treated catalysts. After water treatment, the temperature of the reactor is raised to 480°C to dry catalysts for 10 hours and we carry out n-hexane cracking reaction to test the activity of the catalyst. The conversion of this reaction is utilized to estimate the activity of active sites. The activation energy of the generation of synergistic sites as shown in Figure 11 is 44 kJ/mol corresponding to the rate of new synergistic site generation as discussed above. This value is comparable with the energy barrier of the stepwise immigration of partially dehydrated $[Al(OH)_2]^+$ cation along the super cage in Faujasite zeolite estimated by DFT.[47] In addition, this barrier is significantly lower than predicted barriers reported for dealumination of a framework site. A relatively high energy barrier, E_{act} = 190 kJ/mol has been reported for dealumination of HZSM-5 zeolites by Silaghi et al. [40]

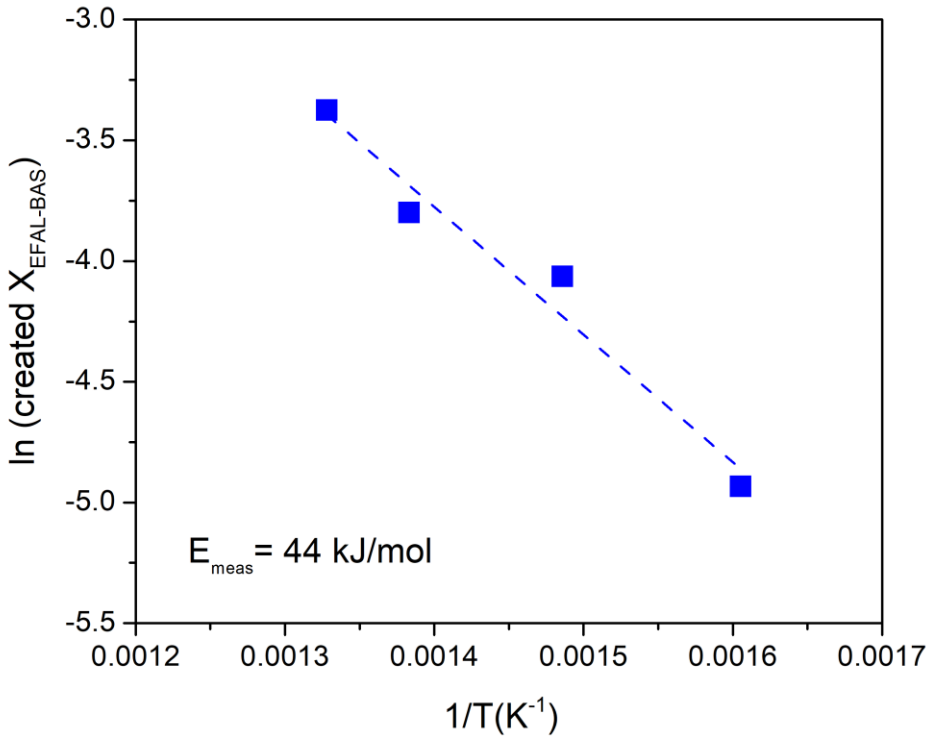

Figure 11. Arrhenius plot of depicting conversion by created synergistic site versus inverse water treatment temperature on HZSM5-11.5.

The migration of $[Al(OH)_2]^+$ to a further location that is away from the framework Al by one more unit of -O-Si-O- is endothermic by 29 - 36 kJ/mol with an activation barrier of 44 - 47 kJ/mol. In other words, for $[Al(OH)_2]^+$ that is further away from the framework Al, there is a driving force for it to migrate toward the framework Al due to the enhanced stability, with an moderate activation barrier of 9 - 18 kJ/mol. We also tested $[Al(OH)_2]^+$ migration in the sinusoidal channel. We intentionally position $[Al(OH)_2]^+$ far from the framework Al to reduce the effect of the electrostatic interaction. We find the migration of $[Al(OH)_2]^+$ from a location close to a T12 site to one close to a T3 site in the sinusoidal channel is a thermodynamically neutral process (ΔE = 2 kJ/mol) and the calculated

activation energy is 23 kJ/mol. These calculations thus suggest the migration of the EFAL cation is moderate and this migration dynamics is driven toward the framework Al, with barriers associated with migration away from local minima to more preferentially stabilized locations, likely pairs of sites, corresponding to barriers consistent with those observed experimentally.

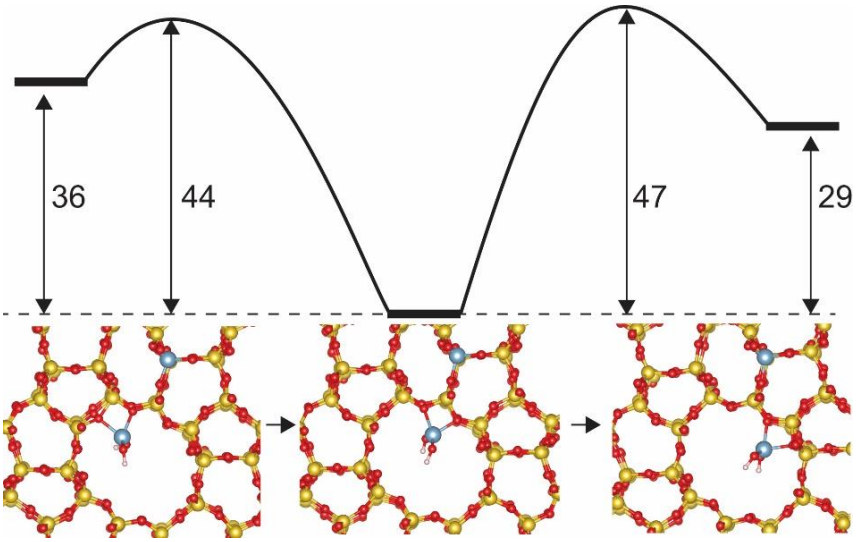

Figure 12. DFT calculations of Al(OH)2+ migration at the intersection of HZSM-5. One framework Al was introduced to balance the charge. The Al, Si, O and H atoms are colored blue, yellow, red and white, respectively. The units in the energy profile is kJ/mol.

2.4 Conclusion

The use of a micropulse reactor to decouple EFAL migration from framework hydrolysis is a revealing way to evaluate the creation of new sites with enhanced activity. The various micropulse treatment conditions employed and further evaluated for n-hexane cracking over HZSM-5 zeolites when contrasted with continuous steam treatments illustrates the important role of water is not only site generation through hydrolysis but also the subsequent Al migration to form metastable synergistic sites prior to Al_2O_3 cluster

formation. During continuous steaming, dealumination converts framework aluminum to EFAL species, which is helpful for enhancing the catalytic activity of the catalyst having low BAS density or low concentration of EFAL species. The activity of catalyst having lower BAS density such as HZSM5-140 could not be enhanced under the treatment condition by both methods, indicating that not only the presence of EFAL is important, but also the density of framework sites. We hypothesize that this is necessary to stabilize EFAL species in the proximity of an adjacent BAS to create the synergistic sites. The micropulse experiments suggest that water enhances the mobility of EFAL species to create synergistic sites. By quantifying strong BAS density as well as n-hexane cracking activity per site, the activation energy associated with the newly created sites, as well as the rate of their creation can be quantified and distinguished from framework dealumination. The apparent activation energy of hexane cracking over synergistic sites is ~75 kJ/mol across all catalysts studied, which is significantly lower than the barrier observed over traditional BAS, ~ 110 kJ/mol. In addition, the energy barrier associated with the creation of new synergistic sites in the presence of water pulses, or the migration of Al, was found to be 44 kJ/mol, far lower than the barrier required for framework dealumination but an essential step for further activity enhancement of cracking activity.

Supporting Information

Determination of the order of the reaction

The rate of n-hexane conversion in the pulse reactor was calculated as the following:

$$rate = \frac{X \times N(nC6)}{W * \tau} = k \times (P_{nC6})^n$$

$$ln(X \times N(0) \times a) + A = B + n \times ln\,(a)$$

$$ln(X \times a) = C + n \times ln\,(a)$$

In which,

P_{nC6} (kPa): partial pressure of n-hexane

W (mg): weight of catalyst

τ (s): contact time of reactant and catalyst

a (%): mole percent of n-hexane in the loop

N(nC6) (mol): mole of n-hexane in the loop

N(0) (mol) : total mole in the loop including He and n-hexane

X (%): conversion of the reaction

A, B, C: constants

Thus, the plot of ln (X × a) vs. ln (a) was used to determine the order of the n-hexane cracking reaction instead of the plot of ln(rate) versus ln (P_{nC6}).

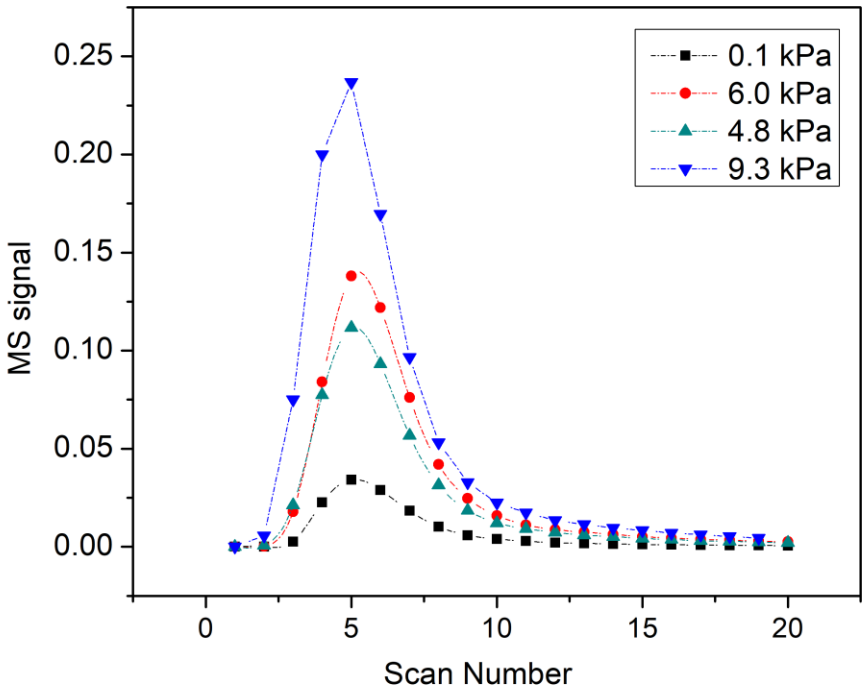

Figure S1. The shape of the pulses with different partial pressure of n-hexane

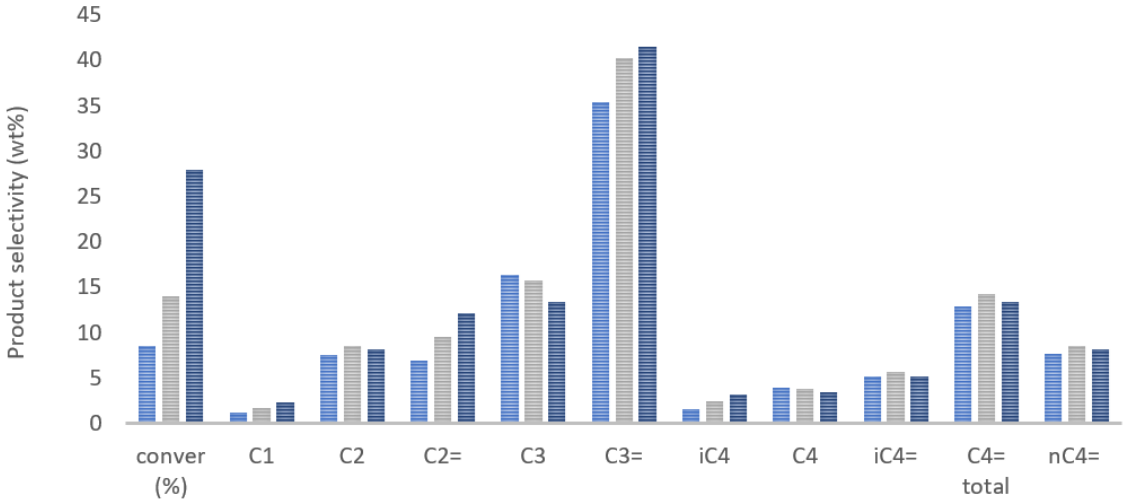

Figure S2. Product distribution as function of conversion level of n-hexane cracking reaction on HZSM5- 11.5 zeolite

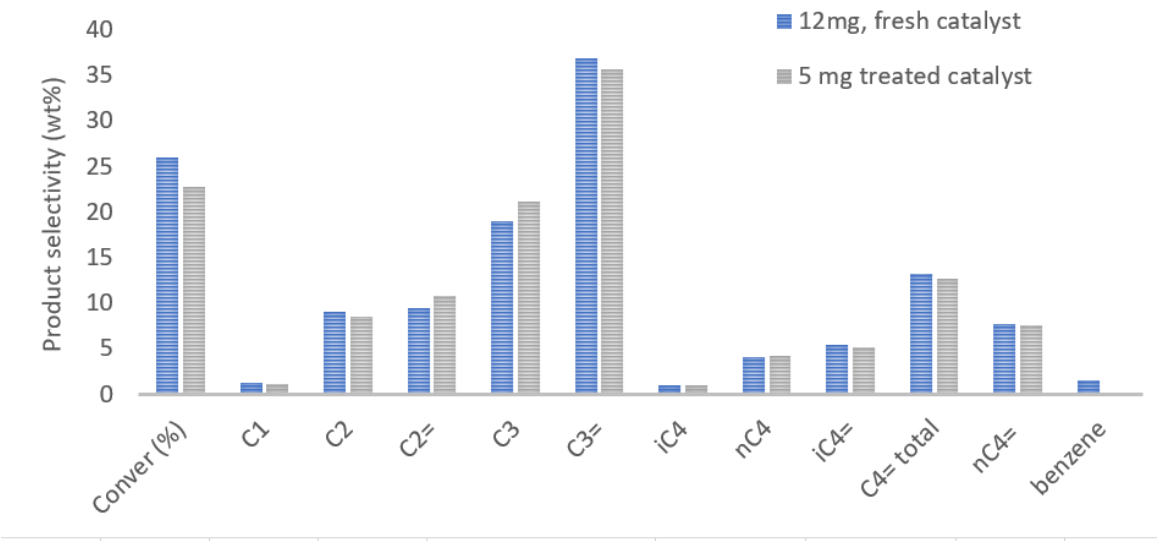

Figure S3. Product distribution of n-hexane cracking reaction on HZSM5- 11.5 zeolite at the same level of conversion

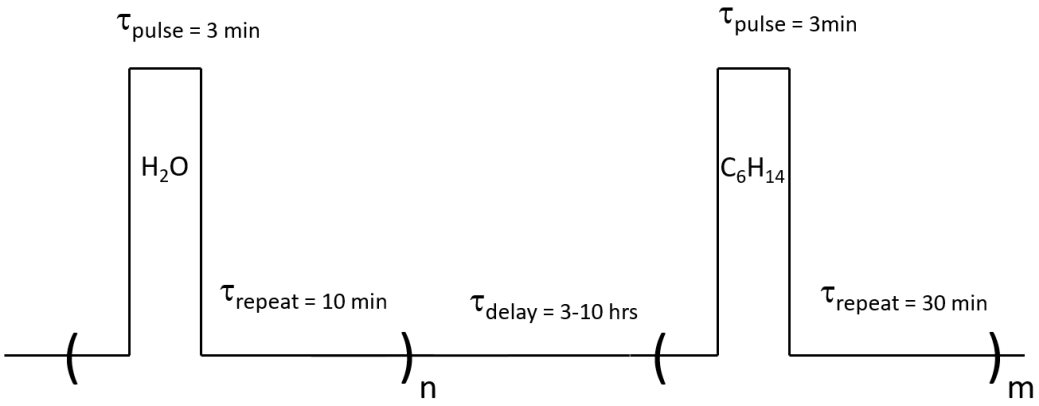

Figure S4. Diagram of pulse experiment

Table S1. Surface area and pore volume of ZSM5-11.5 samples

Catalyst	BET (m^2/g)	Pore Volume (cm^3/g)	Micropore Volume (cm^3/g)
HZSM5-11.5	353.4	0.1786	0.1276
HZSM5-11.5-0.5h S	353.1	0.1826	0.1210
HZSM5-11.5-3h S	344.8	0.1683	0.1203

Table S2. Distribution of specices from H MAS NMR spectra of the HZSM-5 catalysts.[5]

Catalyst	SiOH	H-EFAL	H-EFAL/ Nonxtal	H-EFAL	BAS
	1.9 ppm	2.8 ppm	5-7 ppm	12-15 ppm	4.2 ppm
HZSM5-15	0.18±0.01	0.09±0.01	0.45±0.037	0.059±0.0025	0.56±0.018
HZSM5-15-AHFS	0.20±0.01	0.03±0.003	0.28±0.019	0	0.54±0.02

Unit: mmole/g

REFERENCES

1. Derouane, E. G.; Andre, J.-M.; Lucas, A. A., Surface curvature effects in physisorption and catalysis by microporous solids and molecular sieves. *Journal of Catalysis* **1988,** *110* (1), 58-73.

2. Noh, G.; Shi, Z.; Zones, S. I.; Iglesia, E., Isomerization and β-scission reactions of alkanes on bifunctional metal-acid catalysts: Consequences of confinement and diffusional constraints on reactivity and selectivity. *Journal of Catalysis* **2018,** *368*, 389-410.

3. Gorte, R. J.; Crossley, S. P., A perspective on catalysis in solid acids. *Journal of Catalysis* **2019,** *375*, 524-530.

4. Crossley, S. P.; Resasco, D. E.; Haller, G. L., Clarifying the multiple roles of confinement in zeolites: From stabilization of transition states to modification of internal diffusion rates. *Journal of Catalysis* **2019,** *372*, 382-387.

5. Chen, K.; Abdolrahmani, M.; Horstmeier, S.; Pham, T. N.; Nguyen, V. T.; Zeets, M.; Wang, B.; Crossley, S.; White, J. L., Brønsted–Brønsted Synergies between Framework and Noncrystalline Protons in Zeolite H-ZSM-5. *ACS Catalysis* **2019**, 6124-6136.

6. Chen, K.; Horstmeier, S.; Nguyen, V. T.; Wang, B.; Crossley, S. P.; Pham, T.; Gan, Z.; Hung, I.; White, J. L., Structure and Catalytic Characterization of a Second Framework Al(IV) Site in Zeolite Catalysts Revealed by NMR at 35.2 T. *Journal of the American Chemical Society* **2020,** *142* (16), 7514-7523.

7. Kung, H. H.; Williams, B. A.; Babitz, S. M.; Miller, J. T.; Haag, W. O.; Snurr, R. Q., Enhanced hydrocarbon cracking activity of Y zeolites. *Topics in Catalysis* **2000,** *10* (1), 59-64.

8. Werner O. Haag, L., N.J.; Rudolph M. Lago, Yardley, Pa. Enhancement of zeolite catalytic acivity. 1982.

9. Masuda, T.; Fujikata, Y.; Mukai, S. R.; Hashimoto, K., Changes in catalytic activity of MFI-type zeolites caused by dealumination in a steam atmosphere. *Applied Catalysis A: General* **1998,** *172* (1), 73-83.

10. Ristanović, Z.; Hofmann, J. P.; De Cremer, G.; Kubarev, A. V.; Rohnke, M.; Meirer, F.; Hofkens, J.; Roeffaers, M. B. J.; Weckhuysen, B. M., Quantitative 3D Fluorescence Imaging of Single Catalytic Turnovers Reveals Spatiotemporal Gradients in Reactivity of Zeolite H-ZSM-5 Crystals upon Steaming. *Journal of the American Chemical Society* **2015,** *137* (20), 6559-6568.

11. Niwa, M.; Sota, S.; Katada, N., Strong Brønsted acid site in HZSM-5 created by mild steaming. *Catalysis Today* **2012,** *185* (1), 17-24.

12. van Bokhoven, J. A.; Tromp, M.; Koningsberger, D. C.; Miller, J. T.; Pieterse, J. A. Z.; Lercher, J. A.; Williams, B. A.; Kung, H. H., An Explanation for the Enhanced Activity for Light Alkane Conversion in Mildly Steam Dealuminated Mordenite: The Dominant Role of Adsorption. *Journal of Catalysis* **2001,** *202* (1), 129-140.

13. Zholobenko, V. L.; Kustov, L. M.; Kazansky, V. B.; Loeffler, E.; Lohser, U.; Peuker, C.; Oehlmann, G., On the possible nature of sites responsible for the enhancement of cracking activity of HZSM-5 zeolites dealuminated under mild steaming conditions. *Zeolites* **1990,** *10* (4), 304-306.

14. Schallmoser, S.; Ikuno, T.; Wagenhofer, M. F.; Kolvenbach, R.; Haller, G. L.; Sanchez-Sanchez, M.; Lercher, J. A., Impact of the local environment of Brønsted acid

sites in ZSM-5 on the catalytic activity in n-pentane cracking. *Journal of Catalysis* **2014,** *316*, 93-102.

15. Li, S.; Zheng, A.; Su, Y.; Zhang, H.; Chen, L.; Yang, J.; Ye, C.; Deng, F., Brønsted/Lewis Acid Synergy in Dealuminated HY Zeolite: A Combined Solid-State NMR and Theoretical Calculation Study. *Journal of the American Chemical Society* **2007,** *129* (36), 11161-11171.

16. Zhang, Y.; Zhao, R.; Sanchez-Sanchez, M.; Haller, G. L.; Hu, J.; Bermejo-Deval, R.; Liu, Y.; Lercher, J. A., Promotion of protolytic pentane conversion on H-MFI zeolite by proximity of extra-framework aluminum oxide and Brønsted acid sites. *Journal of Catalysis* **2019,** *370*, 424-433.

17. Maier, S. M.; Jentys, A.; Lercher, J. A., Steaming of Zeolite BEA and Its Effect on Acidity: A Comparative NMR and IR Spectroscopic Study. *The Journal of Physical Chemistry C* **2011,** *115* (16), 8005-8013.

18. Gounder, R.; Jones, A. J.; Carr, R. T.; Iglesia, E., Solvation and acid strength effects on catalysis by faujasite zeolites. *Journal of Catalysis* **2012,** *286*, 214-223.

19. Gounder, R.; Iglesia, E., The catalytic diversity of zeolites: confinement and solvation effects within voids of molecular dimensions. *Chemical Communications* **2013,** *49* (34), 3491-3509.

20. Jones, A. J.; Iglesia, E., The Strength of Brønsted Acid Sites in Microporous Aluminosilicates. *ACS Catalysis* **2015,** *5* (10), 5741-5755.

21. Abdolrahmani, M.; Chen, K.; White, J. L., Assessment, Control, and Impact of Brønsted Acid Site Heterogeneity in Zeolite HZSM-5. *The Journal of Physical Chemistry C* **2018,** *122* (27), 15520-15528.

22. Chen, K.; Abdolrhamani, M.; Sheets, E.; Freeman, J.; Ward, G.; White, J. L., Direct Detection of Multiple Acidic Proton Sites in Zeolite HZSM-5. *Journal of the American Chemical Society* **2017,** *139* (51), 18698-18704.

23. Omegna, A.; Prins, R.; van Bokhoven, J. A., Effect of Temperature on Aluminum Coordination in Zeolites H−Y and H−USY and Amorphous Silica−Alumina: An in Situ Al K Edge XANES Study. *The Journal of Physical Chemistry B* **2005,** *109* (19), 9280-9283.

24. Omegna, A.; Bokhoven, J. A. v.; Prins, R., Flexible Aluminum Coordination in Alumino-Silicates. Structure of Zeolite H-USY and Amorphous Silica-Alumina. *The Journal of Physical Chemistry B* **2003,** *107*, 8854-8860.

25. Garralón, G.; Fornés, V.; Corma, A., Faujasites dealuminated with ammonium hexafluorosilicate: Variables affecting the method of preparation. *Zeolites* **1988,** *8* (4), 268-272.

26. Wan, S.; Waters, C.; Stevens, A.; Gumidyala, A.; Jentoft, R.; Lobban, L.; Resasco, D.; Mallinson, R.; Crossley, S., Decoupling HZSM-5 Catalyst Activity from Deactivation during Upgrading of Pyrolysis Oil Vapors. *ChemSusChem* **2015,** *8* (3), 552-559.

27. Abdelrahman, O. A.; Vinter, K. P.; Ren, L.; Xu, D.; Gorte, R. J.; Tsapatsis, M.; Dauenhauer, P. J., Simple quantification of zeolite acid site density by reactive gas chromatography. *Catalysis Science & Technology* **2017,** *7* (17), 3831-3841.

28. Kresse, G.; Furthmuller, J., Efficient iterative schemes for ab initio total-energy calculations using a plane-wave basis set. *Phys Rev B* **1996,** *54* (16), 11169-11186.

29. Kresse, G.; Joubert, D., From ultrasoft pseudopotentials to the projector augmented-wave method. *Phys Rev B* **1999,** *59* (3), 1758-1775.

30. Blochl, P. E., Projector Augmented-Wave Method. *Phys Rev B* **1994,** *50* (24), 17953-17979.

31. Perdew, J. P.; Burke, K.; Ernzerhof, M., Generalized gradient approximation made simple. *Phys Rev Lett* **1996,** *77* (18), 3865-3868.

32. Grimme, S.; Antony, J.; Ehrlich, S.; Krieg, H., A consistent and accurate ab initio parametrization of density functional dispersion correction (DFT-D) for the 94 elements H-Pu. *J Chem Phys* **2010,** *132* (15), 154104.

33. Zeets, M.; Resasco, D. E.; Wang, B., Enhanced chemical activity and wettability at adjacent Brønsted acid sites in HZSM-5. *Catalysis Today* **2018,** *312*, 44-50.

34. Henkelman, G.; Uberuaga, B. P.; Jonsson, H., A climbing image nudged elastic band method for finding saddle points and minimum energy paths. *J Chem Phys* **2000,** *113* (22), 9901-9904.

35. A. M. Sica, E. M. V., C. E. Gigola, Kinetic Data form a Pulse Microcatalytic Reactor-Hydrogenation of Benzene on a Nickel Catalyst. *Journal of Catalysis 51*, 115-125.

36. Attar, A., Pulsed differential reactors and their use for kinetic studies of gas–solid reactions—application to mechanistic studies of the reactions of hydrogen sulfide and the alkaline minerals in coal. *Review of Scientific Instruments* **1979,** *50* (1), 111-117.

37. Babitz, S. M.; Williams, B. A.; Miller, J. T.; Snurr, R. Q.; Haag, W. O.; Kung, H. H., Monomolecular cracking of n-hexane on Y, MOR, and ZSM-5 zeolites. *Applied Catalysis A: General* **1999,** *179* (1), 71-86.

38. Janda, A.; Bell, A. T., Effects of Si/Al Ratio on the Distribution of Framework Al and on the Rates of Alkane Monomolecular Cracking and Dehydrogenation in H-MFI. *Journal of the American Chemical Society* **2013,** *135* (51), 19193-19207.

39. Jones, A. J.; Carr, R. T.; Zones, S. I.; Iglesia, E., Acid strength and solvation in catalysis by MFI zeolites and effects of the identity, concentration and location of framework heteroatoms. *Journal of Catalysis* **2014,** *312*, 58-68.

40. Silaghi, M.-C.; Chizallet, C.; Sauer, J.; Raybaud, P., Dealumination mechanisms of zeolites and extra-framework aluminum confinement. *Journal of Catalysis* **2016,** *339*, 242-255.

41. Xue, N.; Vjunov, A.; Schallmoser, S.; Fulton, J. L.; Sanchez-Sanchez, M.; Hu, J. Z.; Mei, D.; Lercher, J. A., Hydrolysis of zeolite framework aluminum and its impact on acid catalyzed alkane reactions. *Journal of Catalysis* **2018,** *365*, 359-366.

42. van Bokhoven, J. A.; van der Eerden, A. M. J.; Koningsberger, D. C., Three-Coordinate Aluminum in Zeolites Observed with In situ X-ray Absorption Near-Edge Spectroscopy at the Al K-Edge: Flexibility of Aluminum Coordinations in Zeolites. *Journal of the American Chemical Society* **2003,** *125* (24), 7435-7442.

43. Yi, X.; Peng, Y.-K.; Chen, W.; Liu, Z.; Zheng, A., Surface Fingerprinting of Faceted Metal Oxides and Porous Zeolite Catalysts by Probe-Assisted Solid-State NMR Approaches. *Accounts of Chemical Research* **2021**.

44. Chen, K.; Gan, Z.; Horstmeier, S.; White, J. L., Distribution of Aluminum Species in Zeolite Catalysts: 27Al NMR of Framework, Partially-Coordinated Framework, and Non-Framework Moieties. *Journal of the American Chemical Society* **2021**.

45. Xin, S.; Wang, Q.; Xu, J.; Chu, Y.; Wang, P.; Feng, N.; Qi, G.; Trébosc, J.; Lafon, O.; Fan, W.; Deng, F., The acidic nature of "NMR-invisible" tri-coordinated framework aluminum species in zeolites. *Chemical Science* **2019,** *10* (43), 10159-10169.

46. Mota, C. J. A.; Bhering, D. L.; Rosenbach Jr., N., A DFT Study of the Acidity of Ultrastable Y Zeolite: Where Is the Brønsted/Lewis Acid Synergism? *Angewandte Chemie International Edition* **2004,** *43* (23), 3050-3053.

47. Liu, C.; Li, G.; Hensen, E. J. M.; Pidko, E. A., Nature and Catalytic Role of Extraframework Aluminum in Faujasite Zeolite: A Theoretical Perspective. *ACS Catalysis* **2015,** *5* (11), 7024-7033.

48. Lukyanov, D. B.; Shtral, V. I.; Khadzhiev, S. N., A kinetic model for the hexane cracking reaction over H-ZSM-5. *Journal of Catalysis* **1994,** *146* (1), 87-92.

49. Konno, H.; Okamura, T.; Kawahara, T.; Nakasaka, Y.; Tago, T.; Masuda, T., Kinetics of n-hexane cracking over ZSM-5 zeolites – Effect of crystal size on effectiveness factor and catalyst lifetime. *Chemical Engineering Journal* **2012,** *207-208*, 490-496.

50. Gounder, R.; Iglesia, E., Catalytic Consequences of Spatial Constraints and Acid Site Location for Monomolecular Alkane Activation on Zeolites. *Journal of the American Chemical Society* **2009,** *131* (5), 1958-1971.

CHAPTER 3: Influence of Al in Proximity on Alkane Conversion in MFI Zeolites

ABSTRACT

Extra framework Al species generated during the hydrolysis of framework Al are believed to play a crucial role in the activity of alkane cracking on zeolites. The presence of these extra-framework Al species can enhance the reactivity of the adjacent Brønsted acid sites, resulting in the formation of the synergistic sites. Recently, we have demonstrated that water treatment in a pulse reactor can facilitate the mobility of existing extra-framework Al species in the absence of framework hydrolysis. Here, we investigate the role of framework Al location and proximity in generating synergistic sites in MFI zeolites. Correlations are developed between the cracking rates and the rate enhancement under pulsing water treatment with the concentration of proximate framework Al species. In addition, it is illustrated that sodium and calcium can titrate close framework Al, which we reveal to be essential precursors to synergistic site formation. This approach is utilized to quantify the number of synergistic sites and concludes that these highly active sites are likely located at pore intersections within the MFI framework. In addition, the analysis of experimental transition state energies suggests that these extra-framework Al species help to better stabilize the transition states of alkane cracking reaction by lowering activation enthalpies.

3.1 Introduction

Zeolites are used in many industrial applications such as adsorption, separation, and catalysis due to their uniform structures, diverse topologies, high crystallinity, and large surface area.[1] With excellent chemical and thermal stabilities, MFI-type zeolites, which are the focus of this work, are used as catalysts for many hydrocarbon upgrading processes such as oligomerization, isomerization, and cracking reactions. For traditional Brønsted acid-containing zeolites, active sites result from tetrahedrally coordinated framework aluminum atoms. Many previous studies have claimed that the presence of extra-framework Aluminum (EFAL) proximate to a Brønsted acid site (BAS) can create synergistic EFAL-BAS sites with high activity for alkane cracking reactions.[2-9] While water can participate and influence the reaction rates, selectivity, and mass transfer in many reactions,[10-12] the exposure of zeolites to water can lead to the hydrolysis of framework Al atoms.[13, 14] This results in the generation of framework-associated Al atoms at low temperature and EFAL species at high temperature.[8, 11, 15, 16] In addition, under steaming conditions, water also helps to mobilize EFAL species in zeolite pores, which can be detected by fluorescence microscopy imaging.[17] Decoupling the generation of EFAL species from the subsequent mobility and generation of highly active sites can be challenging due to their concurrent occurrence in persistent steaming environments. We have recently shown that pulsing water treatments can decouple the mobility of EFAL species from the hydrolysis of framework Al, and the consequences of each on alkane cracking activity.[9] While these approaches enable assessment of the creation of new sites, much is still not known regarding the structural features within the zeolite that influence

the generation, diffusion, and stabilization of EFAL species inside zeolite structures to create these highly active sites.

The critical role of EFAL in generating synergistic sites is evidenced by the fact that the rate of alkane cracking increases dramatically during steaming treatment at high temperatures. In addition, the observed activity decreases significantly when the catalyst is treated with ammonium hexafluorosilicate (AHFS) to remove EFAL.[8, 9] However, simply correlating activity with the amount of framework Brønsted sites can often be misleading as well. For example, the generation of a high concentration of EFAL species during longtime water exposure will ultimately result in the formation of Al clusters, resulting in a decrease in reactivity.[2, 18, 19] Prior work suggests that hydrolysis and removal of framework Al are dependent of the local environment within the zeolite lattice, which can be influenced by local confinement, Al distribution, the zeolite structure type, etc.[20, 21] In particular, rates of hydrolysis and removal of framework Al from the lattice increases with the number of T-sites in the ring structures in the order of ferrierite < ZSM-5 < mordenite < beta.[21] In addition, dealumination rates are also influenced by the number of local defects and framework Al density.[21] Silaghi et al. have shown that EFAL species prefer to be stabilized in some specific locations in zeolites.[20] For example, the Pauli repulsion can destabilize the presence of EFAL species in very small cavities, e.g., the hexagonal prism in FAU zeolite. In contrast, in huge pores such as FAU super-cages, the effect of confinement in stabilizing EFAL species is weak. These results imply an ideal confining environment to stabilize EFAL species, which led the authors to conclude that locations with the ideal confining environment, such as the pore intersections in MFI zeolites exhibit the greatest stability of EFAL species such as $Al(OH)_3.H_2O$.

The role of proximate framework sites on the stabilization of extra lattice species is further complicated by the additional consequence that proximate sites may play on a variety of chemistries. For example, the proximity of BAS has been reported to influence the reactivity and selectivity for several chemical reactions such as alcohol dehydration, olefin oligomerization, and alkane cracking.[22-26] For alkane cracking, Song et al. observed a higher rate of pentane cracking on MFI zeolites with higher concentrations of Al in pairs.[25] They attributed the higher rate on the adjacent BAS to the more positive intrinsic activation entropies of the latter transition states, which prefer cracking to dehydrogenation. In agreement with this, Kester et al. reported the rate of propane cracking is linearly correlated with the fraction of Al in pairs in chabazite zeolites.[26] The authors estimated the rate on BAS-BAS sites is ~12× higher than on isolated acid sites due to less negative apparent activation entropies. Another explanation for these results is proposed by Janda and Bell,[27] who attribute rate differences in alkane cracking to the local confining environments surrounding acid sites in different locations. The results suggest a strong preference for dehydrogenation relative to cracking at MFI intersections, which is attributed to the bulky and latter transition states of this reaction. The authors utilized UV-Vis to investigate the location of Al in pairs in cobalt exchanged zeolites and attributed the distribution of Al in pair to the distribution of framework Al sites. In general, it is difficult to decouple the effect of paired Al sites from the local confining environment, since modifications to zeolites during synthesis often modify both features. For instance, adding a small fraction of NaOH in the synthesis solution can promote Al sitting in the channels and lead to an increase in the number of Al in pairs.[28] Many recent works focus on developing synthesis strategies

manipulating the distribution of the active sites in zeolites,[28, 29 30 31] which will help to reveal the effect of Al distribution on the catalytic activity in zeolites.

In this study, we aim to decouple the complex relationship between Al proximity, location, and EFAL species on one of the most industrially important reactions, alkane cracking. The correlation between the cracking reactivity of various MFI samples with different concentrations and locations of Al species will be contrasted with n-hexane cracking activity. Cation exchange is used to modify the concentration and type of acid sites available for cracking, supported by density functional theory (DFT) calculations to determine the preferred cation location during titration. Pulsing water treatments are used to access the ability of these modified zeolites to generate new highly active sites. The results in this work will help to explain many contradicting claims as previously discussed in the literature.

3.2 Experimental section

3.2.1 Catalyst preparation

NH_4-ZSM5 zeolites varying Si/Al ratios purchased from Zeolyst were calcined at 823K for 5h in an air flow to obtain the proton forms of the catalysts. The initial slow ramp rate of 2K/min was applied to minimize the hydrolysis of framework Al sites. After being calcined, all catalysts in proton form are denoted as HZSM5-X with X being the corresponding Si/Al ratio. ZSM5-X-AHFS catalyst was obtained from the chemical treatment of ZSM5-X zeolites with AHFS following the standard procedure to remove EFAL species.[32]

Preparation of partial cation exchanged zeolites. The HZSM-5 samples were exchanged in 0.05 - 0.5 M $NaNO_3$ solution for 0.5 - 12 h at room temperature using the ratio of 20 ml of solution per gram of catalyst. CaHZSM-5-15 samples were obtained by exchanging 1g HZSM-15 zeolites with 90 ml 0.25 M $Ca(NO_3)_2$ solution for 24 h. Afterward, the mixture was centrifuged, and the solid was washed with deionized water 5 times to remove residual nitrate salts. The samples were dried overnight in a vacuum oven at 353 K and calcined at 823 K for 5h before being used for testing reactivity. The obtained catalysts are denoted as NaHZSM5-X (Y, Z, T) and CaHZSM5-X (Y, Z, T); in which X is the corresponding Si/Al ratio, Y (M), Z (K), and T (h) are the concentration of cation in the exchange solution, the temperature and time duration of the cation exchange procedure.

Water pulsing catalysts. Pelletized zeolite samples after calcination were packed into the micro-reactor and exposed to 40 intermittent pulses of water at 480^{o}C with partial pressures of 18.6 kPa. The break time between two pulses is 10 minutes. The catalysts are then dried overnight, and their activity is measured in-situ in that pulse reactor. The other conditions are described in detail in our previous work. [9]

3.2.2 Catalyst Characterization

X-ray diffraction measurement. The X-ray diffraction (XRD) patterns were obtained on a Rigaku diffractometer, using Cu Kα radiation operated at 44 mA and 40 kV; the diffraction angle range 2θ was varied from 5 to 70°.

FI-IR spectroscopy. IR spectra were obtained by a PerkinElmer Spectrum 100 equipped with a high-temperature DRIFT. The background of the measurement was obtained by pelletized KBr powder. Catalysts were pretreated at 573 K for 1 hour in Helium to remove physically adsorbed water. FT-IR spectra of all samples were obtained at 393 K.

Brønsted acid density measurement. The temperature-programmed desorption of isopropylamine (IPA-TPD) was utilized to quantify the density of BAS in all zeolite samples. The procedure was described elsewhere.[9] In brief, 5 - 100 mg catalysts pelletized to 0.25 − 0.35 mm particles and mixed with glass beads were utilized for this measurement. The samples were dried at 753 K for 2 h to remove physically adsorbed water and cooled to 373 K for adsorption of IPA. The catalysts were exposed to 2 µl pulses of IPA to ensure the saturation of IPA uptake and were flushed by a 30 ml/min He flows for a few hours to remove weakly adsorbed IPA. After that, the temperature was increased to 873 K with a 10 K/ min heating ramp, and a peak of released propylene was observed at the temperature range of 623 - 663 K. The propylene was quantified by using an MKS Cirrus mass spectrometer or a GC MS-FID system. The moles of propylene were calibrated with several 500 µL pulses of propylene at a known temperature and pressure condition.

3.2.3 Kinetic measurements

The activity of the catalyst was measured by the n-hexane cracking reaction in a micro-pulse reactor. The experimental details were described elsewhere.[9] In brief, 5-70 mg of catalyst pelletized to 0.24-0.35 mm particles were utilized for the reaction, which occurs at 753 K and 120 kPa pressure in Helium. Before reaction, the pretreatment of catalysts to remove resident moisture was conducted at the reaction temperature for 2h. Several pulses of 0.48 µmol hexane (3.7 mol % of hydrocarbon in He) were sent over the catalyst bed for the cracking reaction by a flow of 75 mL/min He. The reaction conversion and the product distribution were determined by a GC MS-FID system utilizing a HP-PLOT/Al_2O_3/"S" column.

3.2.4 DFT calculation

All periodic computations were performed based on the DFT method as provided in the Vienna ab initio simulation package (VASP). We used the projector-augmented wave (PAW) potential, and the generalized gradient approximation (GGA) described by Perdew-Burke-Ernzerhof (PBE) to simulate the exchange-correlation energy. The DFT-D3 method was employed to consider van der Waals (vdW) interaction. Plane-wave cut-off energy of 400 eV was set, and the residual force and converge criteria for geometry optimization were, respectively, set as 0.02 eV/$Å^{-1}$ and 10^{-6} eV per atom. The ZSM5 zeolite was modeled as a 1 x 1 x 1 unit cell consisting of 96 tetrahedral atoms (Si, Al) and 192 oxygen atoms. This model contains both isolated Al frameworks and Al-Al site pairs as Al-O(Si-O)$_2$-Al sequences. The influence of the Si/Al ratio was not considered in this study. The optimized lattice parameters were set similar as our previous studies: a = 20.078 Å, b = 19.894 Å, c = 13.372 Å.[8, 16, 33]

3. 3 Results and discussion

3.3. 1 Relation between catalytic activity and proximity of framework Al

The high temperatures and low pressures employed here favor a monomolecular cracking mechanism.[2, 3, 19, 27, 34-37] For all tested catalysts, the reaction behaves as 1st order with insignificant shifts in product distribution observed over the range of conversions studied as we have reported previously.[9] Table 3 lists the properties of investigated samples in this work. The utilized samples are commercial catalysts and the number and distribution of Al in pairs were obtained by the cobalt exchange as previously reported by Janda et al.[27] XRD patterns have shown that cation exchange and AHFS treatment do not alter the zeolite

structure, shown in Figure 13-a. Moreover, IR spectra in Figure 13-b show that the 3650 cm^{-1} peak corresponding to the extra lattice Al-OH species is significant in the HZSM5-15 sample while it is negligible in the corresponding AHFS treated sample. This indicates the decrease in the reactivity of this catalyst is a consequence of the loss of EFAL species. Meanwhile, comparing the spectrum of fresh and cation exchanged samples, the intensities of the EFAL-OH peaks do not change significantly. Thus, the decreases in the reactivity of cation exchanged samples discussed in the following sections are attributed to the titration of framework protons.

Table 3. Properties of investigated zeolite samples.

Samples	$Al_{theor.}$ mmol/g	Al_f mmol/g	Al_{non-f} mmol/g	Al_{pair} mmol/g	Fraction of Al_{pair}		
					Straight channels	Intersection	Sinusoidal channels
HZSM5-140	0.12	0.11	0.00	0.01	-	-	-
HZSM5-40	0.41	0.39	0.02	0.13	0.38	0.58	0.04
HZSM5-25	0.64	0.48	0.16	0.23	0.33	0.63	0.04
HZSM5-15	1.04	0.73	0.31	0.41	0.24	0.71	0.05
HZSM5-11.5	1.33	1.08	0.25	0.74	0.23	0.69	0.08

The density framework Al species are measured by IPA-TPD. The numbers of Al in pairs and the fractions of Al_{pair} located at different locations in MFI are obtained by Co(II) distribution from elsewhere. [27]

(a)

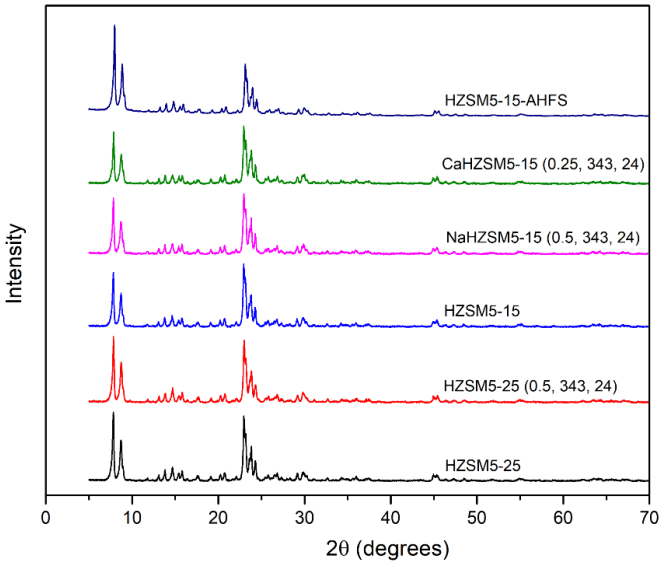

(b)

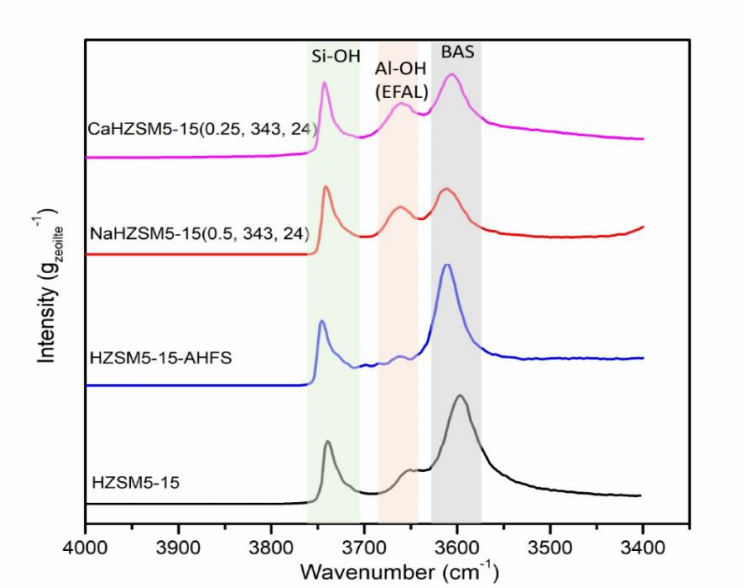

Figure 13. XRD patterns (a) and FTIR spectra (b) of HZSM-5 and cation exchanged sample.

In our previous work, it was demonstrated that the water pulsed treatment does not alter the BAS density of the catalysts; however, the catalytic activities are enhanced via the generation of synergistic sties between BAS and EFAL species.[9] Figure 14 illustrates the correlation between the activity of HZSM-5 catalysts before and after pulsing water treatment and the density of different Al species. A general trend is shown that the catalysts with higher BAS densities have higher activities than the others. In addition, the rate enhancements of these catalysts under pulsing water treatment are more significant compared to the others. This trend does not apply to the fresh HZSM5-11.5, which might be attributed to a lower concentration of EFAL in this catalyst or the ability of this zeolite structure to stabilize EFAL species and generate synergistic sites. In addition, catalysts having insignificant amounts of EFAL species such as HZSM5-140, HZSM5-40, and HZSM5-15-AHFS have significantly lower activity compared to the others. The rate enhancements under pulsing water treatment of these catalysts are also minimal. These results suggest that both BAS density and the concentration of EFAL species are crucial to the reactivity of these catalysts.

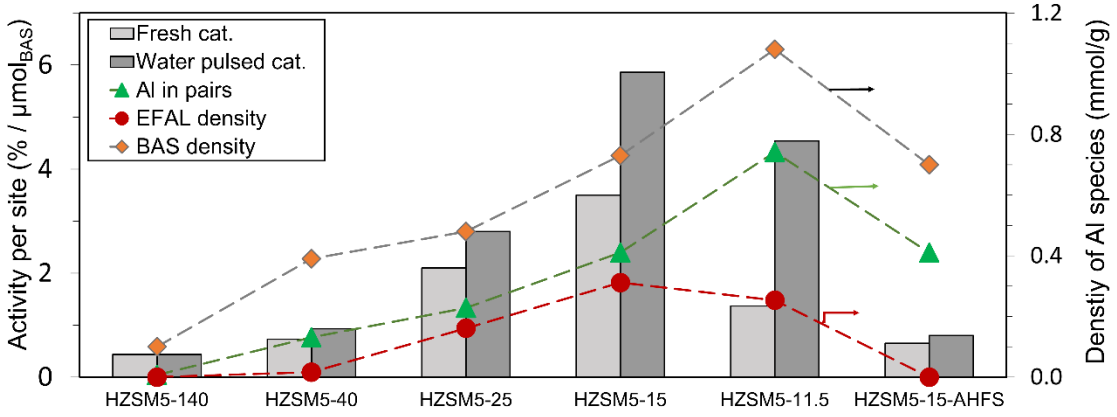

Figure 14. Rate per site of hexane cracking reaction before and after catalysts were treated by pulsing water, obtained from our previous work[9]. and the densities of various Al species

in various HZSM-5 zeolites.[9, 27] *Reaction conditions: T = 753 K,* P_{nC6} *= 4.5 kPa with 0.48 µmol of hexane in each pulse.*

It is important to note that catalysts having higher BAS density will have a higher amount of Al in pairs; noted that the numbers and the locations of these sites are varied with the conditions of the synthesis procedure [28] such as inorganic reagent sources or the structure-directing agents. While Kester et al. have shown that the activities are linearly correlated with the fraction of Al in pairs in CHA zeolites [26], Figure 15 demonstrates that the correlation between the fraction of Al in pairs or EFAL species and the reactivities of MFI zeolites is nonlinear. For example, the activity of HZSM5-11.5 is much lower than the activities of HZSM5-15 and HZSM5-25 despite their high concentrations of Al in pairs. It is important to note that AHFS washing and pulsing/steaming water treatments do not generate more Al in pairs. However, the cracking rate significantly decreases in the AHFS treated sample while significant rate enhancement are observed in some water treated catalysts. These results suggest that the higher cracking rate on Al in pairs cannot explain the discrepancy in the reactivity of MFI zeolites. Therefore, it is proposed that both paired Al sites and EFAL species both play important roles in the generation of synergistic sites.

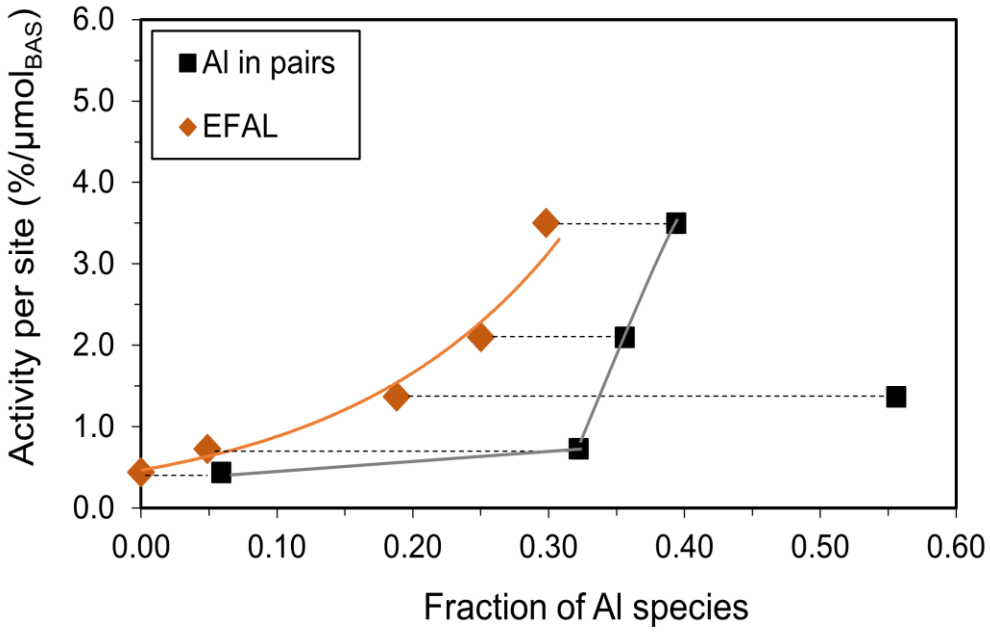

Figure 15.Conversion per site of hexane cracking over HZSM-5 samples as a function of the fraction of different Al species.The dotted line is used to connect the concentration of Al species in the same catalyst. Reaction conditions: T = 753 K, P_{nC6} = 4.5 kPa with 0.48 µmol of hexane in each pulse.

The potential exists for two types of synergistic sites co-existing in MFI zeolites, shown in Figure 16. The first type was proposed by the previous studies, including one BAS and a neighboring EFAL species. The second type of synergistic site might be formed by a pair of framework Al and an EFAL species. Several possible pathways can explain the role of Al in pairs on the generation of synergistic sites in MFI zeolites.

- One framework Al site associated with BAS - BAS pairs is hydrolyzed or exchanged with an EFAL species, which can synergistically enhance the activity of the neighboring framework Al framework, leading to the generation of SBAS (I).

- In the presence of water, EFAL species are mobile and kinetically trapped by Al in pairs, leading to the generation of SBAS (II).

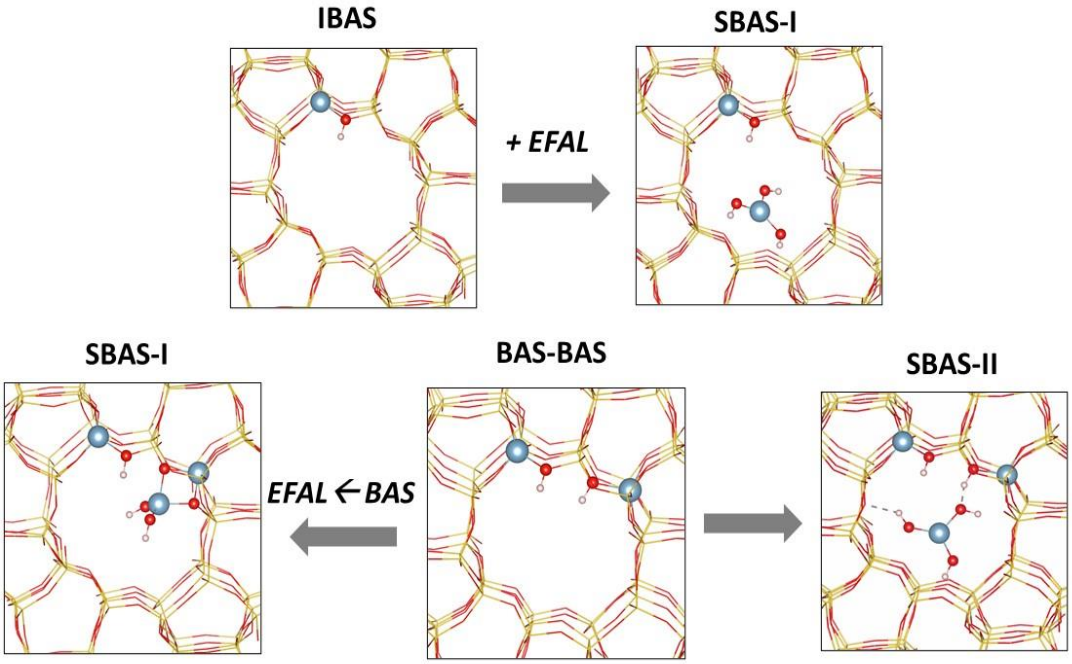

Figure 16. Proposed pathways to generate synergistic EFAL-BAS sites in the presence of water. $Al(OH)_2^+$ and $Al(OH)_3$ are used as examples for EFAL species.

The first pathway is likely attributed to the formation of synergistic sites under steaming treatment or the fast temperature ramping in the presence of moisture, resulting in a loss of active sites. The second pathway likely happens in pulsing water treatment, where the loss of BAS density is not observed.

Figure 17 presents the positive effect of Al in pairs on the generation of synergistic sites under this treatment. The rate enhancement under the water treatment is significant in the catalyst with a high Al fraction in pairs. Under this condition, water helps EFAL species to

mobilize until they are paired with BAS to create synergistic sites. Previous work has claimed that only cation EFAL species play an essential role in the reactivity of the catalysts.[38] Thus, the paired Al sites in zeolites might create metastable locations to kinetically trap these positively charged EFAL species. In addition, other neutral EFAL species such as $Al(OH)_3$ prefer to be formed and stabilized at the MFI intersections, where a high fraction of Al in pairs locate. This can also lead to the formation of SBAS (II). While EFAL species can form H bonds with the neighboring EFAL species, the role of these interactions in stabilizing these species in zeolites is unclear. It is logical to infer that when the EFAL species diffuse in the local environments having a higher density of framework Al, the possibility to create synergistic sites is higher. As a result, the EFAL species will have less freedom moving inside the zeolite pores of the catalysts with a high concentration of Al in pairs. This can be inferred that the synergistic sites are likely located nearby the locations where EFAL species are generated under mild water treatment such as pulsing water. In summary, several pathways to create synergistic sites are proposed, and the Al proximity appears to play a crucial role in stabilizing these synergistic sites.

(a)

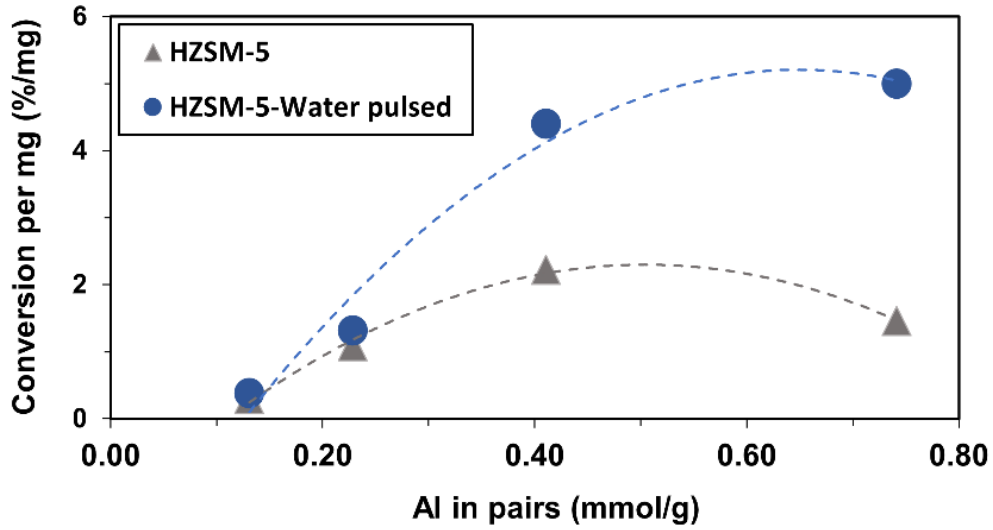

(b)

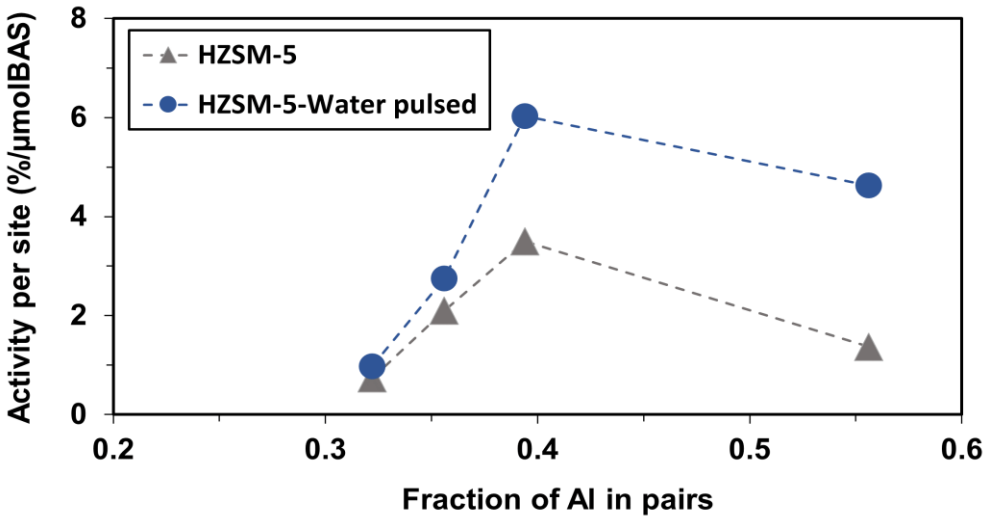

Figure 17. Rate enhancement of hexane cracking when catalysts were treated by pulsing water as a function of the fraction of Al in pairs. Reaction conditions: T = 753 K, PnC6 = 4.5 kPa with 0.48 µmol of hexane in each pulse.

3.3.2 Selective sodium titration of synergistic sites

Previous reports have shown that sodium titration can strongly affect the catalytic activity of alkane cracking over MOR [39] and CHA [26] zeolites. In this work, we show how sodium titration can affect the cracking rate in MFI samples. The correlation between the TOF and the fraction of protons exchanged with sodium is demonstrated in Figure 18-a. The activities of different ZSM5 catalysts decrease significantly when a small fraction of active sites is titrated by sodium. This suggests a strong preference for sodium exchange over these highly active sites. Only a low fraction of acid sites, such as 10% in the case of HZSM5-25, are responsible for most of the catalytic activity. This suggests that the activity associated with these synergistic sites is significantly higher than traditional framework BAS. The catalysts with a high fraction of protons being exchanged with sodium have comparable activities with the one of AHFS washed sample implying that all synergistic sites are titrated by sodium and these catalysts only contain isolated BAS.

In this section, we attempt to estimate the number of these synergistic sites, noting that the activity of the catalyst is affected by both activities of isolated (IBAS) and synergistic (SBAS) sites. The term "IBAS" in this work is used for all framework Al including active sites in Al in pairs, which are not associated with BAS-EFAL synergistic sites, types I and II in Figure 16. The abbreviations in this work are listed as the following:

(a)

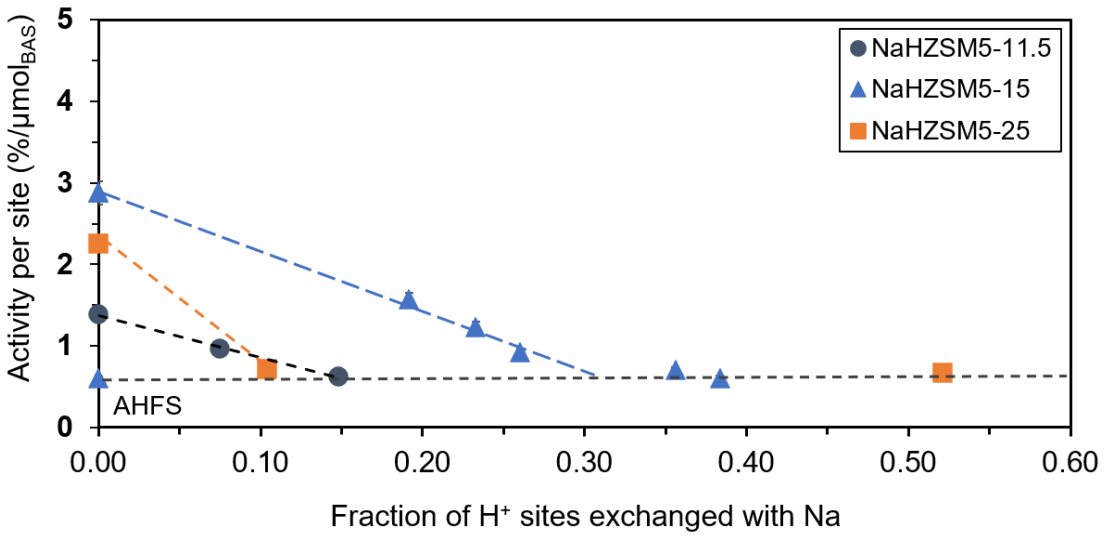

(b)

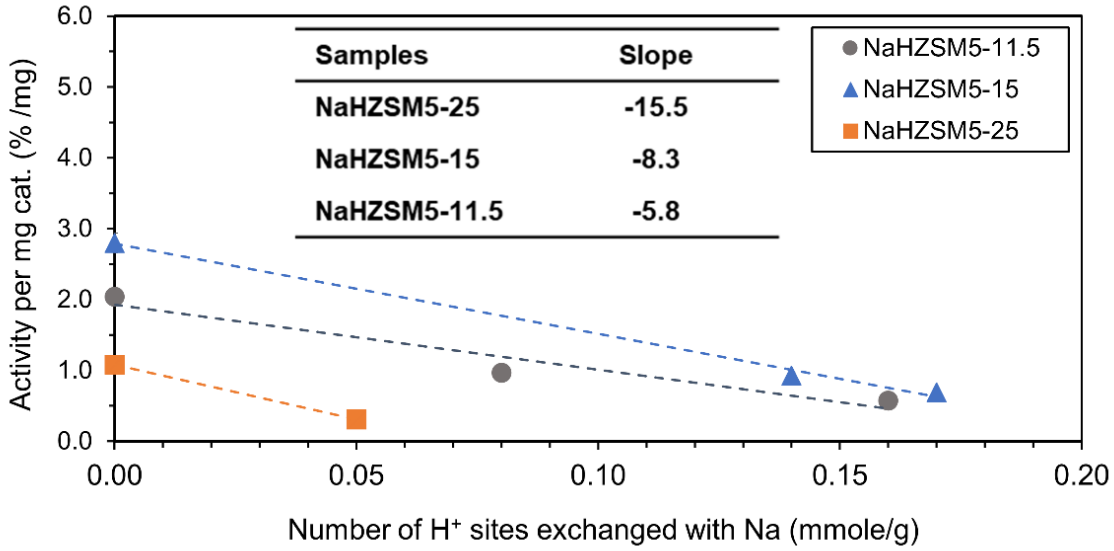

Figure 18. Conversion per site of hexane cracking over NaHZSM-5 samples as a function of the fraction of acid sites being exchanged with sodium (a) and conversion per mg catalyst of hexane cracking of these catalysts as a function of the number of protons

exchanged with sodium (b). Reaction conditions: T = 753 K, P_{nC6} = 4.5 kPa with 0.48 µmol of hexane in each pulse.

The number of each site in the sodium exchanged catalyst can be estimated as the following:

$\bar{X}_{IBAS-0}$, $\bar{X}_{SBAS-0}$, $\bar{X}_0$, $\bar{X}$, $\bar{X}_{IBAS-Na}$, $\bar{X}_{SBAS-Na}$: conversion per mg associated with each site in the fresh catalyst denoted with subscript '-0', and the corresponding ones after sodium exchange (% per mg); X'_{IBAS}, X'_{SBAS}: conversion per site (% per µmol); N_{IBAS-0}, N_{SBAS-0}, N_{BAS-0}, N_{IBAS}, N_{SBAS}: the densities of each site and total active sites in fresh catalysts and the corresponding ones after sodium exchange (mmol/g); $N_{IBAS-Na}$, $N_{SBAS-Na}$, N_{BAS-Na}: the densities of each site and total active sites being titrated by sodium (mmol per g).

The activity of the catalyst after sodium exchange can be estimated as:

$$\bar{X} = \bar{X}_{SBAS} + \bar{X}_{IBAS} = N_{SBAS}.X'_{SBAS} + N_{IBAS}.X'_{IBAS} \quad \text{Eq. (1)}$$

$$N_{SBAS} = N_{SBAS-0} - N_{SBAS-Na} = N_{SBAS-0} - \alpha.N_{BAS-Na} \quad \text{Eq. (2)}$$

$$N_{IBAS} = N_{IBAS-0} - N_{IBAS-Na} = N_{IBAS-0} - (1-\alpha).N_{BAS-Na} \quad \text{Eq. (3)}$$

With α representing the selectivity of sodium titration for the synergistic sites.

$$\alpha = \frac{N_{SBAS-Na}}{N_{BAS-Na}}$$

Replace Eq. (2) and Eq. (3) into Eq. (1):

$$\bar{X} = N_{SBAS-0}.X'_{SBAS} + N_{IBAS-0}.X'_{IBAS} - (\alpha.X'_{SBAS} + (1-\alpha).X'_{IBAS}).N_{BAS-Na}$$

$$\bar{X} = \bar{X}_0 - (\alpha . X'_{SBAS} + (1-\alpha) . X'_{IBAS}) . N_{BAS-Na} \qquad \text{Eq. (3)}$$

Since $X'_{I\text{-}BAS} << X'_{SBAS}$, we have:

$$\bar{X} = \bar{X}_0 - (\alpha . X'_{SBAS} + X'_{IBAS}) . N_{BAS-Na} \qquad \text{Eq. (4)}$$

The slope of the plot of $\bar{X}$ versus $N_{BAS\text{-}Na}$ in Figure 18-b can be utilized to estimate $\alpha . X'_{SBAS}$. Assumed α =1 , the slope of this plot is equivalent to the activity per site of synergistic sites, X'_{SBAS}, according to Eq. (3). Meanwhile, Eq. (4) shows that the slope in Figure 18-b is steeper if the catalyst has higher selectivity for sodium titration of synergistic sites, represented by a higher α value. Since the value of X'_{IBAS} can be obtained from the activity of HZSM5-15-AHFS, we can estimate the number of the synergistic sites for catalysts via the following equations.[9]

$$N_{SBAS-0} = \frac{\bar{X}_0 - X'_{SBAS} . N_{BAS}}{X'_{SBAS}} \qquad \text{Eq. (5)}$$

The difference of α values in various HZSM-5 catalysts, $\alpha_{HZSM5\text{-}25} > \alpha_{HZSM5\text{-}15} > \alpha_{HZSM5\text{-}11.5}$ implies that the BAS density of catalysts strongly affects the selectivity of sodium titration for exchanging protons with sodium. As previously discussed, the density of acid sites can affect the number of paired Al sites and the location of the active sites, which might influence the stabilization of transition states of reactions and modify the rate of reaction. Thus, it is crucial to interrogate further the influence of these factors on the selectivity of sodium exchange using DFT calculations.

3.2.3 Estimation of the energy for sodium exchange by DFT

In this section, we use DFT calculations to explain the different affinities of the sodium exchange in the varying Si/Al samples, see Table 4 and Figure 19. ZSM-5 zeolite has three-

dimensional system channels, comprising straight (5.3 × 5.6 Å) and sinusoidal (5.1 × 5.5 Å) pores.[40] The cavities where these channels intersect are 6.36 Å in diameter. [41] It indicates that the straight and sinusoidal microporous channels possess similar pore sizes, and they are more confined than intersection cages. The results of sodium titration show that IBAS in the straight and sinusoidal channels is slightly more favorable than that at the intersections due to the confinement effect. It has been reported that the sodium cations preferentially stayed in the smaller void of CHA zeolites.[26] However, the differences in sodium exchange are insignificant, which are less than 10 kJ/mol on the investigated sites. We next compare the sodium titrations to IBAS and SBAS, at the intersection, the sodium titration of IBAS and SBAS gain 2 and 45 kJ/mol, respectively, shown in Table 4. These results indicate that the BAS proton in a synergistic site is much easier to be replaced than the isolated BAS. Similarly, the sodium titration to SBAS at straight and sinusoidal pores is dramatically stronger than that to IBAS, given in Table 4. Such a selective titration to the synergistic site is likely caused by the formation of multiple bonds between Na^+ and the oxygen in the $Al(OH)_2^+$. Therefore, when partially introducing sodium to zeolite, the sodium cations replace the BAS protons in synergistic sites first, subsequently eliminating the highly active sites in zeolites. There is also a strong preference of Na^+ titration at synergistic sites of different locations following the same trend as isolated acid centers.

In the case of Al in pairs, the sodium titrations are influenced by Al-Al distance, which strongly affects the interactions of the sodium with the remaining proton and the interaction between two sodium atoms upon the first and second sodium titration of protons in pairs, respectively. Additionally, the local environment and void confinement determine the coordination number of sodium forming with framework oxygen atoms, shown in Figure

19 g-k. At the intersection, the exchange of both Al in pairs is thermodynamically favorable. After being titrated with one sodium cation, the remaining BAS in pairs will react like an IBAS, which agrees with previously reported results. [26] In that work, the energies of these configurations, including a proton and a sodium cation in CHA zeolites, span 50 kJ/mol with different locations of Al site pairs. Further, the configurations in which both the proton and the sodium cation occupy the same 6-MR in CHA zeolite showed the highest energy where the proton pointed out of the ring plane.[26] This result indicates a repulsion between the proton and the sodium exchange in case their locations are sufficiently close.

From Table 4, the first titrations to paired BAS are exothermic at the intersections and straight channels. Since both protons relax into larger voids (Fig. S1 a-b), no repulsion was observed upon the first titration. However, the repulsion due to the short Al-Al distance at the straight channels and the larger size of two sodium cations makes the second exchange of Al-Al sites less thermodynamically favorable. In ZSM5 zeolite, the distribution of tetrahedral sites in straight channels is generally tighter than in intersection and sinusoidal channels. Thus, the Al-Al distances in Al-O(Si-O)$_2$-Al sequence in straight channels are generally shorter than those in the intersection and sinusoidal channels. Meanwhile, in sinusoidal channels, two protons pointed to a smaller void (Fig. S1 c). The first sodium titration to paired BAS at sinusoidal is 14 kJ/mol endothermic due to the repulsion between the proton and the sodium. After the second sodium titration in the sinusoidal channel, two sodium cations relax to further positions to reduce the repulsion and form multiple bonds with framework oxygen, making the second titration 26 kJ/mol easier than the first one. Zeolite samples with higher BAS density will have more Al in pairs at the intersections,

favorably titrated by sodium. However, a high fraction of these sites might not be associated with SBAS leading to a shift in selectivity for the sodium titration of synergistic sites, represented by lower α values. Thus, the distribution of Al sites will strongly affect the α values in various MFI samples.

Table 4. Reaction energies for cation exchange of different active sites and their corresponding locations.

Type of sites	**Reaction**	**Position**	**T-site**	**ΔE (kJ/mol)**
IBAS	ZH → ZNa	intersection	T7-11	-2
		straight	T5-1	-10
		sinusoidal	T9-9	-12
EFAL-BAS	ZH → ZNa	intersection	T7-T12	-45
		straight	T5-T12	-66
		sinusoidal	T5-T7	-88
BAS-BAS	Z_2H_2 → Z_2HNa	intersection	T7-T3	-4
	Z_2HNa → Z_2Na_2			-18
	Z_2H_2 → Z_2HNa	straight	T1-T12	-13
	Z_2HNa → Z_2Na_2			+3
	Z_2H_2 → Z_2HNa	sinusoidal	T5-T7	+14
	Z_2HNa → Z_2Na_2			-12

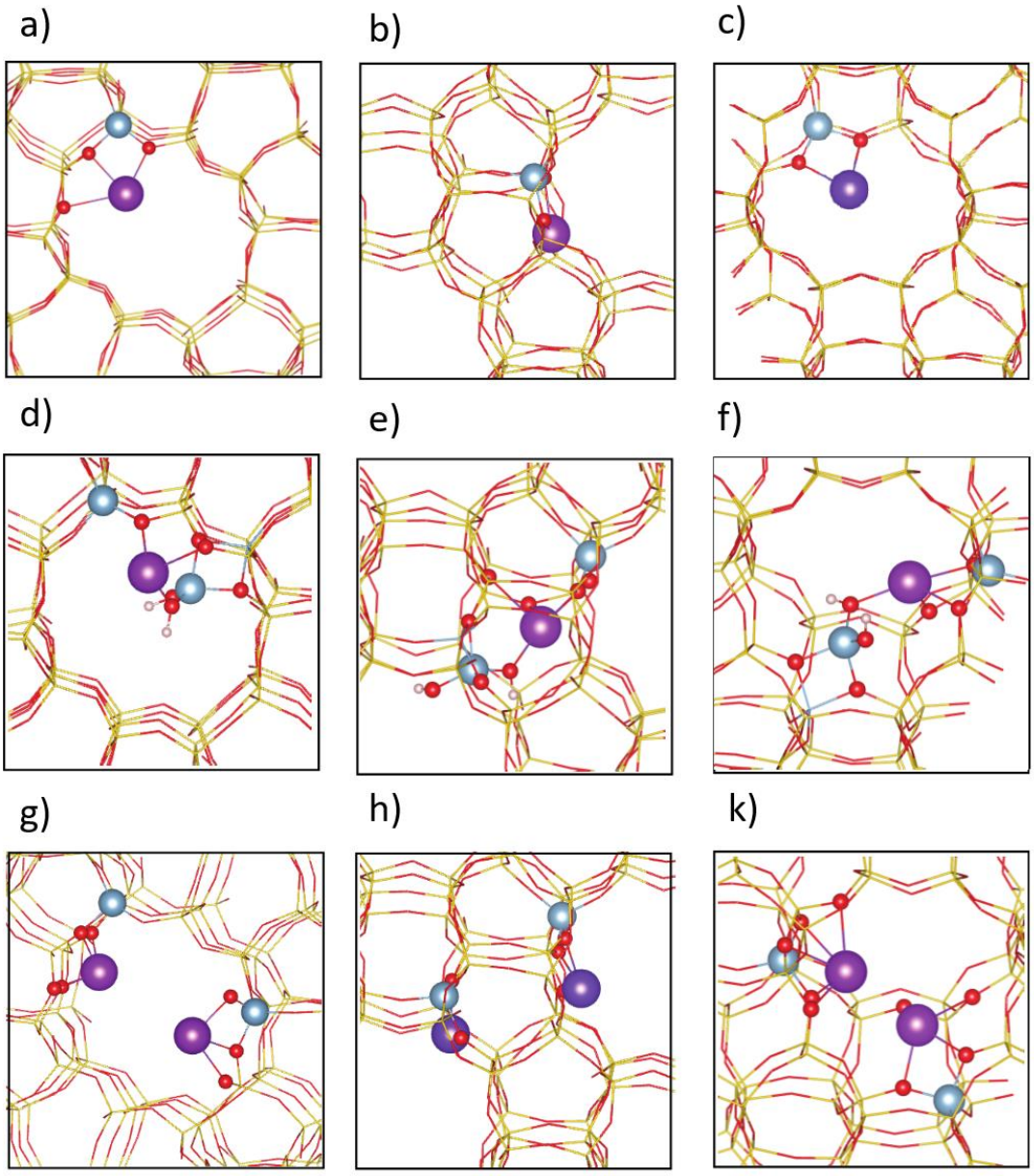

Figure 19. Calculated structures of sodium titration of active sites in zeolite, sodium exchanges with a) isolated BAS at intersection, b) isolated BAS in the straight channel, c) isolated BAS in the sinusoidal channel, d) BAS/EFAL at the intersection, e) BAS/EFAL at the straight channel, and f) BAS/EFAL in sinusoidal channel; Calculated structures of Na^+ titrated to g) paired BAS at intersection h) paired BAS in the straight channel and k) paired BAS at the sinusoidal channel.

3.2.4 Titration of Al in pairs and its effect on cracking rate under pulsing water

Divalent cation titration might provide direct evidence for the role of Al proximity on catalytic activity. Chen et al. have demonstrated that the cationic radius will affect the uptake of divalent cation (Cu^{2+}, Ca^{2+}, and Ba^{2+}) in the divalent cation exchange of protons in MFI zeolites.[8] In addition, the 12-15 ppm peaks representing the interaction between the -OH group of non-framework Al species and the neighboring protons disappears in these divalent-cation exchanged samples. This suggests that the exchange of Al in pairs by divalent cations might titrate the precursors to generate the synergistic sites. In this work, no significant modifications to the activity and the acid site density have been observed on the calcium cation exchanged HZSM5-140 catalyst, which only contains typical isolate BAS. This experiment result suggests that the change in the activity in divalent cation titration is associated with the loss in BAS-BAS pairs. It is shown in Figure 20 that the activity of the catalyst drops significantly when app. 24.5% of sites were titrated by calcium in HZSM-5-15 samples. The activities before and after pulsing water treatment of this catalyst are comparable with the activities of sodium exchange HZSM5-15 samples. In addition, the rate enhancements under pulsing water treatment for those catalysts are also clearly diminished. These results suggest that both sodium and calcium exchange titrate the Al in pairs at the exact location, which is crucial for generating the highly active site for cracking reaction. The titration of Al in pairs may inhibit the hydrolysis of framework Al atoms from creating EFAL species to form SBAS-I from BAS-BAS sites and suppress zeolite structures' ability to stabilize the EFAL species to generate SBAS-II.

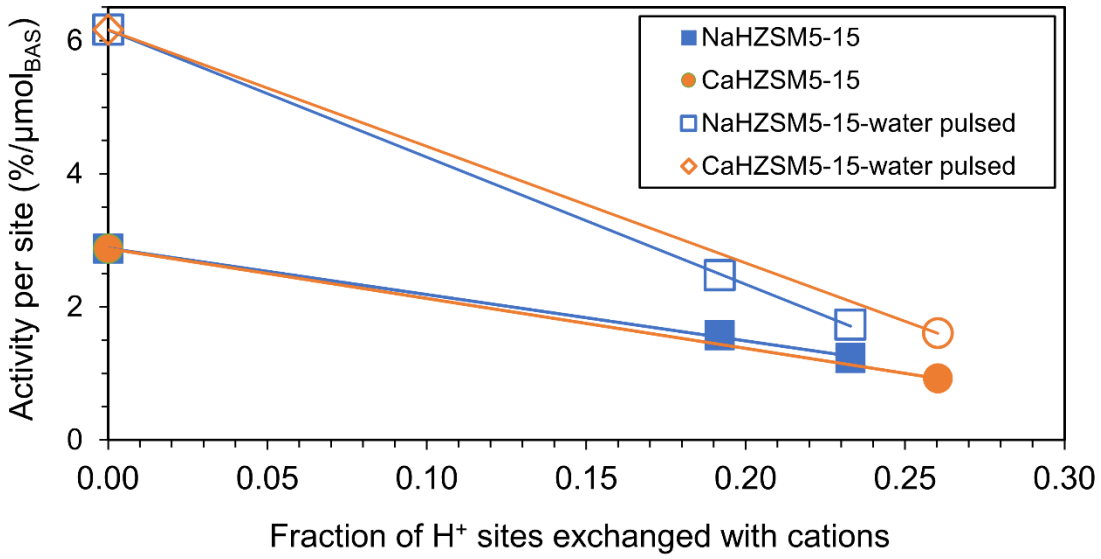

Figure 20. Conversion per active site of HZSM-5 catalysts exchanged with calcium and sodium before and after water pulsing treatment. Reaction conditions: T = 753 K, P_{nC6} = 4.5 kPa with 0.48 μmol of hexane in each pulse.

3.2.5 Estimation of the number of synergistic sites and their location

The results show that sodium titration of HZSM5-25 has the highest selectivity for synergistic sites among the three studied HZSM-5 catalysts because it has a high fraction of synergistic sites, illustrated by its high activity per site in Figure 14. The selectivity in other catalysts can be attributed to a higher concentration of IBAS sites in the more confining voids and especially BAS-BAS sites at the intersections, which are energetically favor being exchanged with sodium, leading to the results of $\alpha_{HZSM5\text{-}25} > \alpha_{HZSM5\text{-}15} > \alpha_{HZSM5\text{-}11.5}$. From Eqs. (3), assuming that $\alpha_{HZSM5\text{-}25} = 1$, which we acknowledge is a conservative estimate, $X'_{SBAS} = 15.5$ (% per μmol_{BAS}). Meanwhile, $X'_{IBAS} = 0.65 \pm 0.5$ % per mg is obtained from the activity of HZSM5-15-AHFS.[8, 9] Now, the number of synergistic sites of various HZSM-5 catalysts may be estimated, shown in Figure 21. Note that, even with

the conservative alpha value mentioned above, the fraction of these highly active sites is less than 10% of the total number of BAS in the HZSM5-25 catalyst. Because it is challenging to obtain the more accurate value of these sites using sodium titration of a lower fraction of acid sites, the actual numbers of the synergistic sites may be lower than the estimated values in this work.

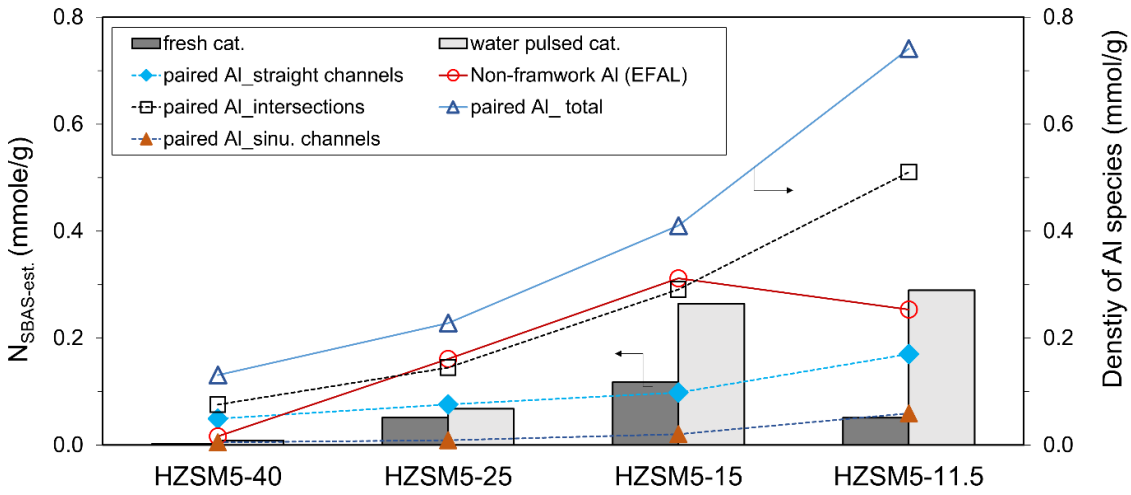

Figure 21. Estimated number of synergistic sites and densities of Al species in HZSM-5 samples. The presented Al distribution is associated with the fresh and water pulsed catalysts. Reaction conditions: T = 753 K, P_{nC6} = 4.5 kPa with 0.48 µmol of hexane in each pulse.

It is observed in Figure 21 that the total numbers of Al in pairs are much higher than the estimated number of synergistic sites. Assuming that both numbers of paired Al and the concentration of EFAL species influence the generation of synergistic sites, the results show that the concentration of active non-framework Al species is the limiting factor for the generation of synergistic sites in some cases. For instance, HZSM5-40 has a negligible number of synergistic sites due to the insignificant concentration of EFAL species. In

addition, the estimated numbers of synergistic sites in HZSM5-15 and HZSM5-11.5 catalysts after exposure to water pulsed treatment are close to the corresponding numbers of EFAL species. Meanwhile, it is observed that the number of synergistic sites in HZSM5-25 is significantly lower than the associated number of Al in pairs and EFAL species. To explain this result, we should note that not all forms of EFAL species can create synergistic sites [38, 42] and the mobility of these species can be influenced by several factors, such as the local confinement of pore sizes,[20] the density of BAS or the distance between active sites. With the catalysts having a high density of BAS, such as HZSM5-11.5, hydrogen bonds formed between the BAS and the neighboring EFAL species might strongly influence the mobility of these species. Instead of generating highly active sites, EFAL-BAS sites with hydrogen bonds might destabilize the transition state of cracking due to a short distance between two species and thus, lower the rate of this reaction. The DFT calculations of alkane cracking reaction on these sites will be studied in another work. The estimated numbers of synergistic sites for water pulsed HZSM5-15 are significantly higher than the ones of Al in pairs in the channels, which suggests a high fraction of the number of synergistic sites formed in the intersections. Most Al in pairs are located at the intersections; thus, these locations will have the highest possibility to form synergistic sites. It has previously been reported that the mean of Co^{2+} exchange energies of different configurations in the intersections is lower compared to the ones in straight and sinusoidal channels; however, the cation exchange energies in each location have a wide range. [28] Therefore, it is difficult to make a definitive conclusion about the location of these sites based on the energies of the divalent-cation exchange due to the high number of paired Al-Al configurations. On the other hand, J. Dedecek et al. showed that Co ions prefer to occupy

the active sites in the 6-MR at the MFI intersections. They also claimed that Ca^{2+} and Ba^{2+} cations located in the less open structures such as intersections and sinusoidal channels are less likely to be replaced by cobalt ions in the following exchange than those in the straight channels.[43] This suggests that Al in pairs at the intersections favor the stabilization of Ca^{2+} cations. In addition, in the previous section, DFT results show that monovalent Na^{+} cations also preferentially exchange locations with proximate framework atoms at MFI intersections. We can infer that the decrease in the cracking rate over sodium and calcium exchanged samples is likely associated with the favorable titration of BAS-BAS pairs at these intersections, which serve as the precursor for the generation of synergistic sites. In addition, in the presence of water, Silaghi et al. have reported that the dealumination of framework Al to form EFAL species in MFI zeolites are kinetically and thermodynamically favorable in the intersections.[20] In summary, these findings indicate that the highly active sites are preferentially formed at MFI intersections.

3.2.6 Analysis of the transition states

In this section, we attempt to analyze the energies of the transition states of the cracking reaction to identify the reason behind the high activity on synergistic sites. By subtracting the cracking rate associated with the typical BAS measured on HZSM5-15-AHFS, we can assess the rate corresponding to the synergistic sties.[9] We have reported that the apparent activation enthalpy for n-hexane cracking reaction on the synergistic sites is significantly lower than the one associated with the typical BAS (~75 kJ/mol vs. ~110 kJ/mol). However, in our previous work, we could not estimate the activation entropy for the cracking reaction because the numbers of the synergistic sites in the studied catalysts were unknown. Thus, in this work, we have utilized the estimated numbers of the synergistic

sites in the previous section to determine the apparent activation entropy of the cracking reaction on the synergistic sites. The activation enthalpies and entropies for the synergistic sites were estimated from HZSM-5 catalysts (Si/Al = 11.5 – 15) after pulsing and steaming water treatments. The obtained values from various samples are comparable, listed in Table 5.

Table 5. Activation enthalpy and entropy of alkane cracking on MFI zeolites.

	ΔH_{app} kJ/mol	ΔS_{app} J/(mol. K)	ΔG_{app} kJ/mol
IBAS	116.9	-131.3	215.8
SBAS	74.3	-161.8	196.2

Previous experiment findings have shown that the presence of EFAL species has an insignificant influence on the adsorption enthalpy of pentane on the active sites in MFI zeolites.[5, 6] In contrast, DFT calculations show that the adsorption of propane on FAU zeolites is slightly favorable on the synergistic sites in terms of activation enthalpy.[38] Thus, the lower apparent activation enthalpy of cracking reaction on synergistic sites suggests that the transition state is better stabilized with the presence of EFAL species, which agrees with the findings from theoretical DFT calculations.[38] However, it is important to note that at high-temperature conditions, the forms and locations of EFAL species can be modified, leading to the difference in the adsorption of alkanes. In addition, we have reported that the presence of water might strongly affect the reaction rate on the synergistic sites,[9] which can also influence the adsorption of the reactant at low temperatures. Thus, we need further

studies to investigate the influence of different EFAL species on the transition states of the cracking reaction. The results in this work follow the compensation effect, showing the lower activation enthalpy and entropy for cracking reaction on the synergistic sites. The result contrasts with the previous reports regarding the larger entropy gain for cracking reaction on the synergistic sites.[6] It is possible that depending on the distance of Al in pairs and the topology of zeolite, the cracking rate might be driven by either entropy or enthalpy. Furthermore, to consider the uncertainty for estimating synergistic sites, we report in Fig. S2 the activation entropy as a function of the number of these sites, which might be significantly lower than the estimated ones in Figure 21 of this work. The significantly lower number of these highly active sites than the estimated value indicates the remarkably higher reactivity per site on the synergistic sites. The conclusion regarding the observed lower activation enthalpy associated with the higher rate on the synergistic sites is still valid even when the actual numbers of these sites in MFI catalysts are overestimated by 90%.

3.4 Conclusions

In this contribution, we have demonstrated the critical role of both extra framework Al species and the proximity of acid sites on the activity of alkane cracking on MFI zeolites. The catalysts having a higher concentration of EFAL species and Al in pairs will have a higher potential to generate more synergistic sites in the parent and water-pulsed catalysts. In addition, selective sodium titration of the highly active sites appears as a promising approach for studying cracking reactions on zeolites, enabling quantification of these highly active synergistic sites. The activity associated with existing synergistic sites and prospective sites assisted by pulsed water EFAL mobility are strongly hindered by low

sodium and calcium titration levels. This result suggests that both cations titrate the Al in pairs, which are essential for generating synergistic sites. Using DFT to estimate the energies for sodium exchange reactions, we infer that the synergistic sites prefer to be generated at the MFI intersections where most Al in pairs locates and EFAL species are preferably formed and stabilized. The higher cracking activity on the synergistic sites is driven by a lower activation enthalpy, which suggests that the presence of EFAL species in the proximity of acid sites helps stabilize better the transition state of alkane cracking reaction on MFI zeolites. By revealing the role of Al in pairs and EFAL species on the alkane cracking rate, the activity of catalysts and the potential to improve their reactivity under water treatments can be assessed. By varying the number of Al in pairs and their location, the concentration, and mobility of EFAL species, catalysts may be synthesized and modified to promote higher rates of alkane cracking. Further studies are needed to investigate the influence of other topologies of zeolites on the generation of these synergistic sites to determine how these findings translate to other zeolite structures.

Supporting Information

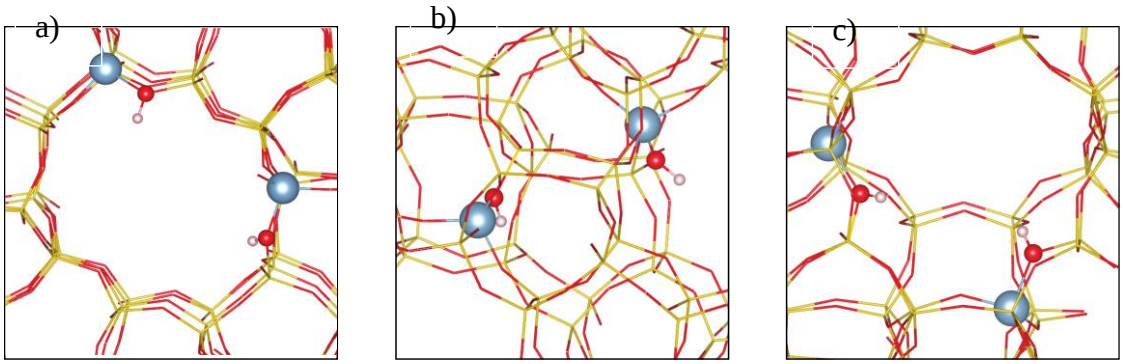

Figure S1. The optimized structures of paired BAS at a) intersection, b) straight channel, c) sinusoidal channel

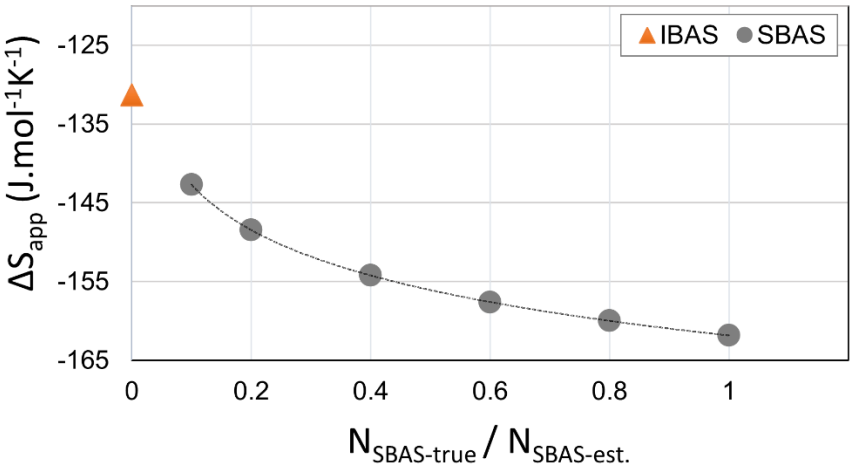

Figure S2. Estimated activation entropy of hexane cracking reaction on the synergistic site (gray) compared with those on the typical BAS site (orange). Reaction conditions: T = 753 K, P_{nC6} = 4.5 kPa with 0.48 μmol of hexane in each pulse.

REFERENCES

1. Corma, A., State of the art and future challenges of zeolites as catalysts. *Journal of Catalysis* **2003,** *216* (1), 298-312.

2. Masuda, T.; Fujikata, Y.; Mukai, S. R.; Hashimoto, K., Changes in catalytic activity of MFI-type zeolites caused by dealumination in a steam atmosphere. *Applied Catalysis A: General* **1998,** *172* (1), 73-83.

3. van Bokhoven, J. A.; Tromp, M.; Koningsberger, D. C.; Miller, J. T.; Pieterse, J. A. Z.; Lercher, J. A.; Williams, B. A.; Kung, H. H., An Explanation for the Enhanced Activity for Light Alkane Conversion in Mildly Steam Dealuminated Mordenite: The Dominant Role of Adsorption. *Journal of Catalysis* **2001,** *202* (1), 129-140.

4. Yu, Z.; Li, S.; Wang, Q.; Zheng, A.; Jun, X.; Chen, L.; Deng, F., Brønsted/Lewis Acid Synergy in H–ZSM-5 and H–MOR Zeolites Studied by 1H and 27Al DQ-MAS Solid-State NMR Spectroscopy. *The Journal of Physical Chemistry C* **2011,** *115* (45), 22320-22327.

5. Schallmoser, S.; Ikuno, T.; Wagenhofer, M. F.; Kolvenbach, R.; Haller, G. L.; Sanchez-Sanchez, M.; Lercher, J. A., Impact of the local environment of Brønsted acid sites in ZSM-5 on the catalytic activity in n-pentane cracking. *Journal of Catalysis* **2014,** *316*, 93-102.

6. Zhang, Y.; Zhao, R.; Sanchez-Sanchez, M.; Haller, G. L.; Hu, J.; Bermejo-Deval, R.; Liu, Y.; Lercher, J. A., Promotion of protolytic pentane conversion on H-MFI zeolite by proximity of extra-framework aluminum oxide and Brønsted acid sites. *Journal of Catalysis* **2019,** *370*, 424-433.

7. Maier, S. M.; Jentys, A.; Lercher, J. A., Steaming of Zeolite BEA and Its Effect on Acidity: A Comparative NMR and IR Spectroscopic Study. *The Journal of Physical Chemistry C* **2011,** *115* (16), 8005-8013.

8. Chen, K.; Abdolrahmani, M.; Horstmeier, S.; Pham, T. N.; Nguyen, V. T.; Zeets, M.; Wang, B.; Crossley, S.; White, J. L., Brønsted–Brønsted Synergies between Framework and Noncrystalline Protons in Zeolite H-ZSM-5. *ACS Catalysis* **2019**, 6124-6136.

9. Pham, T. N.; Nguyen, V.; Wang, B.; White, J. L.; Crossley, S., Quantifying the Influence of Water on the Mobility of Aluminum Species and Their Effects on Alkane Cracking in Zeolites. *ACS Catalysis* **2021,** *11* (12), 6982-6994.

10. Li, G.; Wang, B.; Resasco, D. E., Water-Mediated Heterogeneously Catalyzed Reactions. *ACS Catalysis* **2020,** *10* (2), 1294-1309.

11. Resasco, D. E.; Crossley, S. P.; Wang, B.; White, J. L., Interaction of water with zeolites: a review. *Catalysis Reviews* **2021,** *63* (2), 302-362.

12. Stanciakova, K.; Weckhuysen, B. M., Water–active site interactions in zeolites and their relevance in catalysis. *Trends in Chemistry* **2021,** *3* (6), 456-468.

13. van Donk, S.; Janssen, A. H.; Bitter, J. H.; de Jong, K. P., Generation, Characterization, and Impact of Mesopores in Zeolite Catalysts. *Catalysis Reviews* **2003,** *45* (2), 297-319.

14. Ong, L. H.; Dömök, M.; Olindo, R.; van Veen, A. C.; Lercher, J. A., Dealumination of HZSM-5 via steam-treatment. *Microporous and Mesoporous Materials* **2012,** *164*, 9-20.

15. Ravi, M.; Sushkevich, V. L.; van Bokhoven, J. A., Towards a better understanding of Lewis acidic aluminium in zeolites. *Nature Materials* **2020,** *19* (10), 1047-1056.

16. Chen, K.; Horstmeier, S.; Nguyen, V. T.; Wang, B.; Crossley, S. P.; Pham, T.; Gan, Z.; Hung, I.; White, J. L., Structure and Catalytic Characterization of a Second Framework Al(IV) Site in Zeolite Catalysts Revealed by NMR at 35.2 T. *Journal of the American Chemical Society* **2020,** *142* (16), 7514-7523.

17. Ristanović, Z.; Hofmann, J. P.; De Cremer, G.; Kubarev, A. V.; Rohnke, M.; Meirer, F.; Hofkens, J.; Roeffaers, M. B. J.; Weckhuysen, B. M., Quantitative 3D Fluorescence Imaging of Single Catalytic Turnovers Reveals Spatiotemporal Gradients in Reactivity of Zeolite H-ZSM-5 Crystals upon Steaming. *Journal of the American Chemical Society* **2015,** *137* (20), 6559-6568.

18. Xue, N.; Vjunov, A.; Schallmoser, S.; Fulton, J. L.; Sanchez-Sanchez, M.; Hu, J. Z.; Mei, D.; Lercher, J. A., Hydrolysis of zeolite framework aluminum and its impact on acid catalyzed alkane reactions. *Journal of Catalysis* **2018,** *365*, 359-366.

19. Zholobenko, V. L.; Kustov, L. M.; Kazansky, V. B.; Loeffler, E.; Lohser, U.; Peuker, C.; Oehlmann, G., On the possible nature of sites responsible for the enhancement of cracking activity of HZSM-5 zeolites dealuminated under mild steaming conditions. *Zeolites* **1990,** *10* (4), 304-306.

20. Silaghi, M.-C.; Chizallet, C.; Sauer, J.; Raybaud, P., Dealumination mechanisms of zeolites and extra-framework aluminum confinement. *Journal of Catalysis* **2016,** *339*, 242-255.

21. Müller, M.; Harvey, G.; Prins, R., Comparison of the dealumination of zeolites beta, mordenite, ZSM-5 and ferrierite by thermal treatment, leaching with oxalic acid and

treatment with SiCl4 by 1H, 29Si and 27Al MAS NMR. *Microporous and Mesoporous Materials* **2000,** *34* (2), 135-147.

22. Mlinar, A. N.; Zimmerman, P. M.; Celik, F. E.; Head-Gordon, M.; Bell, A. T., Effects of Brønsted-acid site proximity on the oligomerization of propene in H-MFI. *Journal of Catalysis* **2012,** *288*, 65-73.

23. Di Iorio, J. R.; Nimlos, C. T.; Gounder, R., Introducing Catalytic Diversity into Single-Site Chabazite Zeolites of Fixed Composition via Synthetic Control of Active Site Proximity. *ACS Catalysis* **2017,** *7* (10), 6663-6674.

24. Tabor, E.; Bernauer, M.; Wichterlová, B.; E df ek, J., Enhancement of propene oligomerization and aromatization by proximate protons in zeolites; FTIR study of the reaction pathway in ZSM-5. *Catalysis Science & Technology* **2019,** *9*, 4262-4275.

25. Song, C.; Chu, Y.; Wang, M.; Shi, H.; Zhao, L.; Guo, X.; Yang, W.; Shen, J.; Xue, N.; Peng, L.; Ding, W., Cooperativity of adjacent Brønsted acid sites in MFI zeolite channel leads to enhanced polarization and cracking of alkanes. *Journal of Catalysis* **2017,** *349*, 163-174.

26. Kester, P. M.; Crum, J. T.; Li, S.; Schneider, W. F.; Gounder, R., Effects of Brønsted acid site proximity in chabazite zeolites on OH infrared spectra and protolytic propane cracking kinetics. *Journal of Catalysis* **2021,** *395*, 210-226.

27. Janda, A.; Bell, A. T., Effects of Si/Al Ratio on the Distribution of Framework Al and on the Rates of Alkane Monomolecular Cracking and Dehydrogenation in H-MFI. *Journal of the American Chemical Society* **2013,** *135* (51), 19193-19207.

28. Nimlos, C. T.; Hoffman, A. J.; Hur, Y. G.; Lee, B. J.; Di Iorio, J. R.; Hibbitts, D. D.; Gounder, R., Experimental and Theoretical Assessments of Aluminum Proximity in

MFI Zeolites and Its Alteration by Organic and Inorganic Structure-Directing Agents. *Chemistry of Materials* **2020,** *32* (21), 9277-9298.

29. Yokoi, T.; Mochizuki, H.; Namba, S.; Kondo, J. N.; Tatsumi, T., Control of the Al Distribution in the Framework of ZSM-5 Zeolite and Its Evaluation by Solid-State NMR Technique and Catalytic Properties. *The Journal of Physical Chemistry C* **2015,** *119* (27), 15303-15315.

30. Devos, J.; Robijns, S.; Van Goethem, C.; Khalil, I.; Dusselier, M., Interzeolite Conversion and the Role of Aluminum: Toward Generic Principles of Acid Site Genesis and Distributions in ZSM-5 and SSZ-13. *Chemistry of Materials* **2021,** *33* (7), 2516-2531.

31. Bickel, E. E.; Nimlos, C. T.; Gounder, R., Developing quantitative synthesis-structure-function relations for framework aluminum arrangement effects in zeolite acid catalysis. *Journal of Catalysis* **2021,** *399*, 75-85.

32. Garralón, G.; Fornés, V.; Corma, A., Faujasites dealuminated with ammonium hexafluorosilicate: Variables affecting the method of preparation. *Zeolites* **1988,** *8* (4), 268-272.

33. Zeets, M.; Resasco, D. E.; Wang, B., Enhanced chemical activity and wettability at adjacent Brønsted acid sites in HZSM-5. *Catalysis Today* **2018,** *312*, 44-50.

34. Kung, H. H.; Williams, B. A.; Babitz, S. M.; Miller, J. T.; Haag, W. O.; Snurr, R. Q., Enhanced hydrocarbon cracking activity of Y zeolites. *Topics in Catalysis* **2000,** *10* (1), 59-64.

35. van Bokhoven, J. A.; Williams, B. A.; Ji, W.; Koningsberger, D. C.; Kung, H. H.; Miller, J. T., Observation of a compensation relation for monomolecular alkane

cracking by zeolites: the dominant role of reactant sorption. *Journal of Catalysis* **2004,** *224* (1), 50-59.

36. Olson, D. H.; Haag, W. O.; Lago, R. M., Chemical and physical properties of the ZSM-5 substitutional series. *Journal of Catalysis* **1980,** *61* (2), 390-396.

37. Haag, W. O.; Lago, R. M.; Weisz, P. B., The active site of acidic aluminosilicate catalysts. *Nature* **1984,** *309* (5969), 589-591.

38. Liu, C.; Li, G.; Hensen, E. J. M.; Pidko, E. A., Nature and Catalytic Role of Extraframework Aluminum in Faujasite Zeolite: A Theoretical Perspective. *ACS Catalysis* **2015,** *5* (11), 7024-7033.

39. Gounder, R.; Iglesia, E., Catalytic Consequences of Spatial Constraints and Acid Site Location for Monomolecular Alkane Activation on Zeolites. *Journal of the American Chemical Society* **2009,** *131* (5), 1958-1971.

40. Zeng, S.; Xu, S.; Gao, S.; Gao, M.; Zhang, W.; Wei, Y.; Liu, Z., Differentiating Diffusivity in Different Channels of ZSM-5 Zeolite by Pulsed Field Gradient (PFG) NMR. *ChemCatChem* **2020,** *12* (2), 463-468.

41. Olson, D. H.; Kokotailo, G. T.; Lawton, S. L.; Meier, W. M., Crystal structure and structure-related properties of ZSM-5. *The Journal of Physical Chemistry* **1981,** *85* (15), 2238-2243.

42. Li, S.; Zheng, A.; Su, Y.; Zhang, H.; Chen, L.; Yang, J.; Ye, C.; Deng, F., Brønsted/Lewis Acid Synergy in Dealuminated HY Zeolite: A Combined Solid-State NMR and Theoretical Calculation Study. *Journal of the American Chemical Society* **2007,** *129* (36), 11161-11171.

43. Dědeček, J.; Kaucký, D.; Wichterlová, B., Co2+ ion siting in pentasil-containing zeolites, part 3.: Co2+ ion sites and their occupation in ZSM-5: a VIS diffuse reflectance spectroscopy study. *Microporous and Mesoporous Materials* **2000,** *35-36*, 483-494.

CHAPTER 4: Influence of Extra-framework Al Species and Their Mobility on the Generation of Synergistic Acid Sites in Zeolites

ABSTRACT

Synergistic sites formed between a Brønsted acid site and a neighboring extra-framework Al species are believed to possess a high activity for cracking reaction. Our previous works demonstrated that the formation of highly active sites in zeolite is influenced by the concentration of extra-framework Al species and their mobility inside zeolite pores. Moreover, the distribution of framework Al atoms such as Al in pairs and their locations is essential for stabilizing extra-framework Al species that might result in an enhanced alkane cracking rate. In this work, we further investigate the critical role of Al in pairs in the generation of these highly active sites by water treatments of parent and cation exchange zeolites. In addition, extra-framework Al species are added to MFI zeolites via the cation exchange method to investigate the role of these species on the reactivity of cracking reaction and the ability of zeolite samples to stabilize these species. It is observed that different pre-treatments of the catalysts with liquid water or ammonium nitrate solutions might significantly enhance the reaction rate via the generation of new active sites without modifying the density of Brønsted acid site. The observed rate enhancement can be explained by either the transformation of extra-framework Al species into “active” forms or the enhancement of the mobility of these species in investigated treatment conditions. Density Functional Theory calculations are utilized to investigate the activation energy for the migration of extra-framework Al species in the neighbor of a Brønsted acid site. These results suggest that the H-bonds might kinetically trap extra-framework Al

species resulting in the generation of synergistic sites between these species and the proximal Brønsted acid site.

4.1 Introduction

Zeolites are utilized as catalysts for many important reactions in the chemical industry due to their diversity in the framework topologies with a wide range of sizes and shapes.[1, 2] Active sites in zeolites are framework Al atoms that react as Brønsted acid sites. Depending on the reactions in which these protons participate, their activity might be influenced by the presence of proximal protons or EFAL species, which can modify the surrounding environments of these active sites.[3-9] It was previously reported that the active sites are identically reactive in various H-MFI zeolites samples with a wide range of Al content (Si/Al =15-10,000).[10] However, another explanation for these results is that these investigated samples have similar distributions of specific protons.[11] On the other hand, many recent studies reported that the reactivity of protons in pairs in zeolites is significantly different from the ones of isolated active sites in various reactions such as oligomerization [12, 13] and alkane cracking.[14, 15] To investigate the structure-function relations, it is crucial to develop synthesis pathways to control the distribution of Al, which are the focus of some recent works.[16]

While it is generally accepted that EFAL species are essential for the reactivity of alkane cracking reaction, the generation and nature of these species are not completely understood. In addition, how these species influence the activity of their proximal BAS is an issue of debate. There are several ways to modify the concentration of these EFAL species in zeolite catalysts. The most common way to generate more EFAL species is the exposure of zeolite to high-temperature conditions in the presence of water. Under these conditions, Al atoms

slip out of their framework structures, which results in a loss of BAS density and the permanent decay of the catalysts.[17-21] Steam conditions and catalyst properties might strongly affect the dealumination process. Steaming under mild conditions usually positively affects the reactivity of zeolites for cracking reaction via the generation of synergistic EFAL-BAS sites. However, the reactivity will reach a maximum and decrease with further treatment because, in steaming conditions, EFAL can be mobilized and form aluminum clusters. On the other hand, dealumination can also be done by several post-synthesis modifications such as chemical treatment with EDTA,[22] $(NH_4)_2SiF_6$,[23], or washing with HCl and other acids.[24] These treatments usually remove most EFAL species, which results in a significant decrease in the cracking rate. By using mild conditions for these treatments, the loss of BAS can be minimized. However, it is challenging to preserve all active sites in many cases since hydrolysis of framework Al happens quickly, even at room temperature conditions. After removing EFAL species by ammonium hexafluorosilicate (AHFS) treatment, the following treatment by steaming can significantly enhance the activity of hexane cracking on MFI zeolite.[25] On the other hand, Almutairi et al. reported that AHFS treated FAU zeolites have higher reactivity for propane cracking reaction than the parent zeolites.[26] They claimed that AHFS treatment removes EFAL species and next-nearest-neighbor framework Al atoms in these zeolites, which increases the acidity of acid sites. This is evidenced by the increase of OH stretching vibration on CO adsorbed samples and the enhanced H/D exchange reaction rate.[26] These results suggest that zeolites having a low Si/Al ratio with close distances between two Al atoms in pairs might negatively affect the alkane cracking, which contradicts with the previous results regarding the positive influence of the site proximity on this reaction.[14, 15] In general,

it is difficult to find a unique explanation for the catalytic reactivity of cracking reaction on zeolites, which is generally influenced by the distribution of framework Al and EFAL species.

The conventional methods to extract framework Al atoms and convert them to EFAL species as steaming is challenging to control the fate of these Al species. Thus, it is highly desirable to develop a model zeolite free of EFAL species to which EFAL species are introduced in a controlled manner. Based on this idea, Almutairi et al. attempt to add EFAL species into AHFS treated Y zeolites by incipient wetness impregnation method and ion exchange using $Al(NO_3)_3$ solution.[26] The authors observed an increase in propane cracking rate on those samples, attributed to a small fraction of cationic EFAL species introduced to these zeolites. These positively charged species are believed to be exchanged with protons associated with framework Al atoms and form synergistic sites with neighboring BAS. Another factor that many previous works have not considered is the critical impact of mobility of EFAL on the formation of these sites. For these reasons, in our previous work, we developed a pulsing water treatment method to investigate the mobility of these EFAL species without the modification of BAS density in zeolite samples.[9] Application of this treatment method will be helpful to understand how the structure of parent and modified zeolite can stabilize EFAL species to enhance the alkane cracking.

In the scope of this study, we use cation exchanges of sodium and calcium to investigate the influence of Al in pairs in different MFI zeolites samples. Different treatments of pulsing and steaming are applied to these zeolites, and their catalytic activities are measured by n-hexane cracking reaction. In addition, AHFS treatment is utilized to generate zeolites free from defects and EFAL species; then, we attempt to introduce EFAL

species into these samples by an exchange procedure. Activity before and after pulsing treatment of these modified zeolites will be evaluated the possibility to mobilize those species in zeolite pores and create highly active sites. After that, we investigate the different pretreatment methods of catalysts in water liquid and ammonium nitrate solutions, which help enhance the reactivity of these samples without modifying the number of active sites. Several hypotheses supported by DFT calculations will be proposed and discussed.

4.2 Experimental section

4.2.1 Catalyst preparation

NH_4-ZSM5 zeolites varying Si/Al ratios purchased from Zeolyst were calcined at 823K for 5h in an air flow to obtain the proton forms of the catalysts. The initial slow ramp rate of 2K/min was applied to minimize the hydrolysis of framework Al sites. After calcining, all catalysts in proton form are denoted as HZSM5-X_1, with X_1 being the corresponding Si/Al ratio. ZSM5-X_1-AHFS catalyst was obtained from the chemical treatment of ZSM5-X_1 zeolites with AHFS following the standard procedure to remove EFAL species.[27]

Preparation of partial cation exchanged zeolites. The HZSM-5 samples were exchanged in 0.02 - 0.5 M $NaNO_3$ solution for 0.5 - 12 h at different temperatures using the ratio of 20 ml of solution per gram of catalyst. CaHZSM-5-15 samples were obtained by exchanging 1g HZSM-X_1 zeolites with 90 ml 0.25 M $Ca(NO_3)_2$ solution for 24 h. Afterward, the mixture was centrifuged, and the solid was washed with deionized water 5 times to remove residual nitrate salts. The samples were dried overnight in a vacuum oven at 353 K and calcined at 823 K for 5h before being used for testing reactivity. The obtained catalysts are denoted as NaHZSM5-X_1 (Y, Z, T) and CaHZSM5-X_1 (Y, Z, T). X_1 is the corresponding Si/Al ratio, Y (M), Z (K), and T (h) are the concentration of cation in the

exchange solution, the temperature, and the time duration of the cation exchange procedure.

Preparation of EFAL added samples. 1g of HZSM5-25 or HZSM5-15-AHFS in the proton form was stirred with 20 ml solutions at varying concentrations of $Al(NO_3)_3$ for 3 hours. Catalysts were then washed and centrifuged three times with water, dried, and calcined as previously described. The obtained catalysts were noted as HZ5-25-Al-X_2 M, and HZ5-15-AHFS-Al-X_2 M, with X_2 being the concentration of $Al(NO_3)_3$ solutions.

Preparation of zeolites treated with liquid water and ammonium nitrate solutions. 1g of catalysts was exposed to a 20 ml solution of water or ammonium nitrate for 3 hours at 343 K. The obtained catalysts were centrifuged and calcined at the conditions previously described. These samples are noted as HZ5-NH4-X_3 M, with X_3 being the concentration of NH_4NO_3 solution. HZ5-NH4-0.5M-Al-0.05M was obtained by adding EFAL species to the catalysts treated with NH_4NO_3 0.5M solution. The procedure was previously described.

Water pulsing catalysts. After calcination, pelletized zeolite samples were packed into the micro-reactor and exposed to 40 intermittent pulses of water at 480^oC with partial pressures of 18.6 kPa. The break time between two pulses is 10 minutes. The catalysts are then dried overnight, and their activity is measured in-situ in that pulse reactor. The other conditions are described in detail in our previous work.[9]

4.2.2 Catalyst Characterization

Brønsted acid density measurement. The temperature-programmed desorption of isopropylamine (IPA-TPD) was utilized to quantify the density of BAS in all zeolite samples. The procedure was described elsewhere.[9] In brief, 5 - 100 mg catalysts pelletized

to 0.25 − 0.35 mm particles and mixed with glass beads were utilized for this measurement. The samples were dried at 753 K for 2 h to remove physically adsorbed water and cooled to 373 K for adsorption of IPA. The catalysts were exposed to 2 µl pulses of IPA to ensure the saturation of IPA uptake and were flushed by a 30 ml/min He flows for a few hours to remove weakly adsorbed IPA. After that, the temperature was increased to 873 K with a 10 K/ min heating ramp. A peak of released propylene was observed at the temperature range of 623 - 663 K. The propylene was quantified using an MKS Cirrus mass spectrometer or a GC MS-FID system. The moles of propylene were calibrated with several 500 µL pulses of propylene at a known temperature and pressure condition.

4.2.3 Kinetic measurements

The catalyst activity was measured by the n-hexane cracking reaction in a micro-pulse reactor. The experimental details were described elsewhere.[9] In brief, 5-70 mg of catalyst pelletized to 0.24-0.35 mm particles were utilized for the reaction, which occurs at 753 K and 120 kPa pressure in Helium. Before reaction, the pretreatment of catalysts to remove resident moisture was conducted at the reaction temperature for 2h. Several pulses of 0.48 µmol hexane (3.7 mol % of hydrocarbon in He) were sent over the catalyst bed for the cracking reaction by a flow of 75 mL/min He. The reaction conversion and the product distribution were determined by a GC MS-FID system utilizing a HP-PLOT/Al_2O_3/"S" column.

4.3 Results and discussion

4.3.1 Role of Al in proximity on alkane cracking

As shown in Figure 22, the activities per site of HZSM5 samples with Si/Al = 15 and 11.5 for alkane cracking reaction decrease significantly when a fraction of BAS is titrated with

calcium cations. This result suggests that the Al in pairs being exchanged with calcium are associated with synergistic sites, which have a high activity for this reaction. The activity of HZSM5-15 is significantly higher than that of HZSM5-11.5, which might be associated with a higher fraction of EFAL species in this zeolite sample.[9] This result might be explained by the higher BAS density of this catalyst leading to the formation of H bonds between the EFAL species and BAS. Meanwhile, it might require a certain distance between these two BAS and EFAL species to stabilize the reaction's transition state and form highly active sites inside the zeolites. Furthermore, a newly developed pulsing water treatment is applied to investigate how the influence of calcium titration on the rate enhancement of these catalysts. It is interesting to note that after pulsing water treatment, the activities of these two catalysts are comparable. This implies that a very high concentration of BAS might negatively affect the formation of highly active sites. More systematic studies are needed to address the influence of the distance between Al-Al sites and see how these species can help to stabilize a nearby EFAL species. It is also observed that the fraction of Al in pairs being exchanged with Ca in both samples is comparable (24-24.5%). This result suggests that calcium might prefer to titrate the Al in pairs at similar locations in both catalysts. In addition, when the HZSM5-15 catalyst is exchanged with a solution of $Ca(NO_3)_2$ 0.5 M, which is higher than the concentration of calcium cation used in Figure 22, no significant further decrease in the BAS density is observed, shown in Table 6. This result might be attributed to the repulsion between calcium atoms that inhibits the exchange rate of zeolite samples having a high concentration of these cations. Similar results were illustrated by the DFT results in the previous work for sodium exchange on Al in pairs.

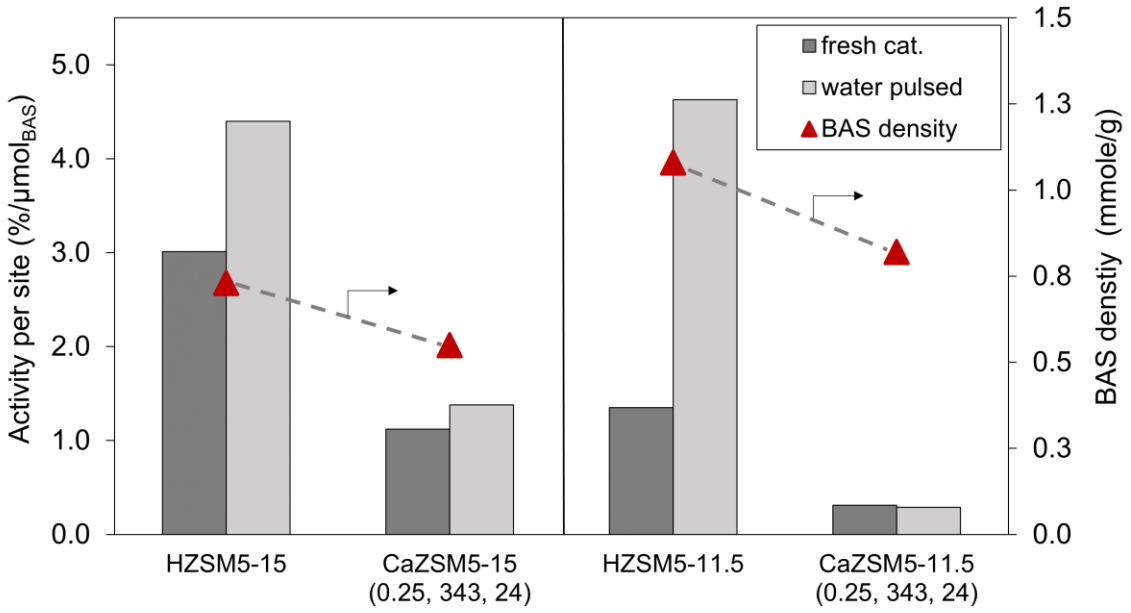

Figure 22. Activity per site of HZSM-5 catalysts exchanged with calcium before and after pulsing water treatment with their corresponding densities of BAS site. Reaction conditions: T = 753 K, P_{nC6} = 4.5 kPa with 0.48 µmol of hexane in each pulse. Water treatment condition: T = 480°C, partial water pressure as 18.6 kPa and 2.85 µmol of water in each pulse; the number of pulses of water is 30 pulses.

Table 6. Densities of framework Al and Al in pairs obtained by IPA-TPD of zeolite samples.

Sample	BAS density (mmol/g)	BAS loss [(1)] (mmol/g)	Al in pairs (mmol/g)
HZSM5-25	0.48	0	0.23 [(2)]
HZSM5-15	0.73	0	0.41 [(2)]
CaZ5-15 (0.5, 343, 72)	0.32	0.41	0 [(3)]
CaZSM5-15 (0.25, 343, 24)	0.55	0.18	0.23 [(3)]
CaZSM5-15 (0.5, 343, 72)	0.51	0.22	0.19 [(3)]
HZ5-15-AHFS	0.45	0.28	0.13 [(4)]
CoZ5-15-AHFS (0.25, 343, 24)	0.32	0.41	0 [(4)]
CaZ5-15-AHFS (0.25, 343, 24)	0.4	0.33	0.08 [(4)]
CaZ5-15-AHFS (0.5, 343, 72)	0.36	0.37	0.04 [(4)]

[(1)] loss of BAS density compared to the corresponding ones of parent zeolite.

[(2)] density of Al in pairs in MFI samples reported elsewhere.[28]

[(3)] calculated concentration of Al in pairs by subtracting the ones of parent zeolite to the ones of the sample after calcium and cobalt exchange, assuming that these divalent cations only titrate the Al in pairs.

[(4)] calculated concentration of Al in pairs by subtracting the ones of the AHFS treated sample estimated by cobalt exchange to those of the sample after calcium exchange.

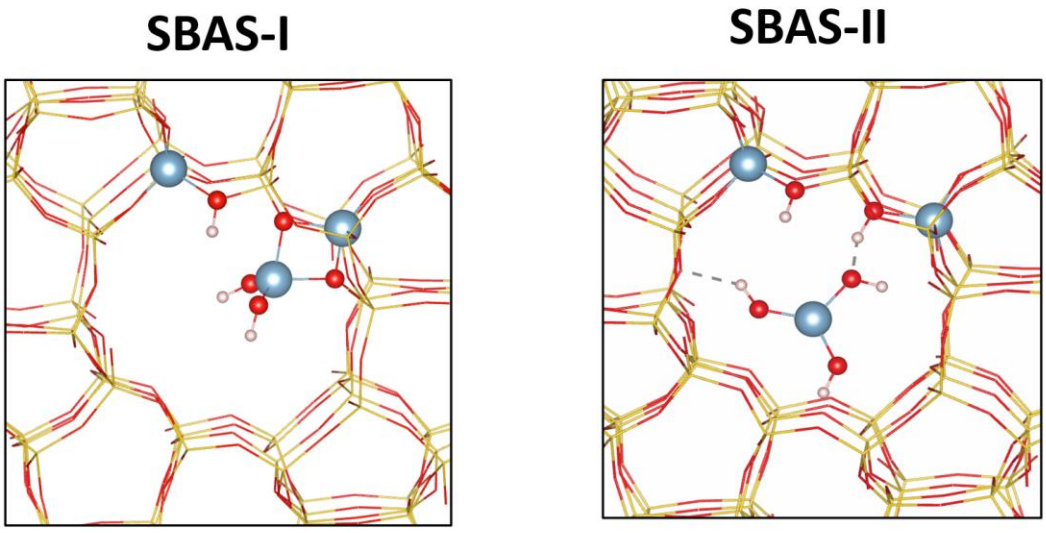

Figure 23. Proposed structure of two types of synergistic sites.

Our previous work claimed that there are possibly two types of synergistic sites co-presented in the MFI catalysts. An EFAL species and one BAS form one type, while the others contain a pair of framework Al atoms and one EFAL species. Al in pairs might play a crucial role in generating both types. The first type might be originated from a pair of Al-Al as one of the framework-Al atoms is hydrolyzed and converted to or stabilize an active non-framework Al species, shown in Figure 23. Meanwhile, Al in pairs might help stabilize the EFAL species resulting in the synergistic sites of the second type. After being titrated with calcium, it is noted that the activity per site of CaZSM5-15 is higher than that of CaZSM5-11.5. As stated previously, repeating the exchange procedure with a higher calcium concentration does not lead to a further decrease in the cracking rate per proton, suggesting the highly active sites are not associated with Al in pairs. Thus, this result can be attributed to a faction of synergistic site type 1 in HZSM5-15, which is not titrated by calcium.

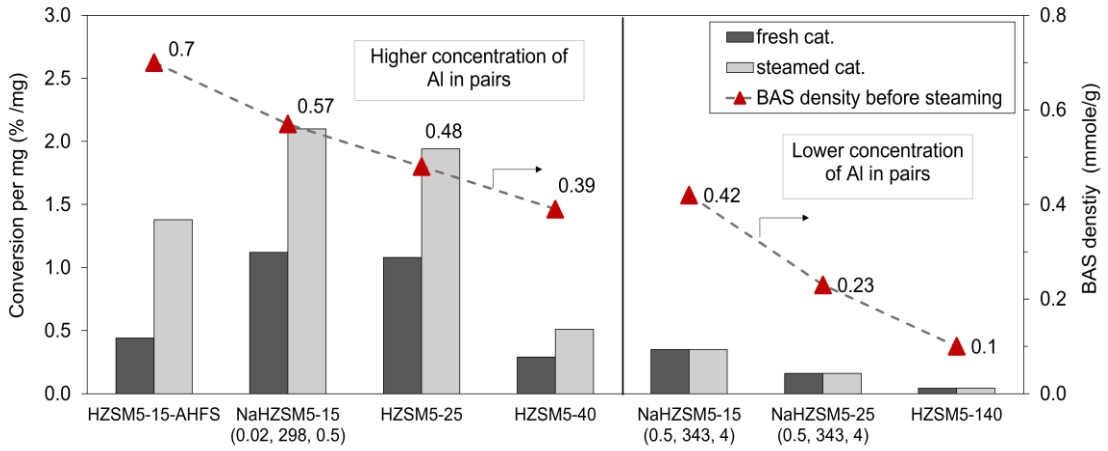

Figure 24. Activity per site of HZSM-5 catalysts exchanged with calcium before and after water steaming treatment. The corresponding BAS density of the catalyst before steaming treatment was plotted. Reaction conditions: T = 753 K, P_{nC6} = 4.5 kPa with 0.48 µmol of hexane in each pulse. Steaming condition: T = 480°C, partial water pressure as 18.6 kPa, the steaming time as 0.5 - 4 hours, maximum reactivity is plotted.

As reported in our previous work, there are several catalysts in which we did not observe the rate enhancement under pulsing water. These include the samples with an insignificant amount of EFAL speices (HZSM5-15-AHFS, HZSM5-40, and HZSM5-140) and catalysts exchanged with sodium (NaHZSM5-15, NaHZSM5-25) and the parent HZSM5-25. To investigate the influence of Al in pairs in the formation of highly active sites, we exposed these catalysts to steam conditions at high temperatures and observed the modification of the activity. The highest activities obtained are reported in Figure 24. Not as pulsing water, steam treatment usually leads to the hydrolysis of framework Al. Synergistic sites will be generated if the resulting EFAL species are stabilized in the nearby BAS sites. The results in Figure 24 show that the rate enhancement under steaming treatment is only observed on the catalysts with high Al fractions in pairs. Our previous work claimed that sodium

exchange might titrate a significant amount of Al in pairs. Thus, even though HZSM5-15 has the same BAS density as HZSM5-40, its activity does not enhance under investigated conditions.

In this section, we showed that Al in pairs is essential for generating synergistic sites under both pulsing and steam treatments. In the pulsing treatment, the cracking rate is enhanced due to the formation of synergistic sites without the modification of BAS density. The role of Al-Al pairs in stabilizing the EFAL species is possibly attributed to the generation of hydrogen bonds between the EFAL species with one of the BAS sites. This interaction might help stabilize the non-framework Al species better and kinetically trap them in the pulsing treatment. Meanwhile, in steaming treatment, the mobility of EFAL species is more vigorous, and the weak interaction as hydrogen bonds might not be sufficient to trap EFAL species and form SBAS-II. On the other hand, in this steaming condition, the hydrolysis of framework Al atoms likely happens on one Al atom of Al-Al pairs, which facilitates the formation of SBAS-I.

4.3.2 Modification of reactivity by adding EFAL species

As previously reported, the incipient wetness impregnation can strongly affect the mesoporous surface due to the formation of larger aluminum oxide clusters at the external surface of the zeolites sample.[26] To void this, EFAL species are added to HZSM5 catalysts by cation exchange procedure in this study. The activities of the resulting catalysts are measured before and after the catalysts are treated by pulsing treatment. Since this water treatment does not modify the BAS densities of the catalysts and only facilitates the mobility of the EFAL species, it was used here to investigate the influence of zeolite structures in stabilizing these added EFAL species. Figure 25 represents the activity of

parent HZSM5-5-15 and samples after treatment with aluminum nitrate solution. The modification of the BAS density of this MFI zeolite is not observed on investigated catalysts, which is different from the previous results reported for Y zeolites elsewhere.[26] This work attributed the loss of BAS density in Y zeolite to the number of framework-Al atoms exchanged with added cation EFAL species. The differences in the topologies of two types of zeolites, their Si/Al ratios, and Al distribution might strongly influence the rate of Al exchange, explaining the insignificant loss of BAS density in MFI zeolite compared to Y zeolite.

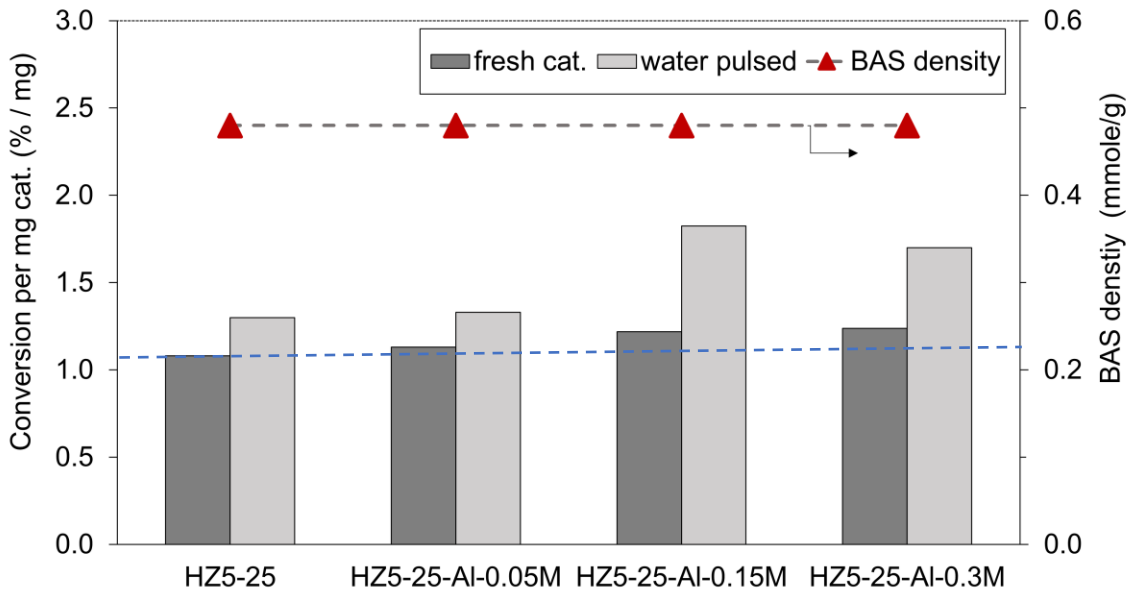

Figure 25. Activity per site of HZSM5-25 catalyst exchanged with aluminum nitrate before and after pulsing water treatment. The corresponding BAS density of the catalyst was plotted, noted that pulsing treatment does not change the density of BAS. Reaction conditions: T = 753 K, P_{nC6} = 4.5 kPa with 0.48 µmol of hexane in each pulse. Water

treatment condition: T = 480°C, partial water pressure as 18.6 kPa and 2.85 µmol of water in each pulse; the number of pulses of water is 30 pulses.

At higher concentrations of $Al(NO_3)_3$ solution, there is no apparent enhancement for hexane cracking rate. We only observed a slight increase in the rate with $Al(NO_3)_3$ 0.15-0.3M solutions. These results suggest that the added EFAL species in these samples are still not located near a BAS, or they are not in the active forms to generate highly active sites. However, after pulsing treatment, we observed a significant increase in the cracking rate compared to the corresponding ones of parent zeolites. This result suggests that added EFAL species might be converted into active forms and migrate inside the micropores to form BAS-EFAL synergistic sites in the pulsing treatment. However, the positive effect of increasing the concentration of $Al(NO_3)_3$ on the rate enhancement under pulsing treatment is not observed. It is not clear how to control the mobility of these EFAL species in zeolite pores. With a higher concentration of the added EFAL species presented on the external surface of zeolites, these might be aggregated to form clusters before moving inside and creat synergistic sites, which is similar to using incipient wetness impregnation. In addition, a high fraction of EFAL species in this catalyst might inhibit the mobility of added EFAL species.

Another factor that can strongly influence the formation of new highly active sites by aluminum treatment is the ability of the structure to stabilize these EFAL species. As being discussed in the previous section, it is hypothesized that Al in pairs might kinetically trap those EFAL species in the pulsing treatment. The density of those Al in pairs and their location is essential in forming those highly active sites. Thus, the number of synergistic sites formed cannot exceed a particular value even if a high concentration of EFAL species

is added to the zeolite structure. Thus, it is difficult for HZSM5-25 to stabilize more EFAL species due to its high concentrations of these species, leading to the lower potential to enhance the cracking rate by this method. One can expect that if the zeolite structures are free from the EFAL species and have more Al in pairs at the desirable location, they will likely be able to uptake more EFAL species from outside sources resulting in catalysts with high activity. Based on this idea, we extract EFAL species from HZSM5-15 by AHFS treatment. The conditions of these treatments will strongly affect the hydrolysis of framework Al atoms, which is not investigated in the scope of this study. Unfortunately, it is impossible to reserve all the active sites in the parent zeolites under the investigated conditions of AHFS treatment, and the BAS density decreases from 0.73 mmol/g to 0.45 mmol/g. After AHFS treatment, we attempt to add EFAL species by the same exchange procedure for HZSM5-25. The activities of the obtained catalysts before and after pulsing water treatment are reported in Fiure 26. Similar to the previous results of HZSM5-25, the BAS density of this catalyst is not changed by the exchange procedure, which is comparable to those of HZSM5-25.

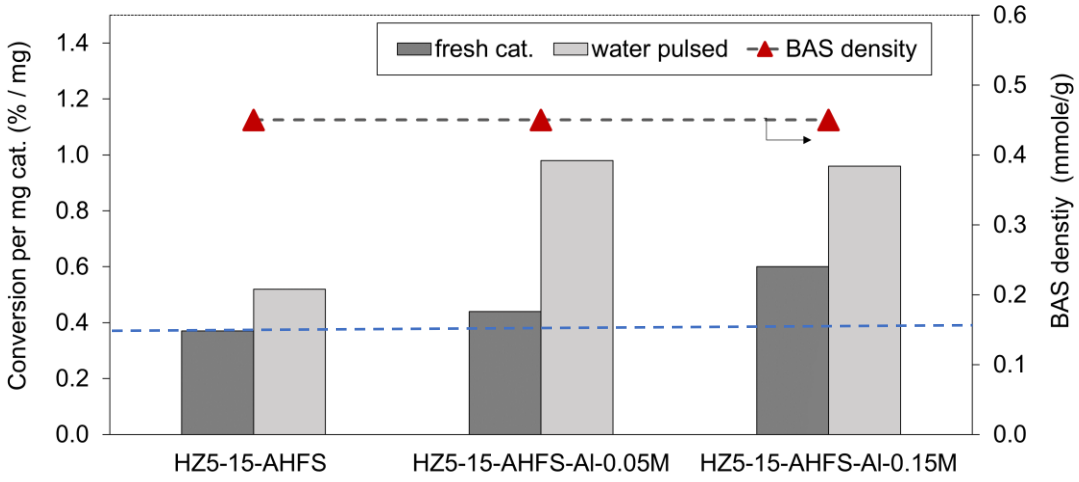

Figure 26. Activity per site of HZSM5-15-AHFS catalyst exchanged with aluminum nitrate before and after pulsing water treatment. The corresponding BAS density of the catalyst was plotted, noted that pulsing treatment does not change the density of BAS. Reaction conditions: T = 753 K, P_{nC6} = 4.5 kPa with 0.48 µmol of hexane in each pulse.

Two catalysts are investigated to compare the ability of their structures to uptake more EFAL species: ones having a high concentration of EFAL species in the parent zeolites (HZSM5-25) and ones being free from these species (HZSM5-15-AHFS). Unlike the results of HZSM5-25, here we can observe the higher activity with increasing concentration of $Al(NO_3)_3$ in the exchange solution. This result suggests that it is easier for catalysts free of EFAL species to uptake more of these species than the others. Pulsing treatment was then applied to mobilize added EFAL species into the zeolite pores. Due to an insignificant amount of EFAL species in the treated AHFS catalyst, its rate enhancement under pulsing water treatment is limited. However, the activity of the HZSM5-15 catalyst after being treated with $Al(NO_3)_3$ 0.5 M can be doubled under pulsing treatment, which is significantly higher than the corresponding rate enhancement for HZSM5-25. These results

also suggest that HZSM5-15-AHFS has a higher potential to uptake more EFAL species than the parent HZSM5-15. It is also observed that increasing the concentration of $Al(NO_3)_3$ in the exchange solution does not result in a higher activity with pulsing water. The activity per mg of catalysts treated with $Al(NO_3)_3$ 0.05M and 0.15M solutions are comparable with parent HZSM5-25 but lower than that of HZSM5-15-Al-0.15. Several reasons can be used to explain these results. First, the mobility of those EFAL species in zeolite pores is challenging to control, which might affect the ability of catalyst structure to stabilize these species more. Instead of migrating toward the inside of zeolite pores, the EFAL species might aggregate to form aluminum clusters, which is similar to adding EFAL species by incipient wetness impregnation.[26] Second, the difference in the number of Al in pairs of those catalysts and their location can influence the stabilization of EFAL species in zeolite structure. The lower activity per gram catalyst of HZSM5-15-AHFS after adding EFAL species compared to those of HZSM5-25 might be attributed to its lower concentration of Al in pairs that can generate BAS-EFAL sites. In agreement with this argument, the ratio of maximum activity per mg of investigated catalysts after adding EFAL species (HZ5-25-Al-0.15M and HZ5-15-AHFS-Al 0.5M) is comparable with the ratio of their corresponding number of Al in pairs. Previous works used the cobalt exchange to estimate the number of Al in pairs in MFI zeolite and their location, which reported that HZSM5-25 and HZSM5-15 have 0.23 mmol/g and 0.41 mmol/g of these species, respectively.[28] In addition, we have shown in the previous section that Al in pairs being exchanged with calcium likely plays an essential role in the catalytic activity of the catalysts before and after pulsing treatment. Thus, in this work, cobalt and calcium exchanges are utilized to estimate the number of all paired BAS-BAS sites. The results of

these cation exchanges are shown in Table 6. After being exchanged with cobalt, the BAS density of HZ5-15-AHFS decreases from 0.45 mmol/g to 0.32 mmol/g. This indicates that the number of paired BAS-BAS in this catalyst is 0.13 mmol/g, which is significantly lower than the density of the Al in pairs in parent zeolite (0.41 mmol/g). Furthermore, the number of Al in pairs in CaZ5-15-AHFS samples are negligible while the ones in CaZSM5-15 samples are still significant. This result suggests the AHFS treatment selectively titrates the Al in pairs that are easily titrated by calcium in the parent zeolite, which are believed to play an essential role in forming synergistic sites. These results also suggest that AHFS treatment causes a significant loss of Al in pairs; thus, this catalyst structure could not stabilize the added EFAL species.

4.3.3 Pre-treatment of zeolite with ammonium nitrate

As illustrated in Figure 27, the activity per site of hexane cracking decreases significantly when a fraction of active sites is titrated by sodium. This result implies that, like calcium, sodium prefers to titrate the highly active sites in HZSM-5, which is reported in our previous work. The presence of EFAL might result in a more confined environment around the active sites, which increases the rate of the cation exchange reaction on these synergistic sites. When sodium exchanged catalysts are exchanged back with NH_4NO_3 in mild conditions, the BAS densities of these catalysts remain unchanged, but the activities increase significantly. Compared to the parent zeolites, their higher activity per site indicates a higher fraction of highly active sites in these catalysts. One hypothesis to explain these results is that synergistic sites titrated by sodium are preferred to exchange back to proton form with ammonium nitrate treatment. However, it is unlikely that the two directions of the same exchange reaction are favorable to happen on the same sites. Another

hypothesis is that the rate increase after ammonium nitrate treatment is related to the mobility of EFAL species under these treatment conditions and the following calcium procedure. To further investigate this hypothesis, parent HZSM-5 zeolites are exposed to NH_4NO_3 0.5M solutions, and the activities of resulting catalysts are measured and presented in Figure 28. The activity of the catalyst treated with liquid water and pulsing water at high temperature in the vapor phase are also reported for comparison purposes.

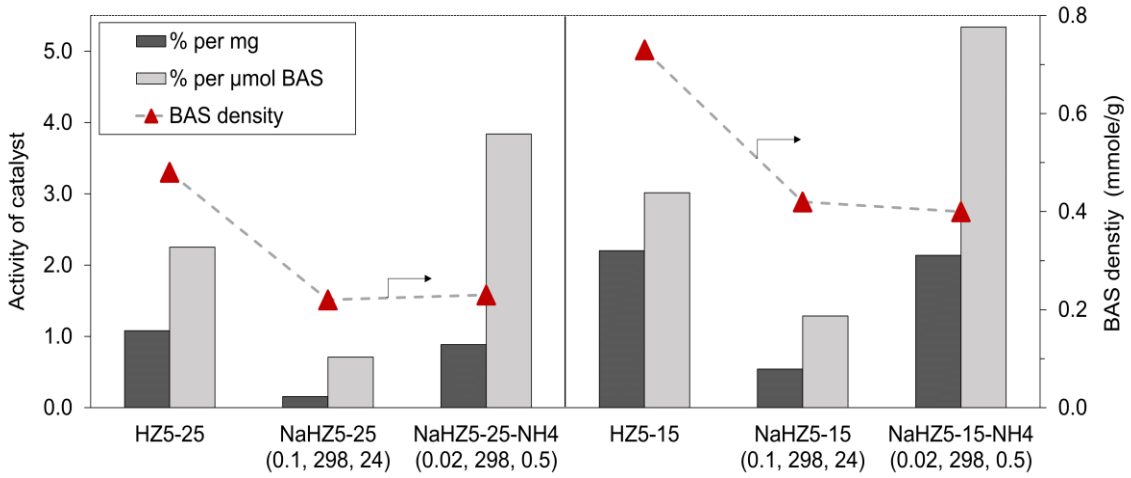

Figure 27. Activity of hexane cracking on HZSM-5 (Si/Al = 15, 25) in the parent samples, sodium exchanged catalysts, and back exchanged samples. The corresponding BAS density of the catalyst was plotted. Reaction conditions: T = 753 K, P_{nC6} = 4.5 kPa with 0.48 µmol of hexane in each pulse.

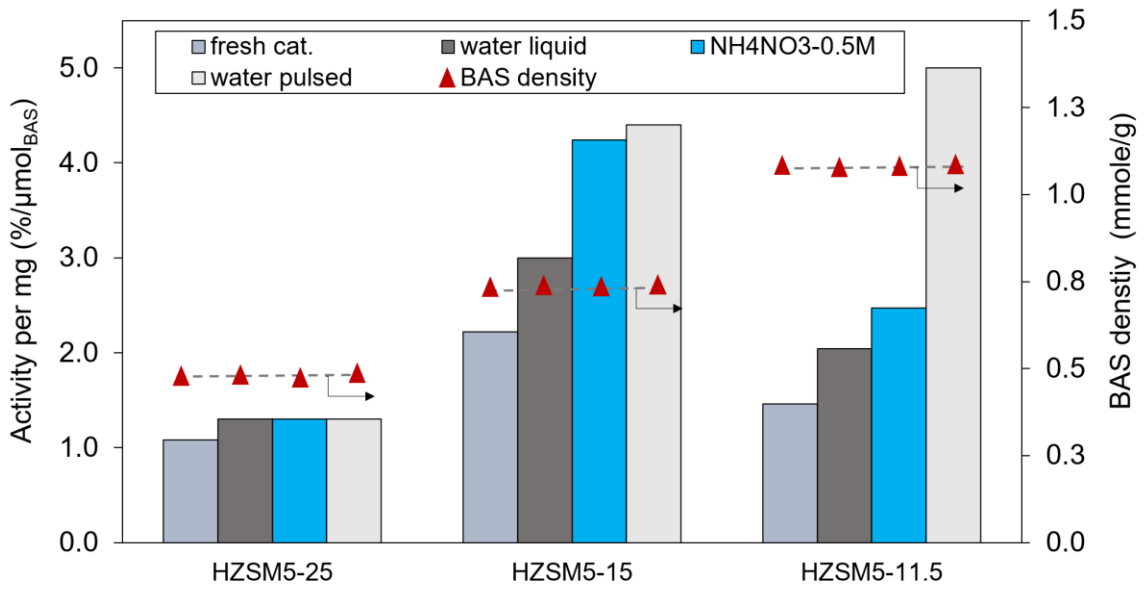

Figure 28. Activity of hexane cracking on HZSM-5 (Si/Al = 15, 25, and 11.5) in parent zeolite and after exposure to various treatments. The corresponding BAS density of the catalyst was plotted. Reaction conditions: T = 753 K, P_{nC6} = 4.5 kPa with 0.48 µmol of hexane in each pulse.

It is important to note that these treatments in both liquid and vapor phases do not lead to the modifications in the BAS densities and facilitate the hydrolysis of framework Al atoms to form EFAL species. Meanwhile, the mobility of EFAL species inside the zeolite pores and the ability of zeolite structure to stabilize EFAL species can strongly affect the formation of SBAS-II. The presence of these highly active sites eventually leads to changes in the reactivity of zeolites.

It is interesting to note that even water liquid treatment can slightly enhance the reactivities of these catalysts. Within different investigated treatments, pulsing water at high temperatures is the most effective method to facilitate the mobility of EFAL species, evidenced by the highest activity observed for hexane cracking reaction. None of these

treatments can significantly increase the reactivity of HZSM5-25, which might be attributed to its low density of Al in pairs. In addition, it is possible that due to a high concentration of EFAL species, this catalyst has a high fraction of framework Al atoms forming hydrogen bonds with EFAL species. This hydrogen bond network might inhibit the mobility of EFAL species and the formation of highly active sites under this treatment. In the case of HZSM5-11.5, the increase in the cracking rate is less pronounced in ammonium nitrate treatment compared to the ones associated with pulsing water. Meanwhile, the rate enhancements of HZSM5-15 by pulsing water and ammonium nitrate treatment are comparable. To explain these results, HZSM5-11.5 has a higher density of Al in pairs that can generate synergistic site type II. Thus, it might require higher energy to mobilize EFAL species from highly active sites, which can be affected by the hydrogen bond network inside this catalyst with high BAS density. In addition, in our separate work, DFT calculations have shown that EFAL species located very close to acid sites and forming hydrogen bonds with that acid site do not positively affect the cracking rate as the ones located at the next nearest neighbor configuration. This result implies that the location of Al in pairs and the distance between Al in pairs also influence the formation of synergistic sites.

We next investigate the influence of ammonium nitrate concentration on the catalyst's reactivity and compare it with the effect of adding EFAL species using $Al(NO_3)_3$ as a precursor. HZSM-5 (Si/Al = 11.5) is utilized because it has a high potential to generate more synergistic sites using ammonium nitrate pre-treatment. It has been shown in Figure 29 that increasing the concentration of ammonium nitrate in the zeolite pre-treatment can significantly enhance the catalytic activity. This effect is similar to pre-treat the catalyst at

a lower concentration of ammonium nitrate followed by a treatment of the zeolite sample with $Al(NO_3)_3$ solution. Even the as-synthesized samples with various pre-treatments have a different activity; the catalytic activities of these catalysts are comparable after pulsing water treatment. The catalyst might reach the limited number of synergistic sites that can form inside this sample. With these experiments, we have shown that the generation of highly active sites inside the zeolite pores is a very dynamic process. In addition, several methods could be applied to modify the concentration of EFAL species and their mobility inside zeolite pores, resulting in higher activity catalysts via the generation of more synergistic sites.

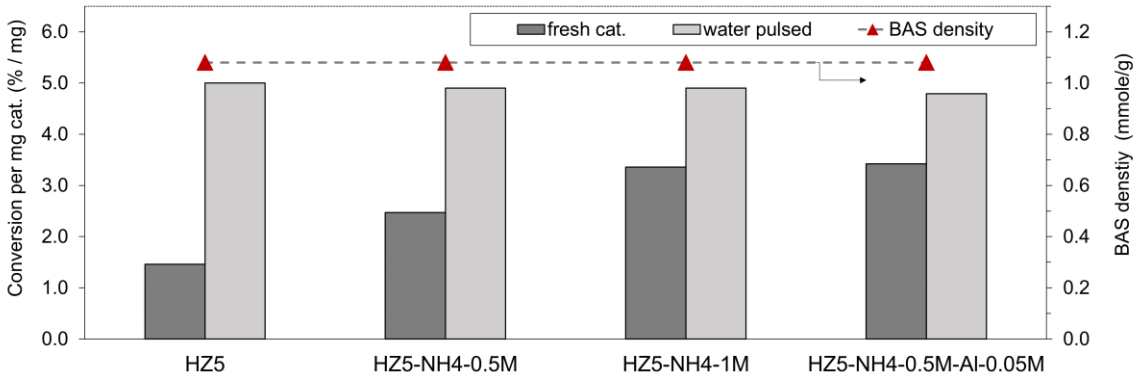

Figure 29. Activity of hexane cracking on HZSM-5 (Si/Al = 11.5) exposed to various treatments. The corresponding BAS density of the catalyst was plotted. Reaction conditions: T = 753 K, P_{nC6} = 4.5 kPa with 0.48 µmol of hexane in each pulse.

4.3.4 Transformation and mobility of EFAL species

The transformation and mobility of EFAL species can be affected by the acidity ofsolutions in the treatment. Solutions with higher concentrations of ammonium nitrate also have lower pH values. It is possible that EFAL species are easier to mobilize in the

acidic environment, or they are converted into active species needed to form highly active sites. In this study, several hypotheses are proposed to explain the observed experimental results using DFT calculations. The reaction energies of transformation of EFAL species in Faujasite zeolite are previously reported by Lui et al.[29] The reactions converting AlOOH into $[Al(OH)_2]^+$ and $[AlO]^+$ into $[Al(OH)]^{2+}$ in the presence of protons are endothermic. As a result, in a low pH environment such as ammonium nitrate solutions, likely, $[Al(OH)_2]^+$ and $[Al(OH)]^{2+}$ are favorably generated. These species might easily mobilize inside the zeolite pores and help stabilize the transition state of cracking reaction on the neighboring BAS than the other EFAL species. This hypothesis can explain why the cracking rate is enhanced by ammonium nitrate treatment.

Scheme 3. Transformation of EFAL species in Faujasite zeolite obtained elsewhere.[29] Energies are reported in kJ/mol.

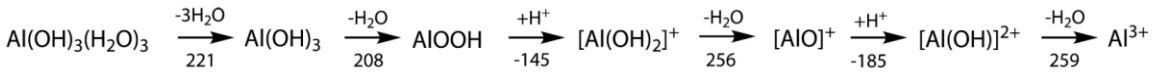

Another factor that can influence the generation of highly active sites is the ability of zeolite structure to stabilize EFAL species, which is hypothetically related to the H bond networks in zeolites. To investigate the influence of the H bonds on the mobility of EFAL species, DFT is utilized to estimate the energy barriers required for this migration, shown in Figure 30. The investigated system includes a BAS and an EFAL speci

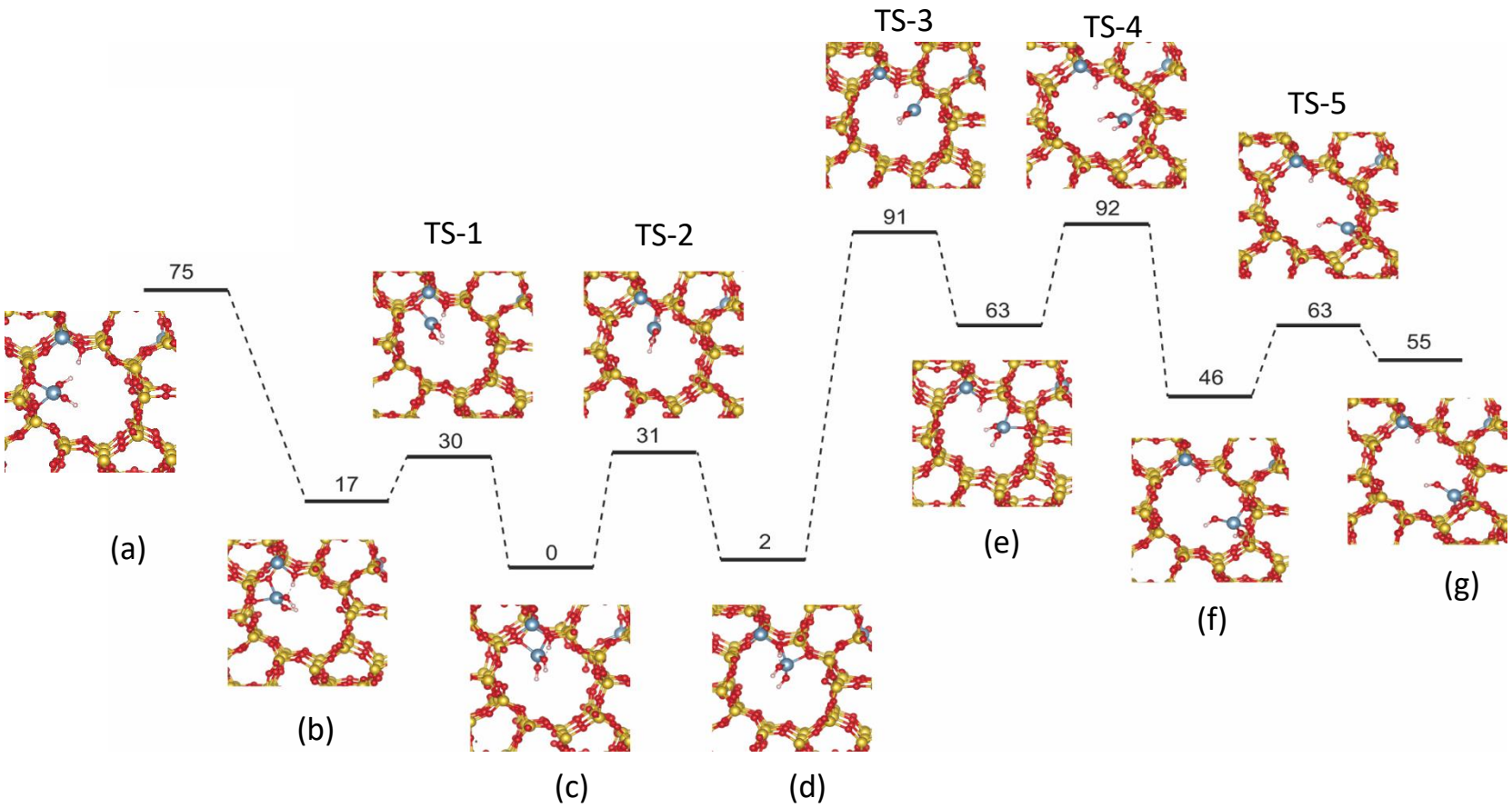

Figure 30. DFT calculations for the energies of Al(OH)2+ migration at the intersection of HZSM5. The energy unit is kJ/mol.

The results have shown that when the EFAL species can form H bonds with BAS easily (Figure 30 a → b) with no activation barrier. The energies of the systems having H bonds between BAS and EFAL (Figure 30 b, c, and d) are significantly lower than the others. Within these three positions, the activation energy for the migration of EFAL species is not profound, about 30 kJ/mol. However, the migration of the EFAL species further away from the BAS from (d → e) and (b → a) requires relatively high energy barriers (58-89 kJ/mol). This result suggests that it is difficult for EFAL species to migrate far away from BAS once H bonds are formed. In other words, EFAL species will be trapped nearby BAS by H bonds. As investigated in separate DFT works, these EFAL-BAS species do not correspond to the higher activity for alkane cracking reaction. However, if there is another neighboring BAS, these EFAL species might synergistically enhance the activity of that BAS. This result will explain why pairs of BAS are required to generate highly active sites. This result will explain the previous results about the generation of synergistic sites during pulsing treatment, in which the highly active sites are very stable under treatment conditions due to the formation of H bonds, as described in our previous work.[9] Furthermore, when EFAL species are far away from the BAS and their movements are not influenced by the presence of BAS, the energy barrier to migrate from (f) to (g) via the TS-5 is not sufficiently high. This result suggests that the migration of EFAL species in the absence of framework Al atoms inside the zeolite pores is typically not an energy-demanding process. While Al-Al pairs are essential for the formation of synergistic sites because the H bond can help trap the EFAL species kinetically, the close distance between BAS sites will negatively influence the generation of synergistic sites for catalysts having high densities of BAS such as HZSM5-11.5. As reported in our previous work, the number of synergistic sites in the

case of pulsed water HZSM5-11.5 is approximately half of the number of Al in pairs at the intersection. This result suggests that one Al in pairs at the MFI intersection can stabilize one EFAL species via H-bonds forming between the EFAL species and BAS.

4.5 Conclusion

This work demonstrates that Al in pairs is essential for generating synergistic sites during both pulsing water and steam treatments. The reactivity of zeolites might be enhanced by adding EFAL species followed by pulsing water treatment in which the role of pulsing water is hypothesized as enhancing the migration of EFAL species inside the zeolite pores. The comparison between adding EFAL species on parent HZSM5-25 and HZSM5-15-AHFS is investigated to illustrate the relationship between the rate enhancement and the potential of catalyst structure to stabilize these EFAL species, which is likely related to the concentration of Al in pairs in these catalysts. Furthermore, besides water treatments at high temperatures, exposure of zeolite to liquid water or ammonium nitrate solutions can significantly enhance the cracking reactivity of obtained catalysts. These treatments can either convert EFAL species into active forms or improve the mobility of these species leading to the formation of highly active sites. DFT calculations have shown that EFAL species can be trapped close by a BAS via the formation of H bonds between them. If the BAS forming H bond with EFAL speices has another BAS in proximity, new synergistic site might be formed.

REFERENCES

1. Haldoupis, E.; Nair, S.; Sholl, D. S., Pore size analysis of >250 000 hypothetical zeolites. *Physical Chemistry Chemical Physics* **2011,** *13* (11), 5053-5060.

2. First, E. L.; Gounaris, C. E.; Wei, J.; Floudas, C. A., Computational characterization of zeolite porous networks: an automated approach. *Physical Chemistry Chemical Physics* **2011,** *13* (38), 17339-17358.

3. Masuda, T.; Fujikata, Y.; Mukai, S. R.; Hashimoto, K., Changes in catalytic activity of MFI-type zeolites caused by dealumination in a steam atmosphere. *Applied Catalysis A: General* **1998,** *172* (1), 73-83.

4. van Bokhoven, J. A.; Tromp, M.; Koningsberger, D. C.; Miller, J. T.; Pieterse, J. A. Z.; Lercher, J. A.; Williams, B. A.; Kung, H. H., An Explanation for the Enhanced Activity for Light Alkane Conversion in Mildly Steam Dealuminated Mordenite: The Dominant Role of Adsorption. *Journal of Catalysis* **2001,** *202* (1), 129-140.

5. Yu, Z.; Li, S.; Wang, Q.; Zheng, A.; Jun, X.; Chen, L.; Deng, F., Brønsted/Lewis Acid Synergy in H–ZSM-5 and H–MOR Zeolites Studied by 1H and 27Al DQ-MAS Solid-State NMR Spectroscopy. *The Journal of Physical Chemistry C* **2011,** *115* (45), 22320-22327.

6. Schallmoser, S.; Ikuno, T.; Wagenhofer, M. F.; Kolvenbach, R.; Haller, G. L.; Sanchez-Sanchez, M.; Lercher, J. A., Impact of the local environment of Brønsted acid sites in ZSM-5 on the catalytic activity in n-pentane cracking. *Journal of Catalysis* **2014,** *316*, 93-102.

7. Maier, S. M.; Jentys, A.; Lercher, J. A., Steaming of Zeolite BEA and Its Effect on Acidity: A Comparative NMR and IR Spectroscopic Study. *The Journal of Physical Chemistry C* **2011,** *115* (16), 8005-8013.

8. Chen, K.; Abdolrahmani, M.; Horstmeier, S.; Pham, T. N.; Nguyen, V. T.; Zeets, M.; Wang, B.; Crossley, S.; White, J. L., Brønsted–Brønsted Synergies between Framework and Noncrystalline Protons in Zeolite H-ZSM-5. *ACS Catalysis* **2019**, 6124-6136.

9. Pham, T. N.; Nguyen, V.; Wang, B.; White, J. L.; Crossley, S., Quantifying the Influence of Water on the Mobility of Aluminum Species and Their Effects on Alkane Cracking in Zeolites. *ACS Catalysis* **2021,** *11* (12), 6982-6994.

10. Haag, W. O.; Lago, R. M.; Weisz, P. B., The active site of acidic aluminosilicate catalysts. *Nature* **1984,** *309* (5969), 589-591.

11. Haag, W. O., Catalysis by Zeolites – Science and Technology. In *Studies in Surface Science and Catalysis*, Weitkamp, J.; Karge, H. G.; Pfeifer, H.; Hölderich, W., Eds. Elsevier: 1994; Vol. 84, pp 1375-1394.

12. Mlinar, A. N.; Zimmerman, P. M.; Celik, F. E.; Head-Gordon, M.; Bell, A. T., Effects of Brønsted-acid site proximity on the oligomerization of propene in H-MFI. *Journal of Catalysis* **2012,** *288*, 65-73.

13. Bernauer, M.; Tabor, E.; Pashkova, V.; Kaucký, D.; Sobalík, Z.; Wichterlová, B.; Dedecek, J., Proton proximity – New key parameter controlling adsorption, desorption and activity in propene oligomerization over H-ZSM-5 zeolites. *Journal of Catalysis* **2016,** *344*, 157-172.

14. Song, C.; Chu, Y.; Wang, M.; Shi, H.; Zhao, L.; Guo, X.; Yang, W.; Shen, J.; Xue, N.; Peng, L.; Ding, W., Cooperativity of adjacent Brønsted acid sites in MFI zeolite channel leads to enhanced polarization and cracking of alkanes. *Journal of Catalysis* **2017,** *349*, 163-174.

15. Kester, P. M.; Crum, J. T.; Li, S.; Schneider, W. F.; Gounder, R., Effects of Brønsted acid site proximity in chabazite zeolites on OH infrared spectra and protolytic propane cracking kinetics. *Journal of Catalysis* **2021,** *395*, 210-226.

16. Bickel, E. E.; Nimlos, C. T.; Gounder, R., Developing quantitative synthesis-structure-function relations for framework aluminum arrangement effects in zeolite acid catalysis. *Journal of Catalysis* **2021,** *399*, 75-85.

17. Resasco, D. E.; Crossley, S. P.; Wang, B.; White, J. L., Interaction of water with zeolites: a review. *Catalysis Reviews* **2021,** *63* (2), 302-362.

18. van Donk, S.; Janssen, A. H.; Bitter, J. H.; de Jong, K. P., Generation, Characterization, and Impact of Mesopores in Zeolite Catalysts. *Catalysis Reviews* **2003,** *45* (2), 297-319.

19. Ong, L. H.; Dömök, M.; Olindo, R.; van Veen, A. C.; Lercher, J. A., Dealumination of HZSM-5 via steam-treatment. *Microporous and Mesoporous Materials* **2012,** *164*, 9-20.

20. Ravi, M.; Sushkevich, V. L.; van Bokhoven, J. A., Towards a better understanding of Lewis acidic aluminium in zeolites. *Nature Materials* **2020,** *19* (10), 1047-1056.

21. Chen, K.; Horstmeier, S.; Nguyen, V. T.; Wang, B.; Crossley, S. P.; Pham, T.; Gan, Z.; Hung, I.; White, J. L., Structure and Catalytic Characterization of a Second Framework Al(IV) Site in Zeolite Catalysts Revealed by NMR at 35.2 T. *Journal of the American Chemical Society* **2020,** *142* (16), 7514-7523.

22. Kooyman, P. J.; van der Waal, P.; van Bekkum, H., Acid dealumination of ZSM-5. *Zeolites* **1997,** *18* (1), 50-53.

23. Han, S.; Shihabi, D. S.; Chang, C. D., Selective Removal of Surface Acidity in ZSM-5 Zeolite Using (NH4)2SiF6 Treatment. *Journal of Catalysis* **2000,** *196* (2), 375-378.

24. Kumar, S.; Sinha, A. K.; Hegde, S. G.; Sivasanker, S., Influence of mild dealumination on physicochemical, acidic and catalytic properties of H-ZSM-5. *Journal of Molecular Catalysis A: Chemical* **2000,** *154* (1), 115-120.

25. Lónyi, F.; Lunsford, J. H., The development of strong acidity in hexafluorosilicate-modified Y-type zeolites. *Journal of Catalysis* **1992,** *136* (2), 566-577.

26. Almutairi, S. M. T.; Mezari, B.; Filonenko, G. A.; Magusin, P. C. M. M.; Rigutto, M. S.; Pidko, E. A.; Hensen, E. J. M., Influence of Extraframework Aluminum on the Brønsted Acidity and Catalytic Reactivity of Faujasite Zeolite. *ChemCatChem* **2013,** *5* (2), 452-466.

27. Garralón, G.; Fornés, V.; Corma, A., Faujasites dealuminated with ammonium hexafluorosilicate: Variables affecting the method of preparation. *Zeolites* **1988,** *8* (4), 268-272.

28. Janda, A.; Bell, A. T., Effects of Si/Al Ratio on the Distribution of Framework Al and on the Rates of Alkane Monomolecular Cracking and Dehydrogenation in H-MFI. *Journal of the American Chemical Society* **2013,** *135* (51), 19193-19207.

29. Liu, C.; Li, G.; Hensen, E. J. M.; Pidko, E. A., Nature and Catalytic Role of Extraframework Aluminum in Faujasite Zeolite: A Theoretical Perspective. *ACS Catalysis* **2015,** *5* (11), 7024-7033.

CHAPTER 5: Confinement effect in zeolites and its impact on cracking reactivity

ABSTRACT

It is generally accepted that the confinement in zeolites can influence the activity of the acid site through the adsorption or stabilization of the transition states of chemical reactions. On the other hand, as discussed in the previous chapters, the reaction rate of alkane cracking is strongly affected by highly active sites in zeolites. The confinement and topologies of zeolites might affect the formation of highly active sites due to their effects on the generation and stabilization of extra-framework Al species. Thus, it is crucial to reveal the influence of confinement on the reactivity of catalysts on the typical BAS and synergistic sites. This chapter investigates the cracking activity of seven zeolite structures, including FAU, BEA, MOR, MFI, MEL, FER, and TON, with varying densities of Brønsted acid sites extra-framework Al species. Activation energies of reaction reveal the effect of confinement on the activity of Brønsted acid sites. Catalytic activities are measured on fresh catalysts and samples after water treatment and sodium titration to evaluate the contribution of synergistic sites to cracking activity.

5.1 Introduction

Zeolites are likely the most widely used solid acid catalysts in the industry.[1-7] To design and utilize zeolites as solid acid catalysts, it is necessary to understand the impact of acid site density, materials structure, and acid strength on the catalytic performance. Furthermore, the local confinement and the intra-channel environment might affect the diffusion of molecules and the stabilization of adsorbed intermediates and transitions states. In previous chapters, we have shown that the rate of alkane cracking reaction in MFI is strongly influenced by the generation of synergistic EFAL-BAS sites. It is crucial to investigate further if these highly active sites exist in other zeolites and the impact of zeolite topologies and confinement on the formation of these sites.

The thermochemical cycle for alkane activation on zeolites is presented in Scheme 4. The acid strength is reflected in the deprotonation enthalpies (DPE) values. These values as 1201 ± 11 kJ mol^{-1}, estimated by DFT, are similar for all framework Al atoms in many investigated zeolites, including MFI, FAU, BEA, MOR, CHA, FER.[8] They do not show any trends with other properties that are usually utilized as indicators of acid strength, such as NH_3 adsorption enthalpies, angles of Si-O-Al bonds, or the length of O-H bonds.[8] Thus, previous works claimed that the differences in catalytic behaviors of different zeolites are not directly related to the acid strength of active sites.[8] Because proton affinities estimated in the gas phase are not affected by the zeolite types, the activation energy of the reaction is strongly influenced by the confining voids around active sites, according to Scheme 4-b. The confinement in zeolites affects the stabilization of intermediates and transition states of reactions, reflected in E_{stab}. The confinement effect of different zeolite structures on alkane cracking reaction has been investigated intensively in many previous works.[9-17] The

explanation for structure-activity relationships by the changes in the activation entropy or enthalpy depends on the reaction pathway (cracking vs. dehydrogenation) and on the alkane. For hexane cracking, previous works have reported that the observed rate of cracking reaction increases with the increasing confinement in the order Y < MOR < MFI.[14, 18] The authors attributed this result to an increase in the heat of adsorption and adsorption equilibrium constant while the intrinsic activation energies are unchanged over these zeolites.[14] For instance, the enthalpy of n-hexane adsorption in Y, MOR, and MFI is about 50, 69, and 86 kJ/mol, respectively.[18] Pore size might strongly influence the energies of alkane adsorption. However, the estimation of the heat adsorption in these studies does not correspond to a reactant state at BAS and is not obtained at the reaction conditions. Thus, the difference in the intrinsic kinetic parameters might be missed. Using Monte Carlo simulations to estimate the energies of alkane adsorption, Janda et al. reported the decreases of the intrinsic activation entropy and enthalpy of hexane consumption with increasing confinement in investigated 10-MR zeolites.[9] This result is different from the conclusions reported in the previous works that intrinsic activation enthalpy [18-22] and entropy [20, 22, 23] are independent of zeolite structure. One of the reasons that can explain these contradictory conclusions in the experiment data and computational simulation might be related to the presence of synergistic sites in zeolites, which strongly influences the alkane cracking rate. For instance, previous works have shown that steaming and hydrothermal treatment can significantly enhance the activity of several zeolites such as Y[18, 24-26], MOR[18, 27, 28] and MFI[18, 28-32] for alkane cracking reaction. The confinement might affect the dealumination process and the stabilization of EFAL species,[33] which eventually influences the generation of EFAL-BAS synergistic sites in zeolites. Thus, it is essential to decouple the effect of

confinement and the presence of synergistic sites on the rate of cracking reaction. In addition, it is desirable to understand the effects of enthalpy and entropy of cracking reaction on the typical and synergistic sites. If the values of E_{meas} of typical and synergistic sites are similar, the reaction rate is likely driven by activation entropies. In the opposite case, the difference in E_{meas} alone can be attributed to the influence of EFAL species on either the absorption of reactants (reflected by ΔH_{ads}) or the stabilization of transition states (reflected by E_{int}). In this case, the transition state with a lower activation enthalpy also has a lower activation entropy due to compensation effect, it is likely that the higher cracking rate on synergistic site is driven by a lower enthalpy.

This chapter aims to reveal the influence of zeolite structure and the generation of synergistic sites on the cracking rate in different zeolite frameworks. Here we investigated the cracking rate of hexane on various zeolite types with differences in pore sizes, the inter-channel networks, Si/Al ratios, etc. As previously reported, pulsing water treatment can significantly enhance the cracking rate on MFI zeolites with low Si/Al ratios without the modification of BAS density. In this work, pulsing water will be utilized to evaluate the potential for generating highly active sites in various zeolite samples. In addition, the activation energies for cracking reactions are estimated to investigate the effect of confinement and the presence of highly active sites in different zeolites.

Scheme 4. (a) Reaction Sequence for Monomolecular Alkane Activation on Brønsted Acid Sites Located within Zeolite Channels (H+Z-).a (b) Thermochemical Cycle for Monomolecular Reactions of Alkanes in Zeolite Channels. This scheme is adapted from Gounder et al. [34]

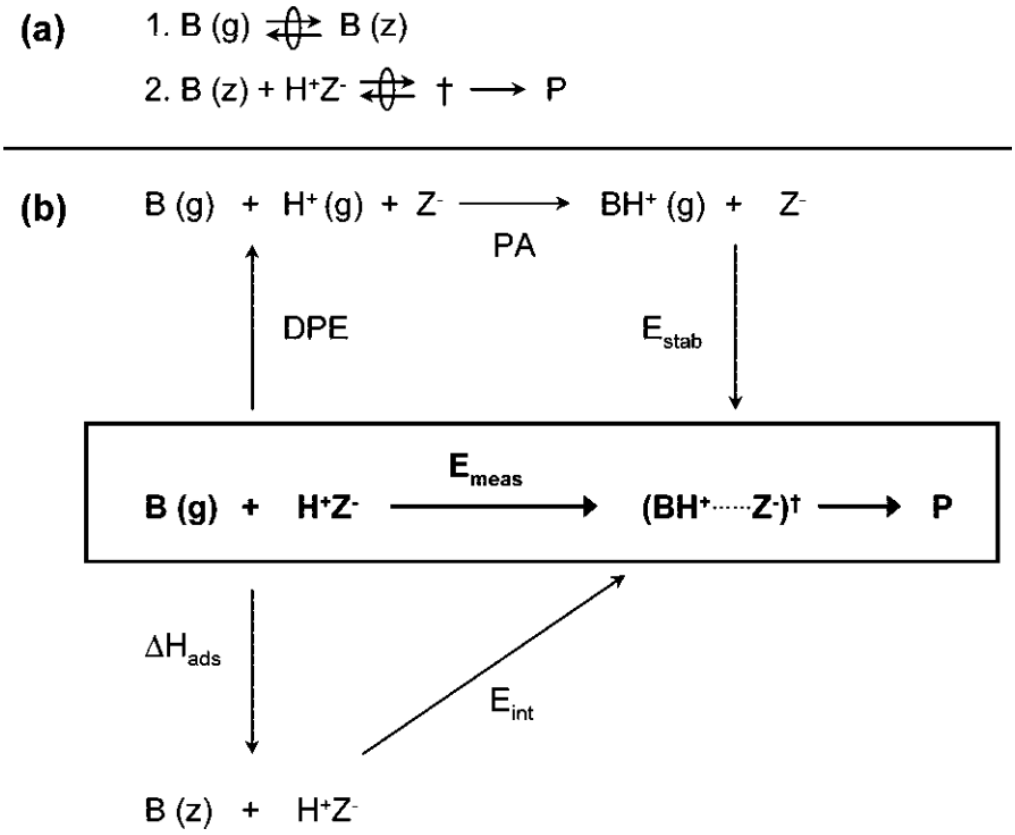

[a] B denotes a reactant base; P denotes products. [b] Measured activation energies (E_{meas}) are related to zeolite deprotonation enthalpies (DPE), gas-phase proton affinities (PA), and ion-pair stabilization energies within zeolite channels (E_{stab}).

5.2 Experimental section

5.2.1 Catalyst preparation

Zeolites varying Si/Al ratios purchased from Zeolyst were calcined at 823K for 5h in an air flow to obtain the proton forms of the catalysts. The initial slow ramp rate of 2K/min was applied to minimize the hydrolysis of framework Al sites. After calcining, all catalysts in proton form are denoted as framework type's name, followed by Si/Al ratio. ZSM5-X1-AHFS catalyst was obtained from the chemical treatment of ZSM5-X1 zeolites with AHFS following the standard procedure to remove EFAL species.[35] Sodium exchange zeolite samples were prepared by the standard exchange procedure in 0.05 - 0.5 M NaNO3 solution for 0.5 - 12 h at different temperatures using the ratio of 20 ml of solution per gram of catalyst**.**

5.2.2 Kinetic measurements

The catalyst activity was measured by the n-hexane cracking reaction in a micro-pulse reactor. The experimental details were described elsewhere.[36] In brief, 5-70 mg of catalyst pelletized to 0.24-0.35 mm particles were utilized for the reaction, occurring at 753 K and 120 kPa pressure in Helium. Before reaction, the pretreatment of catalysts to remove resident moisture was conducted at the reaction temperature for 2h. Several pulses of 0.48 μmol hexane (3.7 mol % of hydrocarbon in He) were sent over the catalyst bed for the cracking reaction by a flow of 75 mL/min He. The reaction conversion and the product distribution were determined by a GC MS-FID system utilizing a HP-PLOT/Al_2O_3/"S" column.

5.3 Results and discussion

5.3.1 Generation of synergistic sites in different zeolites

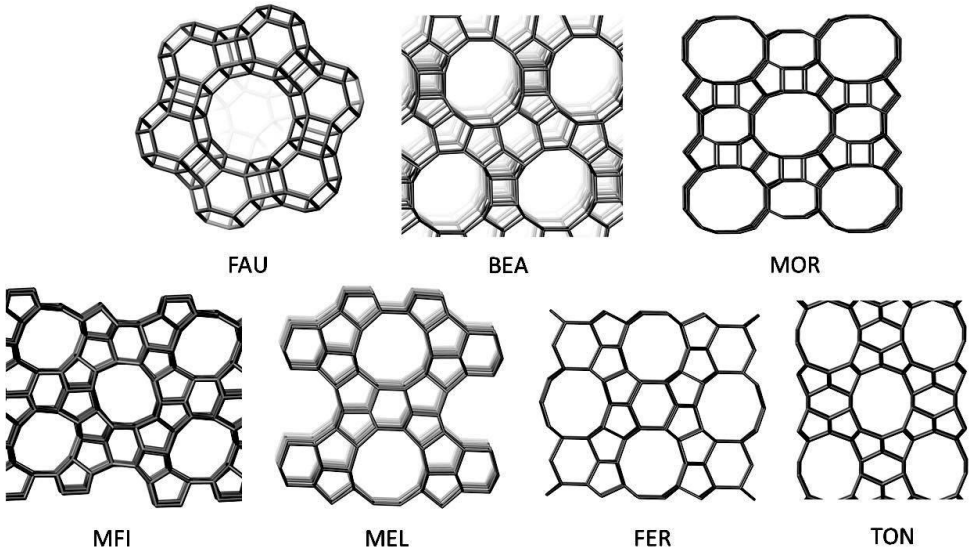

Figure 31. Structures of various zeolite frameworks.[37]

Table 7. Structural properties of investigated zeolites.

Zeolite	Ring sizes	Represented pore size (Å)[a]
FAU	12-6-4	7.35
BEA	12-6-5-4	5.95
MOR	12-8-5-4	6.45
MFI	10-6-5-4	4.46 -4.7
MEL	10-8-6-5-4	5.19
FER	10-8-6-5	3.4-4.69
TON	10-6-5	5.11

[a] Maximum diameter of a sphere that can diffuse along channels, adapted from [37].

Figure 31 and Table 7 present the pore structure of various zeolites samples and their properties in this study. In addition, Table 8 listed the properties of these zeolites and the corresponding activation energies of hexane cracking reaction estimated in the temperature range of 480 – 540 ^{o}C. These investigated zeolites are different in pore sizes and channel structures. To be more specific, FAU has big supper cages with 12-MR pores where most active sites locate and smaller sodalite cages with 6-MR voids. BEA zeolites only have 3D channels of 12-MR pores. MOR zeolites contain 8-MR side pockets connected to their multi-dimensional 12-MR channels zeolites. Although MFI and MEL zeolites have 10-MR structures with similar pore sizes, they have distinct 3D channel systems shown in Figure 1. MEL only has straight channels, while MFI contains straight and sinusoidal channels. Furthermore, FER zeolite has 2D channels that involve 10-MR and 8-MR pores; meanwhile, TON has only a 1D channel structure with 10-MR pores. More information about these zeolite frameworks can be found in the Database of Zeolite Structures.[37] FAU and FER zeolites have low Si/Al ratios and low BAS densities, which suggest that these catalysts have high concentrations of EFAL species. FAU may have a fraction of framework Al atoms located in the sodalite cages that are not accessible for isopropylamine (IPA), a probe molecule to estimate the number of active sites. These types of non-accessible acid sites are usually considered non-active sites. Not similar to FAU and FER, other zeolite samples having low Si/Al generally have high densities of BAS and EFAL species and vice versa. FAU, BEA, and MOR have 12-member ring (MR) channels with large void spaces. The remaining zeolite samples in this work have 10-MR channels with smaller void spaces, and they have different channel structures that can strongly affect the diffusion of molecules in the zeolite pores.

Table 8. The properties of investigated zeolite samples and the activation energies for hexane cracking on these catalysts.

Sample-Si/Al	Al density (mmol/g)			E_{meas} (kJ/mol)	
	Calculated[a]	Al_f [b]	EFAL[c]	Fresh cat.	Water pulsed
FAU-2.6	4.63	0.42	4.21	137	
BEA-19	0.83	0.562	0.268	-	
BEA-133	0.12	0.119	0.001	147.2	
MOR-10	1.52	1	0.52	110.6	99
MFI-11.5	1.33	1.08	0.25	97	76.2
MFI-140	0.12	0.11	0.01	107	
MEL-25	0.64	0.5	0.14	94	
FER-10	1.52	0.085	1.435	92	
TON-40	0.4-0.5	0.31	0.09 - 0.19		

[a] Theoretical BAS density calculated from Si/Al ratio.

[b] BAS density determined by IPA-TPD.

[c] EFAL density estimated by subtracting theoretical BAS density to the experiment ones.

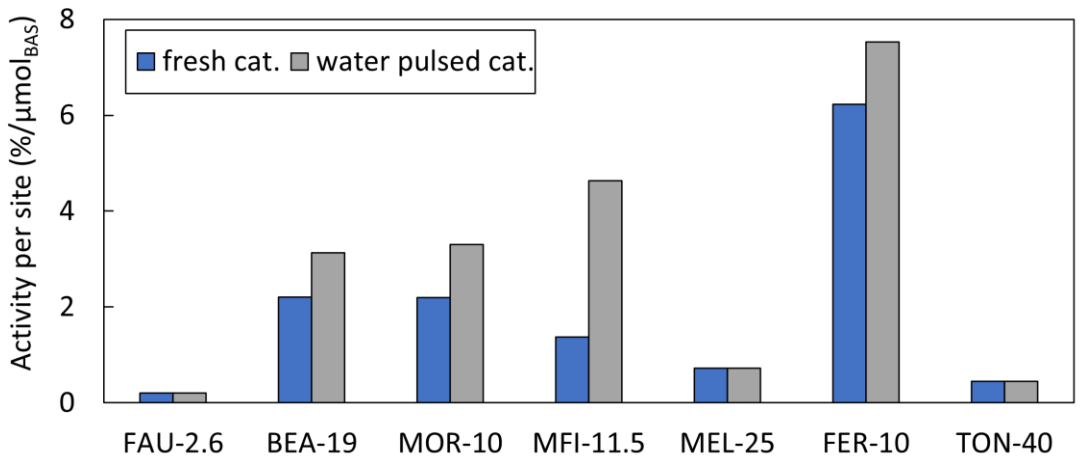

Figure 32. Rate of n-hexane cracking per site of different zeolites before and after pulsing water treatment. Reaction conditions: T = 753 K, P_{nC6} = 4.5 kPa with 0.48 µmol of hexane in each pulse.

According to Table 7, the general trend shows that the measured activation energies of hexane cracking are lower on zeolites with more confining void structures. These results agree with the higher cracking rate on more confined zeolites as FAU-2.6 < BEA-19 < MOR-10, presented in Figure 32. Besides 12 MR channels, MOR zeolite has 8 MR pockets, which are reported to have a higher alkane cracking rate due to their more confining void structures.[13] However, the cracking rates on other 10-MR zeolites such as MFI, MEL, FER, and TON are significantly different, although their pore sizes are comparable. In addition, it has been shown in our previous works that the formation of synergistic sites influences the cracking activities of MFI zeolite varying Si/Al ratios. These results indicate that these highly active sites might affect the reactivity more strongly than the confinement effect in the investigated zeolites in this study.

The potential to generate synergistic sites in fresh and water-treated zeolite samples can be predicted based on the BAS and EFAL density in Table 8. For instance, the cracking rate on BEA-19 (2 % conversion per μmol_{BAS}) at 480 ^{o}C is ~9 times higher than the one on BEA-113 (0.22 % conversion per μmol_{BAS}), which indicates the significant number of synergistic sites in these zeolite samples due to high concentration of EFAL species in this catalyst. In addition, the cracking rate of catalysts treated by pulsing water is significantly enhanced compared to the ones of parent zeolite. Similar results are observed for other low Si/Al catalysts such as MOR-10, MFI-11.5, and FER-10. In addition, significant shifts in the activation energies are observed for MFI-11.5 and MOR-10 after pulsing water treatment. As previously discussed, pulsing water does not change the density of BAS; thus, it cannot modify the distribution of framework Al. As a result, the observed rate enhancement under this treatment cannot be attributed to a higher rate on BAS-BAS pairs or the reactivity of active sites in more confining voids. Water treatments facilitate the formation of highly active sites, and the activation enthalpy required for cracking reaction on these sites is lower than the one on a typical BAS site. Although FAU-2.6 has a high fraction of EFAL species, pulsing water does not enhance the reactivity of this catalyst. This result is possibly related to the formation of EFAL clusters preferentially stabilized in sodalite cages of FAU.[38] It is also reported that the presence of such cationic EFAL clusters in these small cages can increase the propane cracking activity of the neighboring BAS.[38] Thus, once these clusters are formed, likely, water cannot mobilize them to generate more synergistic sites. On the other hand, the cracking activities of other zeolite samples having high Si/Al ratios, such as BEA-133, and MFI-140, are low because these catalysts only contain traditional BAS with low activity. In the absence of highly active sites, the

activation energy for cracking reaction on typical BAS in MFI-140 is lower than the one in BEA-133, which is likely associated with better stabilization of the transition states in more confining voids of MFI. In addition, it is interesting to note that MFI-25 and MEL-15 have similar Si/Al ratios, comparable BAS density, and pore sizes, but they have distinct reactivities. Thus, it is essential to reveal the effect of topologies on the generation of highly active sites in these two catalysts in further discussion.

So far, experiment data suggests that what we observed in MFI zeolite in our previous work is valid for different zeolites. In summary, the formation of highly active sites is influenced by the densities of BAS and EFAL species, which strongly influence the alkane cracking rate. The effect of zeolite confinement on the cracking rate is not as strong as the one of highly active sites. In the presence and absence of synergistic sites in the investigated zeolites, the higher rate of cracking reaction is driven by lower activation enthalpy, which is in contrast to the results obtained for propane cracking reactions in that reaction rate is driven by higher activation entropy, reported elsewhere.[39] However, the results in this study are in good agreement with our previous study showing a clear shift in the activation enthalpy of hexane cracking on synergistic sites versus the one on typical active sites.[36]

5.3.2 Selective titration of highly active sites by sodium

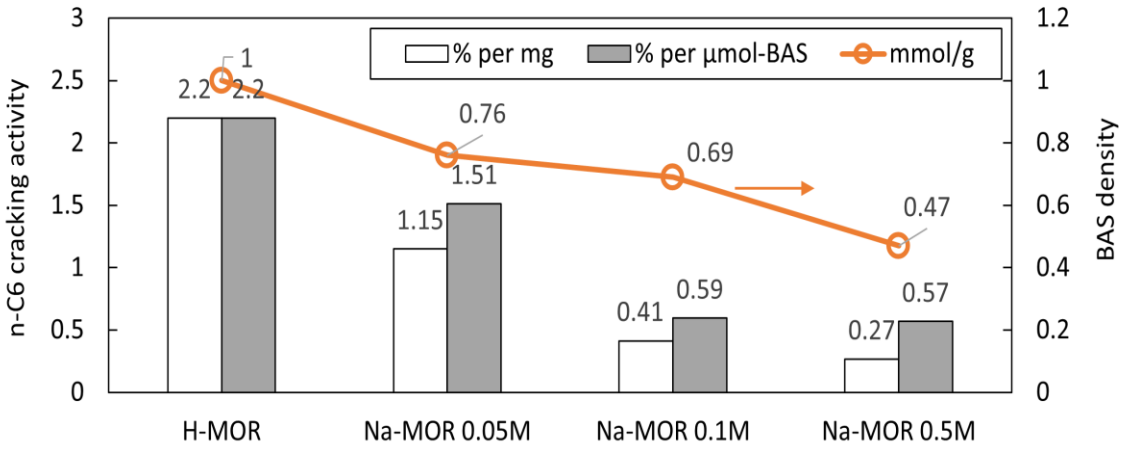

Figure 33. Rate of n-hexane cracking of fresh and sodium exchanged MOR zeolites (Si/Al =10). The corresponding BAS density of the catalyst was plotted. Reaction conditions: T = 753 K, P_{nC6} = 4.5 kPa with 0.48 µmol of hexane in each pulse.

According to our previous works, sodium prefers to titrate the highly active sites in MFI zeolites, resulting in a significant cracking rate decrease. Gounder et al. claimed that sodium prefers to titrate the active sites in 8-MR pockets that have higher activity for C3 cracking for the MOR sample.[34] However, this hypothesis cannot explain the up-to-fivefold enhancement of alkane cracking rate by mild steamed dealumination in MOR.[14] In addition, in this study, we observed significant decreases in alkane cracking rates for MOR-10 and MEL-25 zeolites, shown in Figure 33 and Figure 34, respectively. Sodium exchanged MOR samples are denoted as Na-MOR X M, with X being the concentration of sodium solution.

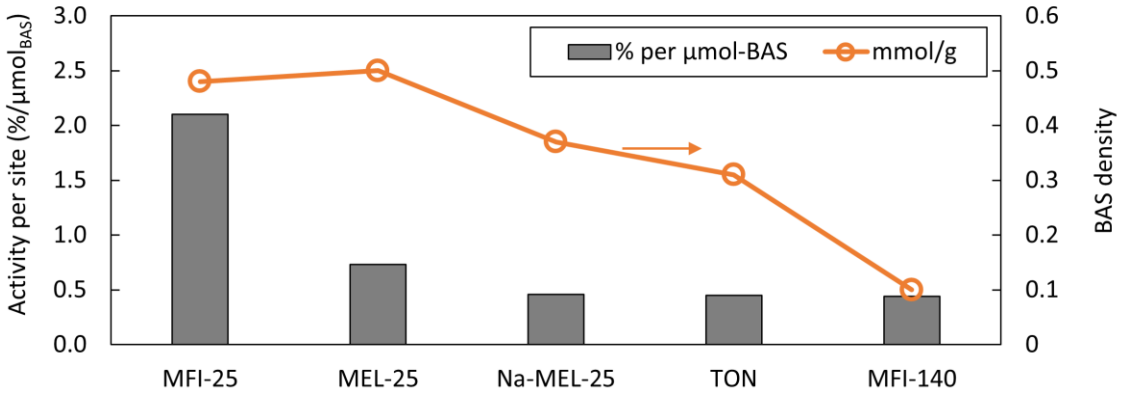

Figure 34. Rate of n-hexane cracking of fresh and sodium exchanged 10MR zeolites. The corresponding BAS density of the catalyst was plotted. Reaction conditions: T = 753 K, P_{nC6} = 4.5 kPa with 0.48 µmol of hexane in each pulse.

In the case of MOR zeolite, activity per site consistently decreases as more active sites are exchanged with sodium while the activity per site decreases and reaches a similar value. This result indicates that most highly active sites are titrated by sodium. The fraction of acid sites in 8-MR pockets of this MOR-10 zeolite estimated by IR spectra is 0.55 (±0.05), reported by Bhan et al.[40] According to this result, Na-MOR 0.1M still has a significant fraction of 8-MR while Na-MOR 0.5 M only contains acid sites in 12-MR channels. If all active sites in 8-MR have higher activity than those in the 12-MR channels, the activity per site in Na-MOR 0.1M must be higher than that of Na-MOR 0.5M. The observed activities on these two catalysts are comparable, implying that the decrease of activity in sodium exchanged zeolites is likely associated with the highly selective titration of synergistic sites in this zeolite. In addition, pulsing water does not enhance the cracking rate of Na-MOR 0.5M, which suggests that sodium titrates the precursor for the generation of highly active sites. The similar results of MFI zeolites discussed in the previous chapter are likely

associated with the titration of Al-Al pairs at MFI intersections. However, the explanation for these results in the case of MOR zeolites might be different. Since previous works reported that Na prefers to titrate active sites in 8-MR pockets, it is possible that synergistic sites are formed in 8MR pockets. Further studies regarding the generation and stabilization of EFAL at the different confining voids in MOR zeolite are needed to address the preferential locations of synergistic sites in this catalyst.

To further investigate the influence of confinement and highly active sites, hexane cracking rates on various zeolite samples having 10-MR pores are compared in Figure 34. The results show that MFI-25 and MEL-25 have distinct reactivity, which might be associated with the higher number of synergistic sites in MFI-25. Although both MEL and MFI zeolites have straight channels and intersections with comparable pore sizes, the absence of sinusoidal channels in MEL zeolite and the differences in the topologies of these catalysts might affect the mobility and stabilization of EFAL species and prevent the formation of highly active sites. The difference in Al distribution, such as the Al-Al distance and the fraction of Al in pairs at the intersections, can also affect the formation of synergistic sites. As previously discussed, the low activity of MEL and FAU shows that zeolite topologies strongly affect the generation of synergistic sites. After sodium exchange, the activity per site of Na-MEL-25 is significantly lower than the one of parent zeolites, which might be attributed to a small fraction of highly active sites or typical BAS sites located at more confining voids that prefer to be titrated with sodium. These sites usually have higher activity than the typical BAS sites located in less confining voids such as intersections. In addition, the activities of Na-MEL-25, TON, and MFI-140 catalysts are comparable despite their apparent differences in Si/Al ratios and densities of BAS and

EFAL species. This result suggests the confinement of active sites in these three zeolites are similar, which determines their cracking reactivity, and these samples only contain typical BAS.

5.4 Conclusions

This work extends our knowledge of the generation of synergistic sites in MFI zeolite to other types of zeolites. The experiment results suggest that the formation of these sites plays a vital role in the catalytic performance of catalysts. The formation of these sites is affected by Si/Al ratios, Al distribution, and topologies of zeolites. These factors also influence the generation and stabilization of EFAL species that strongly affect the rate enhancement under pulsing water treatment. By investigating the zeolites with low Si/Al ratios that only contain typical BAS, we can decouple the effect of confinement from the influence of the presence of highly active sites on the catalytic reactivity of catalysts. The results show that acid sites in more confining voids have a higher catalytic reactivity. In addition, for different zeolites such as MOR, MFI, and MEL, sodium clearly shows the preferential titration of protons associated with highly active sites. Further studies are needed to investigate the location of these sites in different zeolite topologies.

REFERENCES

1. Wang, W.; Hunger, M., Reactivity of Surface Alkoxy Species on Acidic Zeolite Catalysts. *Accounts of Chemical Research* **2008,** *41* (8), 895-904.

2. Corma, A., Inorganic Solid Acids and Their Use in Acid-Catalyzed Hydrocarbon Reactions. *Chemical Reviews* **1995,** *95* (3), 559-614.

3. Corma, A., From Microporous to Mesoporous Molecular Sieve Materials and Their Use in Catalysis. *Chemical Reviews* **1997,** *97* (6), 2373-2420.

4. Clerici, M. G., Zeolites for fine chemicals production. *Topics in Catalysis* **2000,** *13* (4), 373-386.

5. Haw, J. F.; Song, W.; Marcus, D. M.; Nicholas, J. B., The Mechanism of Methanol to Hydrocarbon Catalysis. *Accounts of Chemical Research* **2003,** *36* (5), 317-326.

6. Corma, A., State of the art and future challenges of zeolites as catalysts. *Journal of Catalysis* **2003,** *216* (1), 298-312.

7. Bhan, A.; Iglesia, E., A Link between Reactivity and Local Structure in Acid Catalysis on Zeolites. *Accounts of Chemical Research* **2008,** *41* (4), 559-567.

8. Jones, A. J.; Iglesia, E., The Strength of Brønsted Acid Sites in Microporous Aluminosilicates. *ACS Catalysis* **2015,** *5* (10), 5741-5755.

9. Janda, A.; Vlaisavljevich, B.; Lin, L.-C.; Smit, B.; Bell, A. T., Effects of Zeolite Structural Confinement on Adsorption Thermodynamics and Reaction Kinetics for Monomolecular Cracking and Dehydrogenation of n-Butane. *Journal of the American Chemical Society* **2016,** *138* (14), 4739-4756.

10. Alaithan, Z. A.; Mallia, G.; Harrison, N. M., Monomolecular Cracking of Propane: Effect of Zeolite Confinement and Acidity. *ACS Omega* **2022,** *7* (9), 7531-7540.

11. Kotrel, S.; Rosynek, M. P.; Lunsford, J. H., Intrinsic Catalytic Cracking Activity of Hexane over H−ZSM-5, H−β and H−Y Zeolites. *The Journal of Physical Chemistry B* **1999,** *103* (5), 818-824.

12. Janda, A.; Vlaisavljevich, B.; Smit, B.; Lin, L.-C.; Bell, A. T., Effects of Pore and Cage Topology on the Thermodynamics of n-Alkane Adsorption at Brønsted Protons in Zeolites at High Temperature. *The Journal of Physical Chemistry C* **2017,** *121* (3), 1618-1638.

13. Gounder, R.; Iglesia, E., The Roles of Entropy and Enthalpy in Stabilizing Ion-Pairs at Transition States in Zeolite Acid Catalysis. *Accounts of Chemical Research* **2012,** *45* (2), 229-238.

14. van Bokhoven, J. A.; Williams, B. A.; Ji, W.; Koningsberger, D. C.; Kung, H. H.; Miller, J. T., Observation of a compensation relation for monomolecular alkane cracking by zeolites: the dominant role of reactant sorption. *Journal of Catalysis* **2004,** *224* (1), 50-59.

15. Kadam, S. A.; Li, H.; Wormsbecher, R. F.; Travert, A., Impact of Zeolite Structure on Entropic–Enthalpic Contributions to Alkane Monomolecular Cracking: An IR Operando Study. *Chemistry – A European Journal* **2018,** *24* (21), 5489-5492.

16. Van der Mynsbrugge, J.; Janda, A.; Mallikarjun Sharada, S.; Lin, L.-C.; Van Speybroeck, V.; Head-Gordon, M.; Bell, A. T., Theoretical Analysis of the Influence of Pore Geometry on Monomolecular Cracking and Dehydrogenation of n-Butane in Brønsted Acidic Zeolites. *ACS Catalysis* **2017,** *7* (4), 2685-2697.

17. Kung, H. H.; Williams, B. A.; Babitz, S. M.; Miller, J. T.; Snurr, R. Q., Towards understanding the enhanced cracking activity of steamed Y zeolites. *Catalysis Today* **1999,** *52* (1), 91-98.

18. Babitz, S. M.; Williams, B. A.; Miller, J. T.; Snurr, R. Q.; Haag, W. O.; Kung, H. H., Monomolecular cracking of n-hexane on Y, MOR, and ZSM-5 zeolites. *Applied Catalysis A: General* **1999,** *179* (1), 71-86.

19. Gounder, R.; Iglesia, E., *J. Am. Chem. Soc.* **2009,** *131*, 1958.

20. van Bokhoven, J. A.; Williams, B. A.; Ji, W.; Koningsberger, D. C.; Kung, H. H.; Miller, J. T., *J. Catal.* **2004,** *224*, 50.

21. Xu, B.; Sievers, C.; Hong, S. B.; Prins, R.; van Bokhoven, J. A., *J. Catal.* **2006,** *244*, 163.

22. Ramachandran, C. E.; Williams, B. A.; van Bokhoven, J. A.; Miller, J. T., *J. Catal.* **2005,** *233*, 100.

23. Gounder, R.; Iglesia, E., *Acc. Chem. Res.* **2012,** *45*, 229.

24. Kung, H. H.; Williams, B. A.; Babitz, S. M.; Miller, J. T.; Haag, W. O.; Snurr, R. Q., Enhanced hydrocarbon cracking activity of Y zeolites. *Topics in Catalysis* **2000,** *10* (1), 59-64.

25. Williams, B. A.; Babitz, S. M.; Miller, J. T.; Snurr, R. Q.; Kung, H. H., The roles of acid strength and pore diffusion in the enhanced cracking activity of steamed Y zeolites. *Applied Catalysis A: General* **1999,** *177* (2), 161-175.

26. Biaglow, A. I.; Parrillo, D. J.; Kokotailo, G. T.; Gorte, R. J., A Study of Dealuminated Faujasites. *Journal of Catalysis* **1994,** *148* (1), 213-223.

27. van Bokhoven, J. A.; Tromp, M.; Koningsberger, D. C.; Miller, J. T.; Pieterse, J. A. Z.; Lercher, J. A.; Williams, B. A.; Kung, H. H., An Explanation for the Enhanced Activity for Light Alkane Conversion in Mildly Steam Dealuminated Mordenite: The Dominant Role of Adsorption. *Journal of Catalysis* **2001,** *202* (1), 129-140.

28. Zhu, N.; Wang, Y.; Cheng, D.-g.; Chen, F.-q.; Zhan, X.-l., Experimental evidence for the enhanced cracking activity of n-heptane over steamed ZSM-5/mordenite composite zeolites. *Applied Catalysis A: General* **2009,** *362* (1), 26-33.

29. Schallmoser, S.; Ikuno, T.; Wagenhofer, M. F.; Kolvenbach, R.; Haller, G. L.; Sanchez-Sanchez, M.; Lercher, J. A., Impact of the local environment of Brønsted acid sites in ZSM-5 on the catalytic activity in n-pentane cracking. *Journal of Catalysis* **2014,** *316*, 93-102.

30. Xue, N.; Vjunov, A.; Schallmoser, S.; Fulton, J. L.; Sanchez-Sanchez, M.; Hu, J. Z.; Mei, D.; Lercher, J. A., Hydrolysis of zeolite framework aluminum and its impact on acid catalyzed alkane reactions. *Journal of Catalysis* **2018,** *365*, 359-366.

31. Zholobenko, V. L.; Kustov, L. M.; Kazansky, V. B.; Loeffler, E.; Lohse, U.; Oehlmann, G., On the nature of the sites responsible for the enhancement of the cracking activity of HZSM-5 zeolites dealuminated under mild steaming conditions: Part 2. *Zeolites* **1991,** *11* (2), 132-134.

32. Zholobenko, V. L.; Kustov, L. M.; Kazansky, V. B.; Loeffler, E.; Lohser, U.; Peuker, C.; Oehlmann, G., On the possible nature of sites responsible for the enhancement of cracking activity of HZSM-5 zeolites dealuminated under mild steaming conditions. *Zeolites* **1990,** *10* (4), 304-306.

33. Silaghi, M.-C.; Chizallet, C.; Sauer, J.; Raybaud, P., Dealumination mechanisms of zeolites and extra-framework aluminum confinement. *Journal of Catalysis* **2016,** *339*, 242-255.

34. Gounder, R.; Iglesia, E., Catalytic Consequences of Spatial Constraints and Acid Site Location for Monomolecular Alkane Activation on Zeolites. *Journal of the American Chemical Society* **2009,** *131* (5), 1958-1971.

35. Garralón, G.; Fornés, V.; Corma, A., Faujasites dealuminated with ammonium hexafluorosilicate: Variables affecting the method of preparation. *Zeolites* **1988,** *8* (4), 268-272.

36. Pham, T. N.; Nguyen, V.; Wang, B.; White, J. L.; Crossley, S., Quantifying the Influence of Water on the Mobility of Aluminum Species and Their Effects on Alkane Cracking in Zeolites. *ACS Catalysis* **2021,** *11* (12), 6982-6994.

37. McCusker, C. B. a. L. B., Database of Zeolite Structures:http://www.iza-structure.org/databases/. 1996.

38. Liu, C.; Li, G.; Hensen, E. J. M.; Pidko, E. A., Nature and Catalytic Role of Extraframework Aluminum in Faujasite Zeolite: A Theoretical Perspective. *ACS Catalysis* **2015,** *5* (11), 7024-7033.

39. Gounder, R.; Iglesia, E., The catalytic diversity of zeolites: confinement and solvation effects within voids of molecular dimensions. *Chemical Communications* **2013,** *49* (34), 3491-3509.

40. Bhan, A.; Allian, A. D.; Sunley, G. J.; Law, D. J.; Iglesia, E., Specificity of Sites within Eight-Membered Ring Zeolite Channels for Carbonylation of Methyls to Acetyls. *Journal of the American Chemical Society* **2007,** *129* (16), 4919-4924.

CONCLUSION AND OUTLOOK

In this contribution, we have revealed the influence of highly active EFAL-BAS sites in the catalytic activity of alkane cracking reaction on zeolites. Fundamentals regarding the effect of the aluminum distribution and structural properties of zeolites on the formation of these synergistic sites have been systematically studied using the micropulse reaction system. Hexane cracking is used as a probe reaction to evaluate the catalytic activity of zeolites.

Pulsing water treatment is successfully utilized to examine the potential of the catalysts to generate synergistic sites. This treatment does not lead to modifying the number of active sites; thus, it helps decouple the mobility of EFAL species with the generation of new EFAL species through hydrolysis of framework Al atoms. The results show that activities of MFI catalysts having high densities of BAS and EFAL will be likely increased during pulsing water treatment. Based on the increase in cracking rate, the energy required to generate new sites is estimated, comparable with the barriers to mobilized EFAL species inside zeolite pore obtained by DFT calculations. The high cracking rate on the synergistic sites is attributed to a low activation enthalpy.

By drawing the correlation between the concentration of Al in pairs and the cracking activities of MFI zeolites in fresh and after water treated samples, we proposed that Al in pairs might play an essential role in the generation of highly active sites for this reaction. For instance, one Al atom of the Al-Al pair might exchange with EFAL species or kinetically trap EFAL species through the H-bonds of BAS and -OH groups of EFAL species. As a result, these EFAL species might form the EFAL-BAS with the remaining

BAS of Al in pairs. Cation titration of acid sites by calcium and sodium can significantly diminish the highly active sites in zeolites and the precursor to generate these sites by water treatments. These results suggest these cations selectively titrate Al in pairs associated with synergistic sites, which are likely located at the MFI intersections. It also allows us to quantify the number of these highly active sites and estimate the corresponding activation entropies for cracking reactions on these sites. In agreement with the previous results, a lower activation enthalpy drives the cracking reaction on the synergistic sites.

Furthermore, the transformation and immigration of EFAL species in zeolite might be modified by using several pretreatments of catalysts in water liquid and ammonium nitrate solutions. The results show that these treatments can significantly enhance the cracking activity of MFI zeolites without changing the densities of these catalysts. However, the enhancement is not significant as the pulsing water treatment at high temperatures.

Finally, this work investigated the influence of confinement and topologies on the reactivity of catalysts and the generation of synergistic sites. The results show that the activities are strongly affected by the confinement in catalysts only containing typical BAS sites. The activities of small pore zeolites are higher than those of big pore zeolites. This result is consistent with lower activation energies of cracking on active sites in more confining voids. On the other hand, the activity of catalysts containing synergistic sites is strongly affected by the presence of these sites. The confinement and zeolite topologies can influence the generation, migration, and stabilization of EFAL species inside the pores, thus, alter the formation of new highly active sites.

Although this work has addressed several important issues regarding the generation of highly actives sites for alkane cracking in zeolites, many questions have been raised that

need further investigation. First, what is the nature of EFAL species that can form synergistic sites? To answer this question, we have conducted a follow-up work using the combination of DFT and kinetic measurements that focuses on propane cracking reaction on MFI zeolites. A part of this work will be described in the Appendix of this dissertation. Second, how does the distance of active sites influence the formation of these synergistic sites? Is it possible to observe the change in the distance of Al-Al using characterization techniques such as NMR when new synergistic sites are formed? Third, what kinds of reactions can we observe the high activity on the synergistic sites? If EFAL species can enhance the activity of nearby BAS, it likely modifies the confinement of these active sites, leading to the modification of rates for several reactions on these sites. Fourth, how can the Al in proximity, location of active sites, and zeolites topologies influence the immigration and stabilization of other extra framework species such as La, Zn, and Co in zeolites? In addition, how do these species influence the rate and selectivity of chemical reactions in modified zeolites?.

APPENDIX: Nature and Catalytic Roles of Complex Aluminum Species in H-ZSM5 Zeolites

This work was originally co-authored with Vy Nguyen, Steven Crossley, and Bin Wang. Vy Nguyen conducts DFT calculations, and Tram Pham conducts kinetic measurements. This writing is under preparation for submission of publication.

A1. Kinetic study of propane cracking on H-ZSM5 zeolites

Figure A1 presents the rates of propane conversion on MFI zeolites, which are measured in a pulse reaction. The reaction order is close to 1, shown in Figure A2, suggesting the monomolecular reaction pathway. The products distributions under investigated reaction conditions are comparable, which include C_3H_6 (~ 42 wt.%), C_2H_6 (~ 36 wt.%), CH4 (~ 18wt%), and other light hydrocarbons. These results suggest that propane cracking and dehydrogenation occur under the reaction conditions. It was shown in Figure A1 that HZSM5-15-AHFS catalyst has a significantly lower activity compared to the parent HZSM5-15, which agrees with the results for hexane cracking in the previous chapter. This result suggests that the AHFS treatment removes EFAL species, leading to the loss of synergistic sites. HZSM5-11.5 has lower activity than HZSM5-15, which can be attributed to fewer synergistic sites in this catalyst.

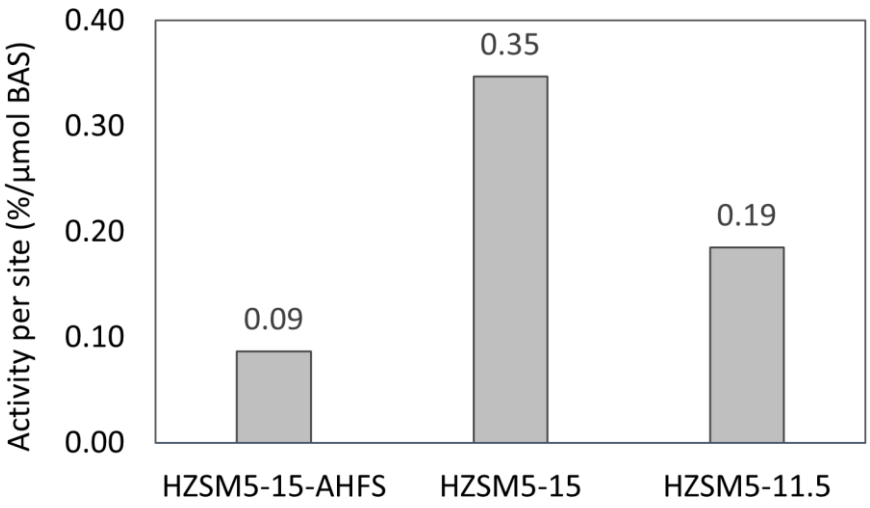

Figure A1. Activity per site of propane conversion in MFI-X zeolites, X is Si/Al ratio.

500 µl pulses of pure propane (>99%) are injected at temperature as 823 K.

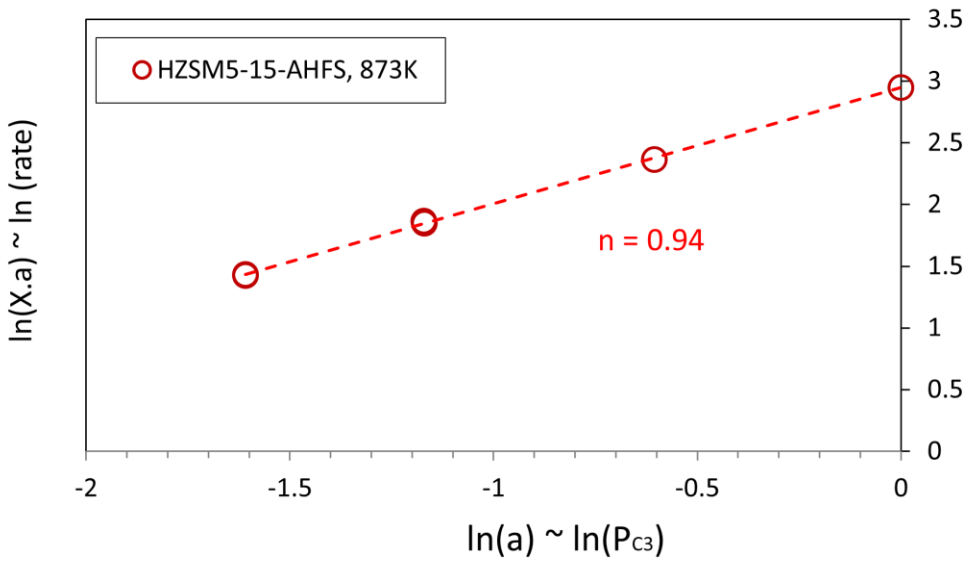

Figure A2. Estimation of the order of propane cracking on HZSM5-15-AHFS. In which X is the reaction conversion, a is the mole percent of propane in the loop, described in the supporting information of chapter 2.

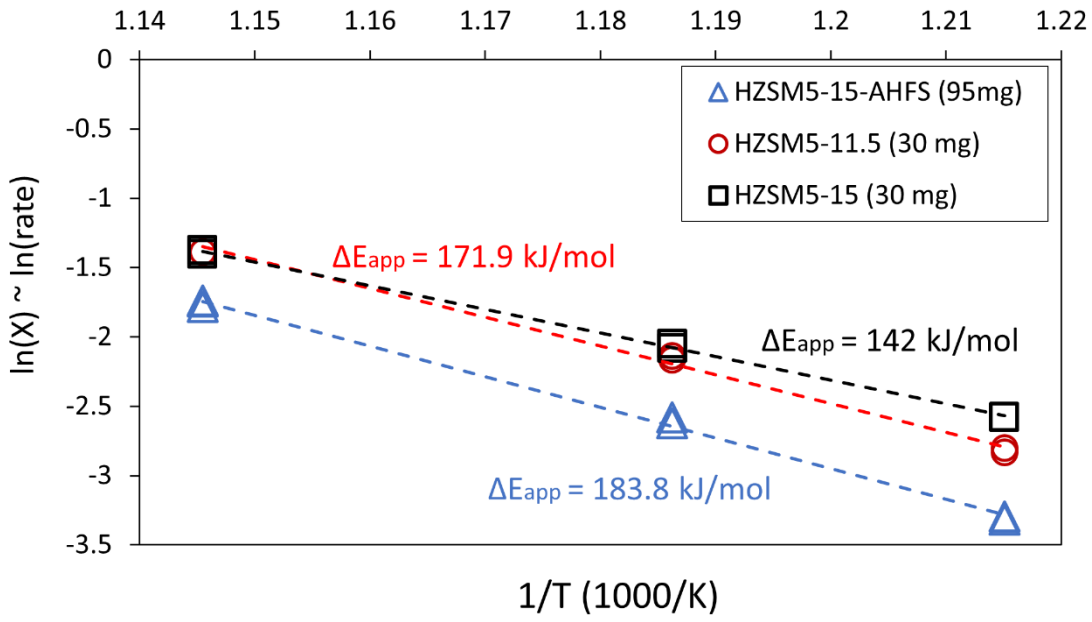

Figure A3. Estimation of apparent activation enthalpy of propane reactions on MFI zeolites.

Figure A3 presents the Arrhenius plot for estimating the activation energies of propane conversion in the investigated catalysts. The amount of the catalyst is varied to maintain comparable levels of reaction conversions. The activation energy for propane conversion is highest in case of AHFS treated catalyst, which is associated with the barrier on typical BAS. This value is lowest in HZSM5-15 catalyst due to a significant number of synergistic sites in this catalyst, as discussed in our previous works.[1] In summary, the rate of propane cracking on HZSM5 zeolite is driven by a lower activation energy. It is important to note that the required barriers of both cracking and dehydrogenation have contributed to the measured activation energies. In the next discussion, DFT calculation will be utilized to estimate the barrier for only propane cracking, not for propane dehydrogenation, which is expected to be significantly lower compared to the values we obtained here. In agreement

with the experiment results, DFT calculations show that the presence of some EFAL species nearby a BAS helps to stabilize better the transition state of propane cracking reaction on MFI zeolites.

A2. Identification of nature of synergistic sites by DFT

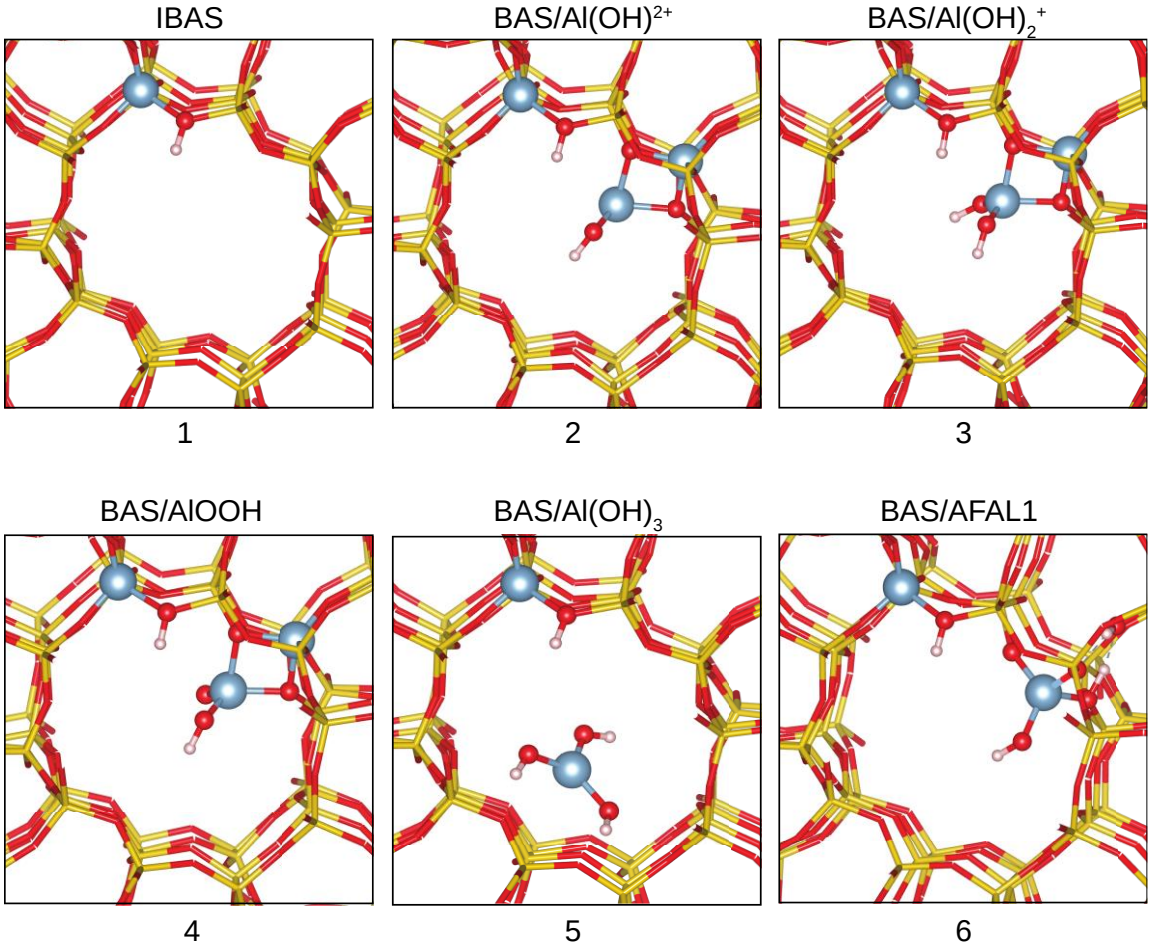

Figure A4. Possible active sites, including isolated BAS and synergistic sites in H-ZSM5 zeolite.

To further study the impact of non-framework Al on catalytic performance, monomolecular cracking of n-propane was modeled on various active sites consisting of I-BAS and synergistic sites, illustrated in Figure A4. Energy, entropy, and free energy for

each step of reactions were evaluated and compared among different active centers. The cracking process is limited by the initial protonation of the C-C bond or C atoms to form the propyl carbonium intermediate (Scheme A1). The C-C bond of the propane molecule that undergoes cracking is located directly over the O-H group of BAS. All the adsorption-related values were calculated at this position of propane.

Scheme A1. Propane cracking reaction mechanism with the rate-limiting step 1) protonation to C-C bond and 2) protonation to terminal C.

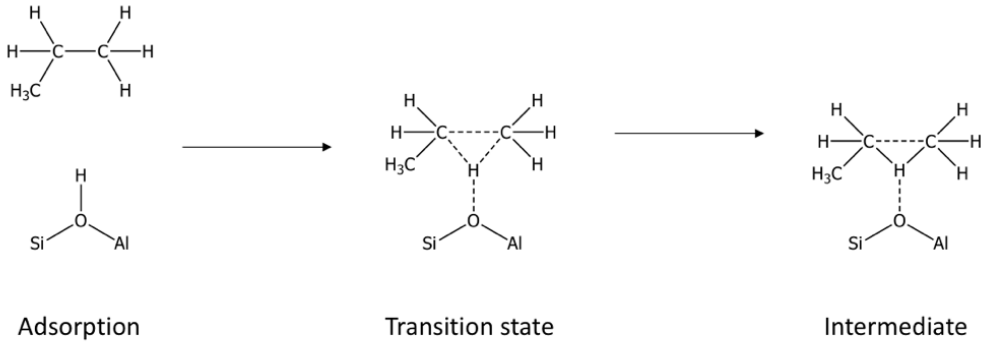

Table A1. The adsorption enthalpy, intrinsic and activation enthalpies for propane cracking on different active sites calculated at 773 K.

Sites	structure	ΔH_{ads} (kJ/mol)	$\Delta H^{\ddagger}_{int}$ (kJ/mol)	ΔH_{app} (kJ/mol)	$\Delta H_{intermediate}$ (kJ/mol)
I-BAS	1	-46	161	115	107
BAS/Al(OH)$^{2+}$	2	-45	151	106	88
BAS/Al(OH)$_2^+$	3	-52	149	97	97
BAS/AlOOH	4	-62	153	91	91
BAS/Al(OH)$_3$	5	-64	130	66	71
BAS/AFAl1	6	-65	162	97	79

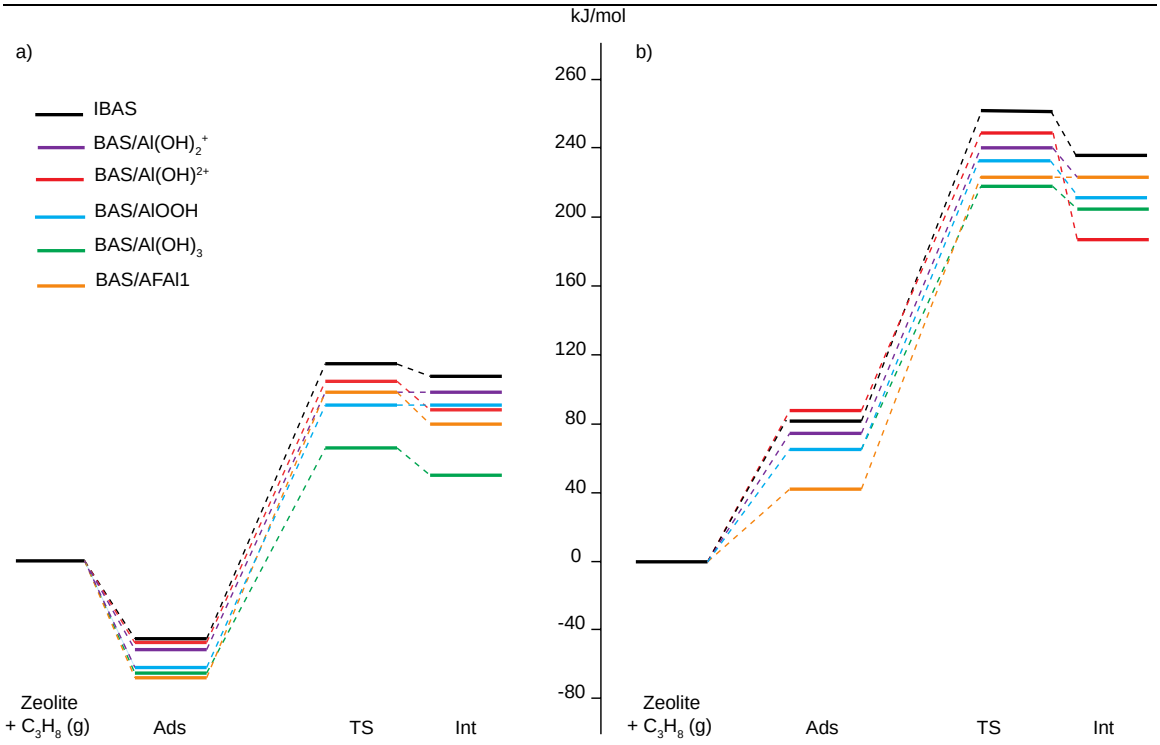

Figure A5. a) Enthalpy profiles of propane cracking and b) Gibb free energy profiles of propane cracking on different active sites

The adsorption, the intrinsic activation, and the apparent activation enthalpy of propane cracking on various active sites are presented in Table A1 and Figure A5-a. The adsorption heat of propane over isolated BAS at the intersection is -46 kJ/mol, in good agreement with previous computational and experimental works.[2-4] The experimental value reported by Moor et al. was -41 kJ/mol, which was shown insensitive to temperature and the reported computational values were about -64 and -53 kJ/mol for propane adsorption in the straight and sinusoidal channel, respectively.[4] Moreover, Swisher et al. reported a value of -37.8 kJ/mol using the configurational bias Monte Carlo method at 773^{o}K.[3] In the presence of EFAL or AFAL, adsorption heat is higher compared to that of isolated BAS due to the more effective van der Waals interaction.

For the same BAS at T7, the activation barriers depend on the local environment of the active sites. The cracking reaction shows significantly lower apparent activation enthalpies, ranging from 66-106 kJ/mol, among six distinct synergistic sites (compared to 115 kJ/mol for isolated BAS sites). The activation enthalpy in this work is in general agreement with previous literature. For instance, the intrinsic activation barrier of propane cracking reaction at 773 K using DFT (PBE functional) on cluster model, reported by Bell group,[3] is 156.2 kJ/mol, which is very close to our value for an isolated BAS (161 kJ/mol). However, it has been known that PBE, the calculation method used in this work, would lead to underestimation of the barrier height.[5]

Table A2. Charge transfer from propane to zeolite at the transition states.

Sites	Structures	Charge transfer (e)
I-BAS	1	0.19
BAS/$Al(OH)^{2+}$	2	0.75
BAS/$Al(OH)_2^{+}$	3	0.53
BAS/AlOOH	4	0.40
BAS/$Al(OH)_3$	5	0.18
BAS/AFAl1	6	0.42

From Table A2, the charge transfer between TS and zeolite framework on all synergistic sites, except BAS/$Al(OH)_3$, are 0.21-0.56 e higher than that of I-BAS. The positive values of charge transfers indicate electron transfer from propane molecule to zeolite. The atomic distances of TS structures (Table A5) indicate that the proton approaches closer to the molecule on these synergistic sites and attract more electron from the molecule, evidenced by the shorter C1-H and C2-H distances. Additionally, the charge transfers at TS are highest on synergistic sites containing cation EFAL ($Al(OH)^{2+}$ and $Al(OH)_2^{+}$) due to the fact that these cation EFAL species can also withdraw electrons from the molecule. These results suggest that the electrostatic interactions at TS are stronger on synergistic sites. The cation EFAL species can also stabilize the anion deprotonated framework, leading to lower activation barriers. Liu et al. reported that the multi-nuclear cationic EFAL in sodalite in FAU could enhance the catalytic activity of BAS in its proximity. The negative charge of the deprotonated zeolite framework was more effectively compensated by the multiple charge cationic EFAl, leading to the decrease of the activation barrier of the propane

cracking reaction.[6] Unlike positively charged cationic EFAL, the AFAl1 species possessing tetrahedrally coordinated aluminum centers to four oxygen atoms have negative charges stabilized on aluminum. Our previous study, using the chemical shift and CQ data, showed that the Al(IV)-2, which were assigned to hydrolyzed aluminum species, possesses a negative formal charge.[7] These negative charges in the reaction environment can stabilize the positive carbonium ion at TSs.

The activation barrier decreases dramatically on synergistic sites BAS/Al(OH)3, 49 kJ/mol lower than I-BAS. The $Al(OH)_3$ species at the intersection make the pore tighter, resulting in more effective van der Waals interactions between the TS and zeolite and additional dispersion force between the TS and the $Al(OH)_3$ species. In general, the more effective van der Waal and electrostatic interactions make the activation enthalpies on synergistic sites considerably lower than that of I-BAS.

It has been shown that the entropy loss upon adsorption in zeolite is a function of confinement.[4] In the case of MFI zeolite, P. J. Dauenhauter and O. A. Abdelrahman showed that considering one translational and one rotational degree of freedom loss in entropy upon n-alkane adsorption led to underestimation of the entropy loss. However, they argued that losing all the three translational degrees of freedom would result in an overestimation of the entropy loss. Additionally, the entropy loss of linear alkane upon adsorption on MFI was about 38% of their gas-phase entropy. Moor et al. proposed that the n-alkane adsorption could be addressed by considering two degrees of rotational freedom and one degree of translational freedom loss for the molecule entropy upon adsorption.[4] In this study, to compare the entropic changes of propane in different local environments, we assume the adsorption of reactant on active sites are strong enough that the propane

molecule is an immobile adsorbate the rotational motion is negligible. Further, the solid zeolite also possesses negligible rotational and translational entropy, thus all entropic effects come from the change in the harmonic vibrational modes. It should be pointed out that this method is the only one that is capable of differentiating entropy loss at the TSs from those in the stable states, leading to some estimation for the contribution from entropy change along the reaction pathway in the activation barriers.

Table A3. The adsorption, apparent and intermediate activation entropies for propane cracking on different active sites calculated at 773 K.

Sites	**structure**	**ΔS_{ads} (J/mol/K)**	**ΔS_{app} (J/mol/K)**	**$\Delta S_{intermediate}$ (J/mol/K)**
I-BAS	1	-165	-188	-155
BAS/$Al(OH)^{2+}$	2	-170	-185	-181
BAS/$Al(OH)_2^{+}$	3	-164	-186	-164
BAS/AlOOH	4	-165	-179	-161
BAS/$Al(OH)_3$	5	-167	-196	-177
BAS/AFAl1	6	-159	-165	-166

Table A3 lists the entropy change for elementary steps compared to the gas phase along the reaction coordinate. The adsorbed entropies of propane on the studied active sites are not considerably different. Although this entropy model overestimates the entropy losses, it still provides an acceptable comparison between different active sites. Moor et al. reported the calculated entropy loss upon adsorption to be roughly -100 J/mol.K, while the experimental value calculated based on statistical thermodynamic equations was -94

kJ/mol.K.[4, 8] Grounder et al. reported that the measured and intrinsic entropy of propane cracking reaction in MFI was about -110 and -10 J/mol.K. The activation entropies on most of the synergistic sites, including BAS/$Al(OH)^{2+}$, BAS/$Al(OH)_2^+$, BAS/AlOOH, BAS/$Al(OH)_3$, and BAS/AFAL1 are insignificantly different from that of I-BAS. Notably, the activation entropy on BAS/AFAL1 is 23 kJ/mol.K less negative than I-BAS. On BAS/AFAL1 site, the TS is a late one and resembles the product, that is evidenced by the elongated C-C bond. Particularly, the C-C bond of TS on I-BAS is 1.71 Å while C-C bond on BAS/AFAL1 is 2.12 Å., shown in Table A4.

Table A4. Atomic distances of transition states on different site, with C1: terminal C, C2: middle C, H: BAS and O: the protonated oxygen.

site	structure	C1-C2 (Å)	C1-H (Å)	C2-H (Å)	O-H
I-BAS	1	1.71	1.48	1.73	1.26
BAS/$Al(OH)^{2+}$	2	1.88	1.22	1.32	2.29
BAS/$Al(OH)_2^+$	3	1.79	1.28	1.41	1.75
BAS/AlOOH	4	1.71	1.23	1.63	1.73
BAS/$Al(OH)_3$	5	1.68	1.49	1.79	1.29
BAS/AFAl1	6	2.12	1.21	1.33	2.42

Since the enthalpies and entropies for propane cracking are known, the Gibb free energies can be easily calculated as:

$$\Delta G = \Delta H - T\Delta S \quad (1)$$

The calculated values of Gibb free energy are given in Table A5 and Figure A5-b. Owing to the overestimated entropy losses as discussed earlier, the free energies in this study would be generally overestimated, but to a similar extent, leading to reliable activation barriers. The free energy of activation barriers of propane cracking on BAS in 8-MR and 12-MR of mordenite zeolite reported by R Grounder et al. were about 227 and 234 kJ/mol, respectively.[8] This work suggests that the free energy of activation barriers on I-BAS at the MFI intersection is 260kJ/mol. There are significant decreases in free energies of activation on synergistic sites, which is dominantly contributed by lower activation enthalpies. However, on BAS/AFAl1 site, the lower activation of free energy is affected by both enthalpic and entropic activation.

Table A5. The adsorption and apparent activation of Gibb free energies for propane cracking on different active sites calculated at 773 K.

Sites	**Structure**	**ΔG_{ads} (kJ/mol)**	**ΔG_{app} (kJ/mol)**	**$\Delta G_{intermediate}$ (kJ/mol)**
I-BAS	1	82	260	235
BAS/$Al(OH)^{2+}$	2	87	249	187
BAS/$Al(OH)_2^{+}$	3	74	241	226
BAS/AlOOH	4	65	230	216
BAS/$Al(OH)_3$	5	65	218	208
BAS/AFAL1	6	58	228	207

REFERENCES

1. Pham, T. N.; Nguyen, V.; Wang, B.; White, J. L.; Crossley, S., Quantifying the Influence of Water on the Mobility of Aluminum Species and Their Effects on Alkane Cracking in Zeolites. *ACS Catalysis* **2021,** *11* (12), 6982-6994.

2. Mallikarjun Sharada, S.; Zimmerman, P. M.; Bell, A. T.; Head-Gordon, M., Insights into the Kinetics of Cracking and Dehydrogenation Reactions of Light Alkanes in H-MFI. *The Journal of Physical Chemistry C* **2013,** *117* (24), 12600-12611.

3. Swisher, J. A.; Hansen, N.; Maesen, T.; Keil, F. J.; Smit, B.; Bell, A. T., Theoretical Simulation of n-Alkane Cracking on Zeolites. *The Journal of Physical Chemistry C* **2010,** *114* (22), 10229-10239.

4. De Moor, B. A.; Reyniers, M.-F.; Gobin, O. C.; Lercher, J. A.; Marin, G. B., Adsorption of C2−C8 n-Alkanes in Zeolites. *The Journal of Physical Chemistry C* **2011,** *115* (4), 1204-1219.

5. Zimmerman, P. M.; Tranca, D. C.; Gomes, J.; Lambrecht, D. S.; Head-Gordon, M.; Bell, A. T., Ab Initio Simulations Reveal that Reaction Dynamics Strongly Affect Product Selectivity for the Cracking of Alkanes over H-MFI. *Journal of the American Chemical Society* **2012,** *134* (47), 19468-19476.

6. Liu, C.; Li, G.; Hensen, E. J. M.; Pidko, E. A., Nature and Catalytic Role of Extraframework Aluminum in Faujasite Zeolite: A Theoretical Perspective. *ACS Catalysis* **2015,** *5* (11), 7024-7033.

7. Chen, K.; Horstmeier, S.; Nguyen, V. T.; Wang, B.; Crossley, S. P.; Pham, T.; Gan, Z.; Hung, I.; White, J. L., Structure and Catalytic Characterization of a Second Framework Al(IV) Site in Zeolite Catalysts Revealed by NMR at 35.2 T. *Journal of the American Chemical Society* **2020,** *142* (16), 7514-7523.

8. Gounder, R.; Iglesia, E., The Roles of Entropy and Enthalpy in Stabilizing Ion-Pairs at Transition States in Zeolite Acid Catalysis. *Accounts of Chemical Research* **2012,** *45* (2), 229-238.